Clean Energy, 2023, Vol. 7, No. 2, 436–491
https://doi.org/10.1093/ce/zkac079
Advance access publication 8 April 2023
Review Article

Combined cold, heat and power (CCHP) systems and fuel cells for CCHP applications: a topological review

Nganyang Paul Bayendang*, Mohamed Tariq Kahn and Vipin Balyan

Cape Peninsula University of Technology (CPUT), Bellville Campus, Symphony Way (off Robert Sobukwe Road), Department of Electrical, Electronic and Computer Engineering (DEECE), 7535, Cape Town, Western Cape, Republic of South Africa
*Corresponding author. E-mail: bayendangn@cput.ac.za

Abstract

As the basis for the study, this manuscript was written at a time when the energy crisis is affecting most parts of the world and most especially the prevailing and rampant electricity crisis in most developing countries. As a result, 50 combined cooling, heating and power (CCHP) systems studies were reviewed, which included the internal combustion engine (ICE), Stirling engine, biomass, micro turbine, solar and biogas, photovoltaic (PV) and gas turbine, wind turbine, PV and micro-turbine, solid-oxide and phosphoric-acid fuel cells (FCs), ICE and thermoelectric generator, low-temperature (LT) polymer electrolyte membrane (PEM), inlet air throttling gas turbine, ground source heat pump (GSHP) micro gas turbine and PV, ICE and GSHP, ICE with dehumidification and refrigeration, 5-kW PEM FC, thermoelectric cooler and LT-PEM FC, Stirling engine and molten carbonate FC, thermo-acoustic organic Rankine cycle, solar-thermal, geothermal, integrated energy systems, power- and heat-storage systems, energy-conversion systems, thermodynamic and thermo-economic optimization strategies, working fluids based on hydrogen, helium as well as ammonia, H_2O, CO_2 etc. Of these reviewed CCHP systems, FC-based CCHP systems were of the greatest interest, particularly the PEM FC. Consequently, FCs were further investigated, whereby the seven popular types of FCs identified and classified were summarily compared with each other, from which the PEM FC was preferred due to its practical popularity. However, PEM FCs, like all FCs, are susceptible to the fuel-starvation phenomenon; therefore, six FC-assisted schemes were examined, from which the FC assisted with the supercapacitor and battery technique was the most widely applied. In sum, the significance of the study entails assorted CCHP systems, FCs, their highlights, their applications and their pros and cons in a single reference document that anyone can easily use to holistically understand the characteristics of the CCHP systems. The study concludes with our perspective, by which we formulate and propose an alternative innovative unique CCHP system model under research, which is based exclusively on green technologies: FCs, lithium-ion battery, ultracapacitor, thermoelectricity and an energy-management system using MATLAB®.

Graphical Abstract

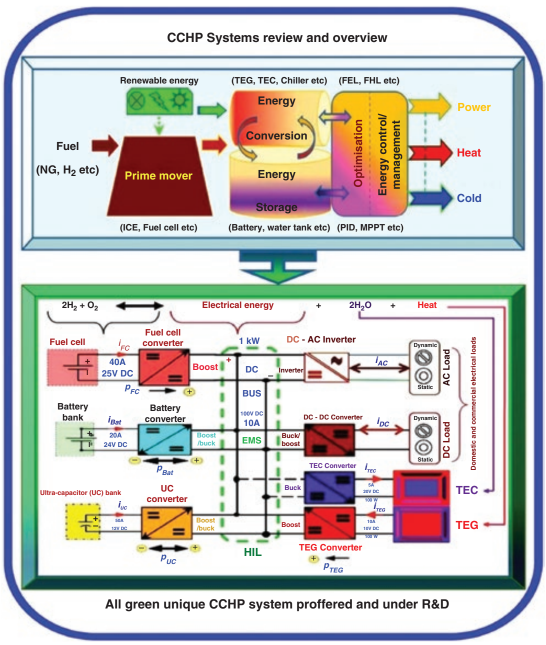

Keywords: CHP/CCHP systems; fuel cells; full cells fuel starvation; hybrid power and renewable energy

Received: 29 August 2022. **Accepted:** 28 November 2022

Introduction

The national electricity grid in most developing countries is perpetually unstable [1], resulting in huge adverse effects on the economy of these countries and on the livelihood of their citizens, as electricity is now very important for daily activities of many people. Furthermore, with ongoing conflicts around the world, it is now paramount for countries, corporations and individuals to diversify and control their energy supplies without relying on a single energy supplier or source. As a result, a variety of potential alternative energy/power initiatives are being exploited and developed around the world to address the raging energy/power crises. To this effect, this article topologically articulates in detail various research studies on combined cooling, heating and power (CCHP) systems, as well as fuel cells (FCs). Unlike the reviewed CCHP studies (summarized below in Table 1) that focused on parametric analyses, this review paper uses a case-study approach from an application perspective. This is to expose/establish inventions and innovations that can be developed and deployed for the implementation of energy-efficient hybrid power systems for purposefully residential and commercial CCHP applications. As indicated in [2–66], CCHP, also known as trigeneration, is a parallel-combined heating and power (CHP) energy system (cogeneration) with extra cooling. As per Fig. 1, it concisely comprises a prime mover, energy conversion and storage, and management processes, which can efficiently produce power, heat and cold when fuelled, allowing it to provide direct stand-alone energy utility to homes and businesses. According to [2, 3, 29], CCHP systems, especially those based on FCs, are becoming trendy as a result of their energy-saving, environmentally friendly, cost-saving and flexible features. However, FCs are prone to intrinsic FC fuel starvation—which is further investigated in this study. Presented next is the review of CCHP systems, followed by FCs with a focus on various types of FCs and the FC fuel-starvation phenomenon, as well as mitigation methods, followed by our proposed CCHP system model that is undergoing research and finally closing remarks are drawn to conclude the study.

1 CCHP systems

CCHP systems produce heat and power simultaneously in the same process, with cooling later obtained from the generated power and/or from the heat, depending on the type of hybrid implementation. With a properly designed CCHP system, total energy efficiency could exceed 90%. Typically, CCHP prime movers vary and comprise various energy sources and conversion techniques and, from the literature analysis and as stated in [4, 5], a specific CCHP system name will usually be derived from its prime mover or power generation unit (PGU). As mentioned in [2], a CCHP system is designed to (i) follow the electrical load, (ii) follow the thermal load and (iii) follow the electrical thermal load, with following the electrical load being the most popular. However, more advanced schemes are being used, as CCHP systems are traditionally based not only on the hardware aspects, but also now on the software aspects. Furthermore, a CCHP system should be designed and deployed with four main objectives, which are to maximize the (i) energy, (ii) exergy, (iii) environmental benefits and (iv) economic benefits. Miscellaneous CCHP studies were examined and in what follows are 50 studies which show that the building blocks are not only physical and consist of diverse types of PGUs, energy-conversion and storage mechanisms, but also different types of optimization/control strategies.

1.1 CCHP system

As studied in [4], internal combustion engines (ICEs) infuse fuel and air into cylinders where combustion occurs, causing the fuel and air mixture to produce useful work. This process occurs in cycles, making it difficult to complete the burning of the fuel, leading to noise and pollution. Contrary to modern ICE CCHP systems, the earlier ones were based on automotive engines transformed to work with natural gas; as a result, they were unreliable and required very high maintenance. In [2], an ICE CCHP system consisting of four different cooling mechanisms under following the electric load (FEL) and following the thermal load (FTL) was researched and its performance and optimization techniques were compared in terms of its energy, economy and environmental benefits. It was found that FEL performed best in terms of energy, economy and environment, and the ground source heat pump (GSHP) with the absorption chiller cooling mechanism shown in Fig. 2 performed best out of the four versions. According to [5], ICEs have matured with relatively low cost, high efficiency and rapid start-up time, and can be powered by natural gas and petrol (gasoline) fuels.

1.2 ICE or Stirling-engine CCHP system

As researched in [4], the most popular micro CCHP systems are external combustion engines (ECEs), as they are mainly suitable for static or continuous active use. A typical example is a Stirling engine, which employs s simple ambient pressure combustor, equivalent to a hot-water heater or furnace, to generate a continuous heat source that is passed to a gas that enlarges to move a piston to do work. After the gas completes the work, it passes through a regenerator (a heat exchanger) where any residual usable heat left is brought back to preheat the inflowing gas, which is then recycled and re-used to always remain in the engine, making ECEs more efficient and environmentally friendly compared to ICEs. Furthermore, the efficiency of micro CCHP systems depends on the efficiency of each individual component and also on the cogeneration coefficient of performance of the whole system. In addition, the cogeneration index of the micro CCHP system with the Stirling engine is close to that of the micro CCHP system with FCs, which further motivates why CCHP systems with absorption chillers are better than CCHP systems with compression types. Fig. 3 shows a micro CCHP system based on a Stirling engine.

1.3 Biomass CCHP system

As stated in [31], biomass incineration-based CCHP systems have already established their worth in some functional settings. However, their energy and ecological performances may also be poorer relative to traditional stand-alone power-production systems. To make provisions for procedures concerning their environmental viability, a life-cycle assessment (LCA) workflow was employed to assess biomass CCHP systems and the model result was compared to that of a developed primary energy-saving ratio (PESR) analysis. A thermodynamic model that took into account the incorporation of various dimensions of cooling and cogeneration units was advanced to suitably characterize the life cycle inventory stage. The LCA findings disclosed that CCHP plants based on biomass combustion are environmentally friendly if the plant cooling-to-heating ratio is small but not when large. The PESR findings revealed that LCA alone was not sufficient to evaluate the static performance of such plants, because it could instead reduce the practicability of the plant when

Table 1: Summary of reviewed CCHP system case studies

CCHP research reviewed	Highlights	Advantages	Disadvantages
Case Study 2.1 [5] (Bozchalui MC, Sharma R, 2012)	ICEs CCHP system	Has advanced with comparatively fast start-up time, high efficiency and affordability. Fuels can be natural gas or petrol (gasoline)	Noisy, noxious and requires high maintenance
Case Study 2.2 [4] (Badea N, *et al.*, 2010)	Stirling-engine CCHP system. Works by reusing the fuel (gas) back and forth	Green and relatively more efficient. Inclusion of renewable energy increased efficiency	Suitable mostly for motionless or non-stop working applications
Case Study 2.3 [31] (Maraver D, *et al.*, 2013)	Biomass CCHP system	A thermodynamic model that takes into account various CHP sizes/cooling units	Needs lots of space to implement
Case Study 2.4 [7] (Xu AD, *et al.*, 2014)	Micro-turbine CCHP system. By means of pressure, air is pumped to the cold side to combine with heat for cold production	Low emissions, compact, uses various fuels	Needs high temperature to produce more power. Low fuel-to-electricity efficiency
Case Study 2.5 [25] (SU Z, *et al.*, 2016)	Biomass and solar CCHP system	Using a genetic algorithm to realize a model to acquire an optimum operation technique, considering energetic criteria, the environment and economics	It significantly requires sunlight to work well
Case Study 2.6 [27] (Wongvisanupong K, Hoonchareon N, 2013)	Gas-turbine and PV CCHP. Simulated online economic functionality	Optimum execution having the smallest cost and modelled as a LP problem using MATLAB®	Requires sunlight to function well. Low efficiency without cogeneration
Case Study 2.7 [26] (Zhao H, *et al.*, 2018)	Micro-turbine, PV and wind-turbine CCHP system	HOMER® was used to model an optimum economic operation model of a microgrid having net current cost as optimization purpose. It has reasonable energy-saving and contamination effects	High revolution per minute works only well when there is sunlight and wind
Case Study 2.8 [8] (Wang R, *et al.*, 2018)	PAFC and SOFC CCHP system. Thermal, electrolysis and technical economies as well as factors that protect the environment were investigated	SOFC has high CHP efficiency. No catalyst was needed because of the high temperature. PAFC is stable and CO-tolerant even at 200°C. Low vapour pressure	SOFC needs high temperature that relatively slows down the start-up time. PAFC produces less power relative to other FCs of the same size and weight
Case Study 2.10 [18] (Cozzolino R, 2018)	LT-PEM FC CCHP system	Their research results revealed better execution based on exergy and energy in the overall functional field of the CCHP (trigeneration) scheme	LT PEMFC requires expensive Pt catalyst
Case Study 2.11 [9] (Wang Z, *et al.*, 2018)	IAT gas-turbine CCHP system	Their findings showed that their CCHP scheme is better than the discrete scheme in yearly review, regardless of the working system used	Requires high temperature
Case Study 2.12 [16] (Lu S, *et al.*, 2018)	PV CCHP and GSHP micro gas turbine	An optimization of the regional multi-energy energy-supply system was performed	However, it is very expensive to install
Case Study 2.13 [15] (Li B, *et al.*, 2019)	GSHP and ICE CCHP. The hybrid scheme execution with a heat exchanger was superior to the same system without a heat exchanger	The heat exchanger enhanced the system	It is not environmentally friendly—high temperature, noisy and large
Case Study 2.14 [14] (Jiang R, *et al.*, 2017)	ICE with cooling and dehumidification CCHP system	A thermo-economic model was instituted and a constrained NLP resolve was employed to maximize the system blueprint and functioning strategy	Poor economy and sizable CO_2 emissions
Case Study 2.15 [12] (Chen X, *et al.*, 2018)	A 5-kW PEM FC CCHP system. It was optimized using an evolution algorithm	The intake gases and small working temperature are paramount for improving the system competence, exergy and emission	Requires high pressure and relative humidity to be efficient. Bulky system
Case Study 2.16 [19] (Ebrahimi M, Derakhshan E, 2018)	LT-PEM FC with TEC hybrid CCHP system	Proficient in producing 26.8 W of cold, 3.04 kW of heat and 2.79 kW of power with an overall efficiency of ~77% and 43.25% of fuel savings. Portable, low temperature and thus longer durability	Water-management issues. Costly catalyst because of the low temperature. Low cooling
Case Study 2.17 [17] (Mehrpooya M, *et al.*, 2017)	Stirling-engine and MCFC CCHP system. MCFC is the primary source of power and its exhaust heat was used to provide the Stirling engine, from which it delivers heat to the cold generator, the absorber chiller	The combined cold, heat and power that were generated were respectively 1372, 2137 and 6482 kW. No catalyst was needed because of the high temperature	Usually, very high temperature is involved. However, in order to be less durable, the high temperature and corrosiveness of the electrolyte reduce the cell life span

Table 1. Continued

CCHP research reviewed	Highlights / Advantages / Disadvantages	CCHP research reviewed	Highlights / Advantages / Disadvantages
Case Study 2.9 [11] (Wang JL, *et al.*, 2014)	ICE and TEG CCHP system. ICE used to produce power, cold and heat, which is stored in hot water The heat exchanger and TEG were used to effectively recover heat emitted by ICE exhaust gas It is power-efficient because of the incorporation of TEGs, but may have environmental issues because of the usage of ICE		
Case Study 2.18 [34] (Wu D, *et al.*, 2019)	CCHP–ST–ORC system harmonizes fossil fuel with renewable energy. Performance was assessed based on thermodynamics. CCHP–ST and CCHP systems are also evaluated CCHP–ST–ORC system could produce 5.1 kW more power. Has an energy ratio of 22.6% more than CCHP system. Uses 12.4% less energy than CCHP–ST system CCHP–ST–ORC has similar exergy efficiency of 40% compared to the traditional CCHP and CCHP–ST systems	Case Study 2.27 [43] (Lingmin C, *et al.*, 2021)	A wind, solar and natural-gas CCHP system for a remote tourist area with energy hub for electric power and heat with cold supplied by the chillers Heat- and power-storage devices assist the PGU during power outages to supply the bulk of the power to reduce waste and also enhance the system performance Reliance on the PGU to supply most of the power during wind and solar outages. Complex system to install and control
Case Study 2.19 [35] (Mao Y, *et al.*, 2020)	CCHP is a promising technology to provide cascaded efficient energy System performance can be enhanced by integrating PV/thermal panels as well as energy storage. Their system has better cost and primary energy savings of ~17% Enhanced performance relies on sunlight to provide usable light and heat energy	Case Study 2.28 [44] (Lombardo W, *et al.*, 2020)	CCHP system based on micro-ORC plant, PV and adsorption chiller with built-in real bioclimatic NZEB modelled using TRNSYS® Annual efficiency of the system ranged from 32% to 42%. The system is suitable for use in home ventilation. With incentives, the return on investment of the system is estimated to be ~6 years The effectiveness is affected by solar irradiance, location and weather conditions
Case Study 2.20 [36] (Lingmin C, *et al.*, 2020)	CCHP multi-energy system incorporating gas, solar and wind energy, as well as power storage controlled by PSO method FEL-generated power can reach >50% during peak load periods Bulky and requires sunshine and wind	Case Study 2.29 [45] (Wu D, *et al.*, 2021)	Theoretical model of the integrated multiscenario CCHP system. A novel self-adaption technique based on exhaustive search Reduced yearly cost by 0.67%. IES is economical for a large energy-supply area Not suitable for small/isolated scenarios
Case Study 2.21 [37] (Cao Y, *et al.*, 2020)	CCHP system based on a developed owl search technique Waste heat from hot gases is recycled while at the same time producing power, enabling >85% system energy efficiency The improved overall yearly cost saving, however, reduced the system capacity	Case Study 2.30 [46] (Ma H, *et al.*, 2020)	CCHP–ORC system. Used TRNSYS® to develop a simulation model Stabilize irregular power/heat demands. Enhance the versatility/changeability of the heat-to-power ratio on the source side Low heating and cooling in the transitional season, releasing a lot of wasted heat
Case Study 2.22 [38] (Farmani F, *et al.*, 2018)	A smart EMS concept of a microgrid CCHP system for buildings, to control the schedules of the energy-storage and renewable-energy systems The CCHP system fitted with a smart controller could significantly lower a building's energy operating cost The application is based on data collected by smart meters	Case Study 2.31 [47] (Miao N, *et al.*, 2020)	Cascaded CCHP systems. Analysis is required and two operating modes, namely 'fixing power based on heat' and 'fixing heat based on power', were evaluated Fixing heat based on power is the better operating mode (in their case) and had a lower yearly cost. Reduced emission Their provisions are challenging for optimal set-up
Case Study 2.23 [39] (Zare V, Takleh HR, 2020)	A geothermal CCHP system with the ejector TRCC fitted with a traditional Rankine cycle Replacement of the gas cooler resulted in 30.9% exergy efficiency, 49.1% net power output and 75.8% cooling output Replacing the gas cooler also resulted in a 39.1% loss in the heating output	Case Study 2.32 [48] (Ji J, *et al.*, 2020)	A novel CCHP system with an integrated hybrid energy-storage system and ORC was developed with the aim of evaluating its performance In one of the case studies, the efficiency ranged from 35.70% and 42.70%, with the efficiency improvement of >40% relative to traditional CCHP systems ORC uses a combustible fluid that can pose an environmental hazard if leaked
Case Study 2.24 [40] (Mohammadi K, Powell K, 2020)	New configurations of integrated cogeneration and trigeneration systems using a CO_2 parallel compression economization–vapour compression refrigeration cycle with 1-MW capacity The main contribution is an in-depth techno-economic assessment of the numerous possible variations for such systems Very bulky system	Case Study 2.33 [49] (Jia J, *et al.*, 2021)	A CCHP–ORC–ST system was studied and had better thermodynamic performance it is versatile with greater power-production capability, more energy and more waste-heat efficiency Compared to conventional CCHP systems, the annual cost savings raised were 15.0% in commercial buildings and 27.0% in office buildings The ORC efficiency is ~10% on average

Table 1. Continued

CCHP research reviewed	Highlights	CCHP research reviewed	Highlights
	Advantages		**Advantages**
	Disadvantages		**Disadvantages**
Case Study 2.25 [41] (Chahartaghi M, Sheykhi M, 2019)	Dual Stirling-engine CCHP system with H_2 and helium as functioning gases	Case Study 2.34 [50] (Li J, *et al.*, 2021)	Evaluation of traditional CCHP systems based on fossil fuels and modern types based on IES with renewable energy
	The power, cold, heat productions, CCHP efficiency and CoP results using helium were, respectively, 15.24 kW, 19.65 kW, 12.65 kW, 70% and 64.4%, and using hydrogen were 22.52 kW, 21.65 kW, 14.43 kW, 72.29% and 66.7%. H_2 offered better results		The IES approach is paramount for co-ordinating and maximizing the different energy flows in both an independent and isolated CCHP system set-up. Uncertainty modelling methods were evaluated to ensure the accuracy of the methods and to decrease adverse circumstances on the upper grid
	Very bulky system. Requires external heat. Slow start. High economic cost		Unlike fossil fuels, renewable energy, though clean, is unstable due to outages
Case Study 2.26 [42] (Parikhani T, *et al.*, 2020)	A new ammonia–water mixture CCHP system driven by a LTHS which is a customized version of a Kalina cycle. Thermodynamics and thermo-economic balance equations for the performance analysis of the thermal system were used to investigate the viability of the proposed system		
	The energy and exergy efficiencies were respectively found to be 49.83% and 27.68%. The optimum electrical, cooling and heating capacities were also, respectively, 0.253, 1.610 and 1.972 MW		
	Greater energy efficiency requires increasing the evaporation temperature and basic ammonia concentration		
Case Study 2.35 [51] (Qian J, *et al.*, 2021)	A wind–solar CCHP. A MODM method rooted in Fuzzy-AHP, anti-entropy and game theory is proposed to compute the index weight. A Kendall rank correlation coefficient established the correlation between the CCHP and wind–solar CCHP systems, and with the CCHP system as a reference, the FCE method was used to assess the integrated performance of the system	Case Study 2.43 [59] (Yang X, *et al.*, 2022)	The PV CCHP hybrid system has many parts, making it prone to failure at any time during operation. Their work compared/analysed with a focus on 3E, the performance of three PV CCHP systems—SPV CCHP, MPV CCHP and RPV CCHP. A two-stage optimization technique was employed and the three systems were tested. RPV CCHP is best
	Comprehensive performance and superior to other CCHP systems due to many optimization techniques		The RPV CCHP performance was 16.20% and 13.99% better than the MPV CCHP and SPV CCHP systems, respectively
	Defective indexing. Prone to outages when there are no wind and no sunshine		Costly and bulky due to redundancy
Case Study 2.36 [52] (Zhao H, *et al.*, 2022)	A CCHP–microgrid system focused on 3E. The MCDM framework was designed using two modular steps: (i) integrated AEW and grey-DEMATEL and (ii) ranking the assessed cases using an improved TOPSIS with DQGRA	Case Study 2.44 [60] (Wang M, *et al.*, 2022)	Efficient transcritical CO_2 CCHP system. Their findings revealed that, by introducing the ejector, the ER CCHP system can yield more net output power than the TR CCHP system
	Their MCDM scheme compared to four MCDM models had good potency and relevance for the 3E performance of the CCHP–MG system. Gains in system energy supply, savings, utilization and equivalent emission reduction		Their results showed that at 230°C and 20 MPa, the TR CCHP and ER CCHP systems could respectively produce optimal exergy efficiencies of 26.9% and 27.9%, and maximum net output powers of 7.5375 and 7.9103 MW
	The module needs modification to be used with other MCDM		CO_2 has a high critical pressure (7.37 MPa) and a low critical temperature of 31.1°C
Case Study 2.37 [53] (Xu J, *et al.*, 2021)	A thermo-acoustic CCHP system for LNG cold-energy/waste-heat recovery. Their research novelty is based on acoustically matching the alternator and thermo-acoustic unit impedance for total maximum exergy efficiency by varying the alternator's external electric impedance	Case Study 2.45 [61] (Deng Y, *et al.*, 2022)	A CCHP–GSHP-SF–SE with SF = 0.4 is better than CCHP–GSHP–SE and CCHP–SE systems. In terms of comprehensive performance, the CCHP–GSHP–SE and CCHP–GSHP-SF–SE systems, respectively, reached 3.05% and 10.92% relative to the CCHP–SE system
	Their results showed that their CCHP system can function effectively for various energy/power-supply modalities		CCHP–GSHP-SF–SE produced energy, economy and CO_2 savings of 5.25%, 0.68% and 4.58%, respectively
	LNG has issues with greenhouse gas emissions (GHG) emissions. LNG has a very low temperature, which requires special materials to store. Dangers of leaks		GSHP has a relatively high instillation cost. Less efficiency on sandy soil. Bulky and can be tricky to retrofit in small spaces
Case Study 2.38 [54] (Li Y, *et al.*, 2021)	ICCHP system whereby an interactive operation strategy is based on the energy-augmentation characteristics of FEL, FTL and FHL	Case Study 2.46 [62] (Xu Y, *et al.*, 2022)	A SOFC CCHP system with a LiBr absorption chiller and water tank. Focused mainly on the 4E evaluation criteria: energy, environmental, exergy, economy, and 4E benefits of a CCHP system
	Their findings showed that CCHP systems with different loads can use energy augmentation of operation means to enhance the ICCHP system		Examined the effects of the working conditions of the FC stack and the absorption chillers in 4E. Increasing the temperature increased the generated electricity
	However, CCHP systems with the same loads can only rely on energy augmentation of the operation strategies, leading to lower performance		The system involves a very high temperature. Increasing the temperature also decreased the generated thermal power. Absorption chillers are bulky

Table 1. Continued

CCHP research reviewed	Highlights / Advantages / Disadvantages	CCHP research reviewed	Highlights / Advantages / Disadvantages
Case Study 2.39 [55] (Kang L, *et al.*, 2022)	Their work analysed the mismatched/delay of thermal energy using principal component and correlation analyses	Case Study 2.47 [63] (Nondy J, Gogoi T, 2022)	Two 4E-based CCHP systems with the same recuperative gas-turbine topping cycle but different bottoming cycles to give Systems I and II were researched and compared
	Their results show that the linear regression correlation coefficient between the measured and predicted heating load is 90.97% and the mean absolute percentage error is 6.84% for cooling and 5.43% for heating loads		The PESA-II and TOPSIS techniques were used to obtain optimal results. System I with a bottoming cycle with recuperative–regenerative ORC, steam turbine and two absorption cooling systems was better than System II
	GSHPs are bulky and costly to install		Steam turbines generally take a long time to start. Gas turbines are bulky and more complex
Case Study 2.40 [56] (Yan R, *et al.*, 2022)	Hybrid renewable-energy system. Their study novelty lies in the integration of stochastic and robust optimization into a two-stage stochastic–robust capacity-optimization model to adequately address the multi-uncertainties and to robustly obtain optimal results	Case Study 2.48 [64] (Lu Z, *et al.*, 2022)	CCHP–ISCC–double-effect absorption lithium bromide refrigeration (DEALBR) system. Thermal and solar energy influence performance analysis conducted. The results showed that their CCHP system can generate 494.1 MW of electricity, 7.55709 MW of cold with 1.09 CoP and 57.95625 MW of heat
	Their findings revealed that the appropriate scenario number can allow scenario-based stochastic optimization to save 97.71% of the calculation time and protect the reliability of the optimized results		Their CCHP system has better ability to perform work and with lower CO_2 emissions, as well as simultaneously meeting the demands of users for electricity, heating and cooling loads
	However, the uncertain budget value greatly affected the installed capacity of the successive device, while it hardly impacted the discrete device numbers		MCFC-generated power requires a higher temperature and H_2-utilization rate. The high temperature reduces the durability of the system
Case Study 2.41 [57] (Fu C, *et al.*, 2022)	Developed an improved-FEL (IFEL) and an improved-FTL (IFTL) strategies, to adequately control the flow of energy	Case Study 2.49 [65] (Salimi M, *et al.*, 2022)	Examined green features of various CCHP systems when used in different sectors
	Demonstrated that the Pareto solutions acquired using the proffered IMOMVO algorithm were distributed evenly and can give a set of representative solutions. The IFEL strategy gave the best all-round results		Key drivers to reduce carbon and water footprints are enhancing the system parts such as the combustion engine and extending the system to multigeneration systems and incrementing productivity of the product with smallest carbon footprint
	Complex algorithms and operation strategies		Multifunctional CCHP system is complex and costly
Case Study 2.42 [58] (Yang L, *et al.*, 2022)	Geothermal energy CCHP system. A water heater is used to utilize the exhaust geothermal water for heating, whereas the throttled valve of the basic flash cycle was replaced by an ejector for cooling output	Case Study 2.50 [66] (Ren F, *et al.*, 2022)	Reviewed a broad analysis of assorted CCHP systems integration as well as optimization technologies and techniques. The application scenarios at the building, neighbourhood, district and city levels were examined and their concerns were noted
	Detailed mathematical models were instituted and validated to assess the performance of the CCHP system. Showed various factors affecting exergy		Optimal equipment capacity, network layout and functioning methods are used to manage/improve the total performances of distributed energy systems
	The increase in the temperature of the water heater affects the system exergy of the system. Geothermal energy is location-limited, costly, bulky and not sustainable		Distributed systems research difficulties can be summarily classified into five groups—green sources, efficient conversion, good network, load predictions and planning

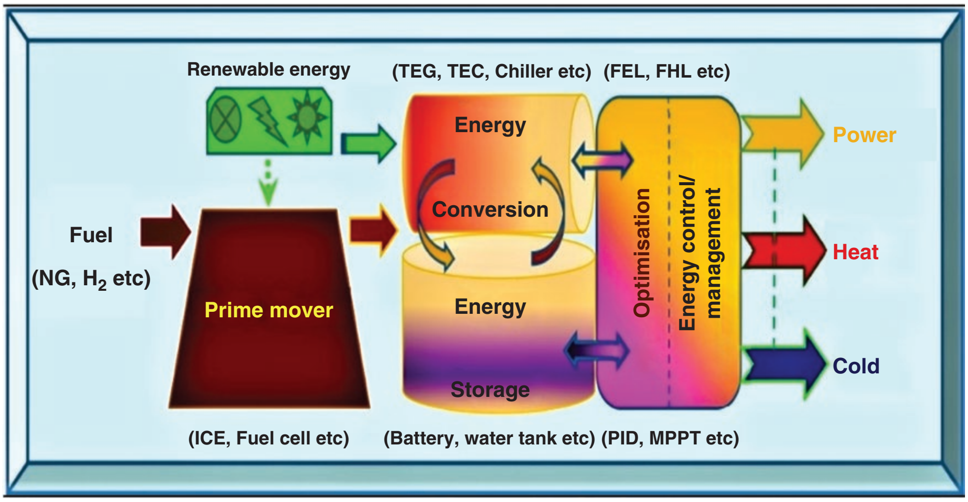

Fig. 1: Overview of the CCHP system.

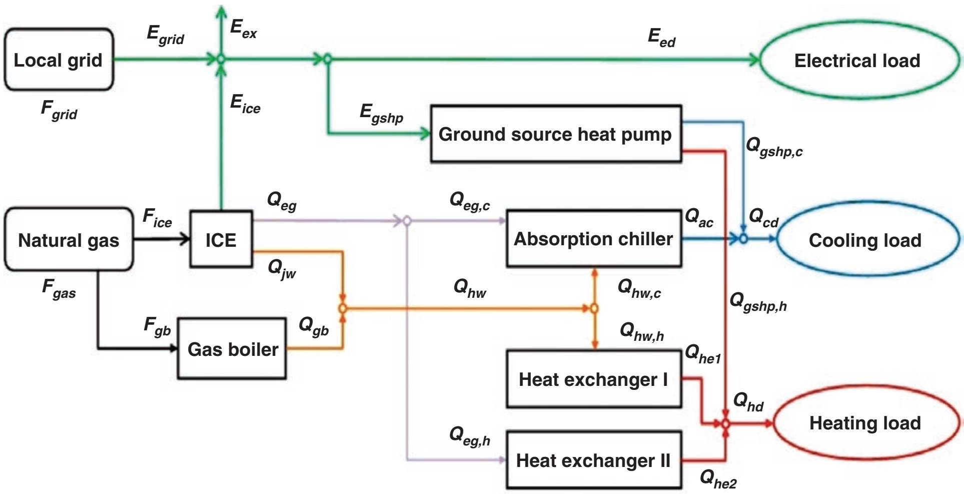

Fig. 2: Natural-gas (fossil-fuel) ICE CCHP system. Reprinted from [2] with permission from Elsevier.

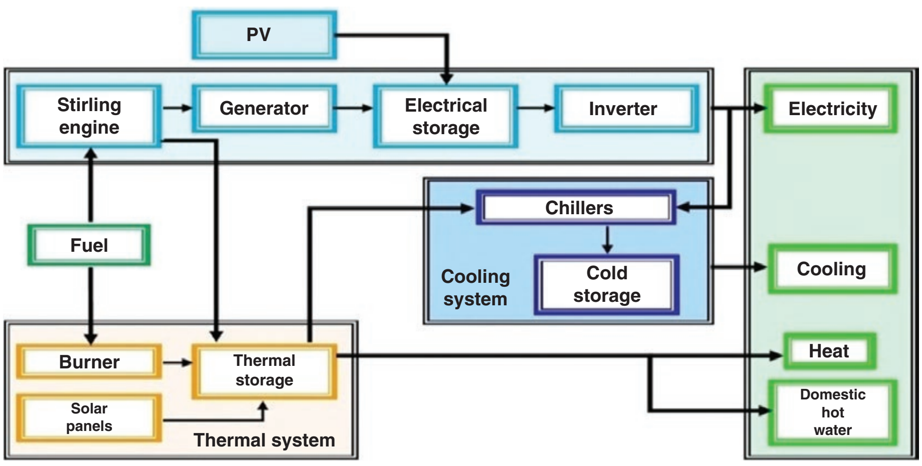

Fig. 3: Stirling-engine CCHP system. Redrawn from [4] with permission from IEEE.

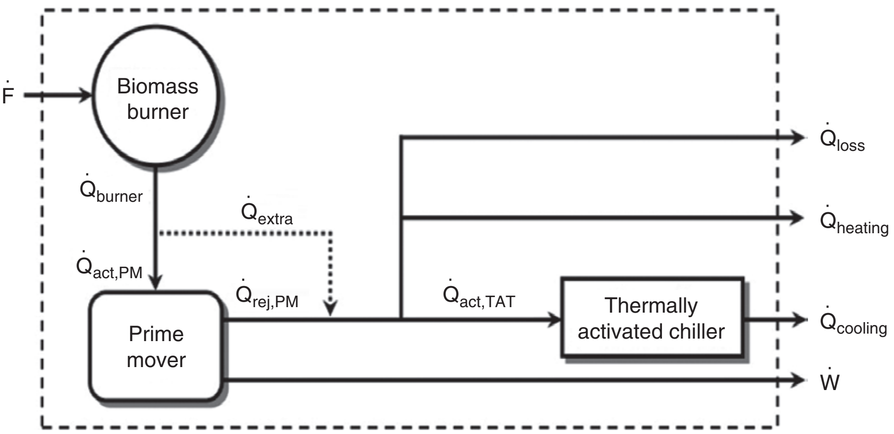

Fig. 4: Biomass CCHP system. Reprinted from [31] with permission from Elsevier.

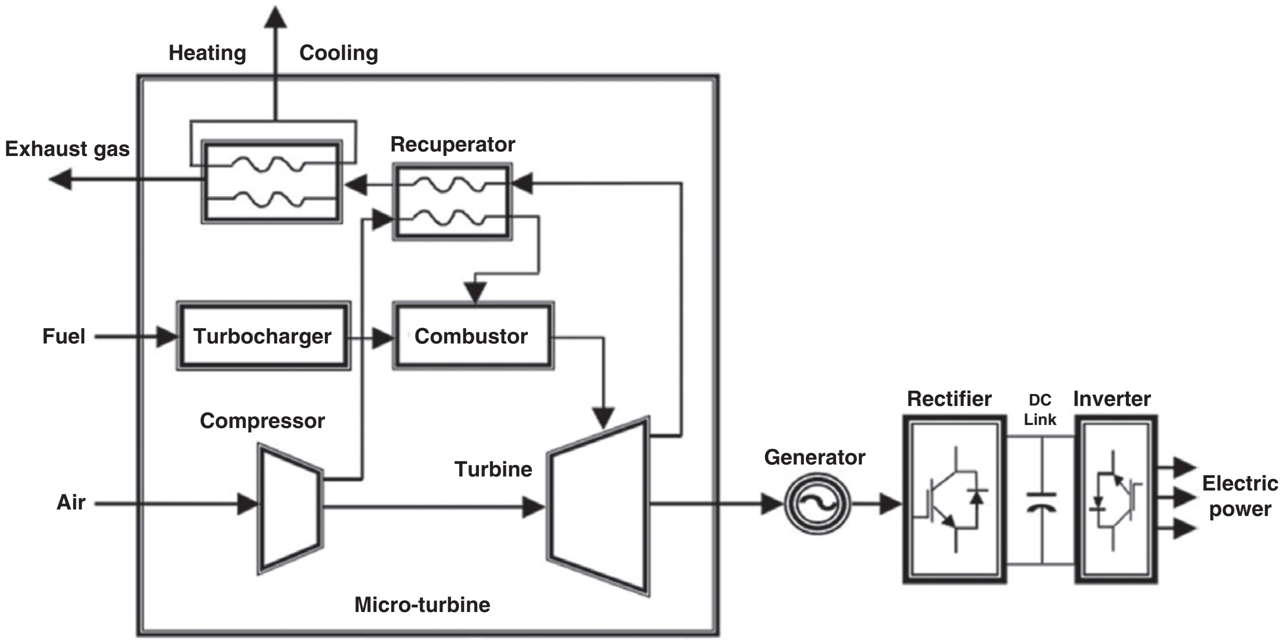

Fig. 5: Micro-turbine CCHP system. Redrawn from [7] with permission from IEEE.

environmentally friendly benefits could have been achievable. Fig. 4 shows their biomass CCHP system.

1.4 Micro-turbine CCHP system

Similarly to a usual gas turbine and according to [7, 23], in the micro-turbine CCHP system, air is initially drawn into the compressor, where it is pressurized and pumped to the cold side of the recuperator to effectively combine with exhaust heat to generate cold with the absorption refrigerating machine, as presented in Fig. 5. The presented CCHP system used spot pricing, unlike peak-valley pricing, to sell surplus electricity to the grid when the grid electricity price was high; however, when the grid electricity price was low, the CCHP system had no real economic benefits. When switching between different operating modes using spot pricing, the operating cost of the system could be reduced. Therefore, the conclusion drawn was that CCHP systems when compared to decentralized systems were more economical, especially when CCHP and the decentralized systems had a large load difference. In addition, the electricity pricing system was very vital to optimizing the operations of the electrical network.

1.5 Solar and biogas CCHP system

In [25], a photovoltaic (PV) and biomass CCHP system was proposed, consisting of a smaller biogas PGU, solar cell, auxiliary boiler, absorption chiller, solar-thermal collector (STC), etc., as shown in Fig. 6. Their model was implemented using a genetic algorithm to obtain an optimal functional approach considering economic, environmental and energetic criteria, and the result was compared with a separation production (SP) system. The SP was operated by prioritizing the electric load satisfied by the power grid, the heating load satisfied by the biogas boiler and the cooling load was satisfied by the electric chiller powered by the grid. In their proposed scheme, the PV cell and STC converted solar energy into electricity and hot water, respectively, thus minimizing fossil-fuel usage and pollution. The electricity generated could be used to meet the user's power demand and excess power could also be sold to the power grid and during peak periods, thus improving energy consumption and cost. Their findings revealed that the proposed optimal operation strategy had paramount effects in minimizing the running cost, pollutant emission and the primary energy usage—relative to the FEL and FTL operation modes.

1.6 PV and gas-turbine CCHP system

As per [27], a proposal was presented for an online economic optimal functioning PV and CCHP system. Linear programming (LP) was used to formulate and model the system using MATLAB®. The simulation results showed that a hybrid CCHP and PV system with optimum projected operation obtained the lowest cost of operations. Fig. 7 shows the proposed CCHP system. The CCHP system mainly produced power and heat to the electrical and thermal loads, respectively, whereas the PV system and electrical grids compensated for power shortfalls. The additional heat produced at the same time by the CCHP system could be recovered and stored in the heat-storage tank, as well as supplied to the absorption chiller, which converted it into cold energy. The auxiliary boiler produced heat to compensate for any heat shortage and to supply the absorption chiller, after which excess could also be stored in the heat-storage tank. Their simulation results concluded that the online model had the potential to determine real-time operating points of each component in the energy-management system, as it could minimize the total cost to ~17%.

1.7 Wind-turbine, PV and micro-turbine CCHP system

In [26], a combination of wind and PV energy was used together with a gas micro turbine to generate power and supply heat and cold as per Fig. 8. In their set-up, the electrical load was connected to a central bus supplied by the grid, PV, wind turbine, micro turbine and battery, whereas the thermal load was supplied by the boiler, which was driven by the micro turbine, and finally the cooling load was furnished by the refrigerator, which was driven by the boiler. They claimed that it saved energy better and without pollution effects, which was validated by comparing the optimum strategy under the condition that only the grid supplies the load. HOMER software was used to model an optimum economic functioning framework of a microgrid with the objective of the optimization of net present

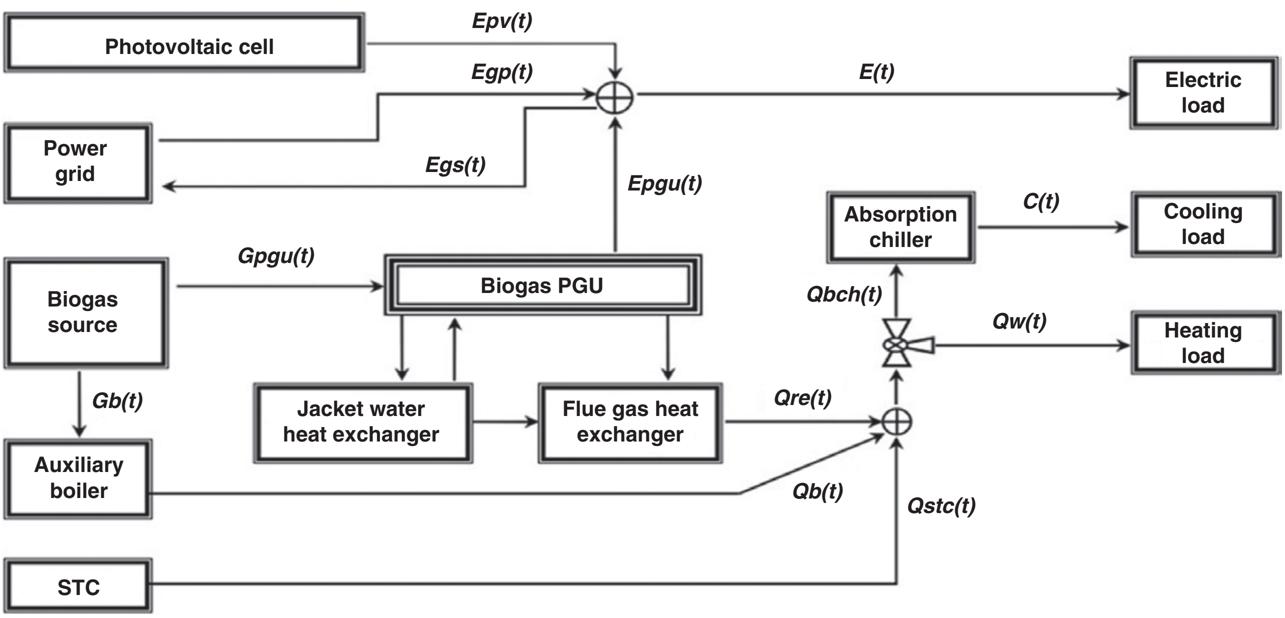

Fig. 6: Biomass and solar CCHP system. Redrawn from [25] with permission from IEEE.

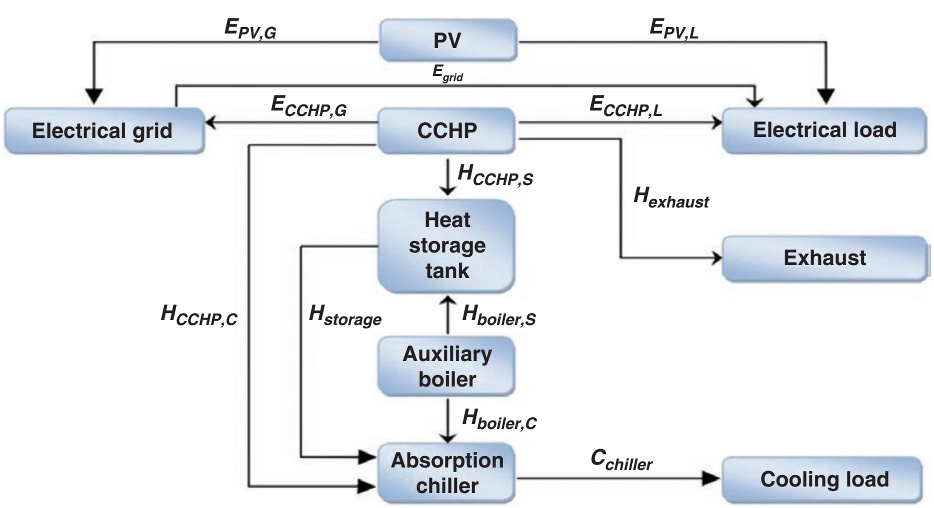

Fig. 7: Gas-turbine and PV CCHP system. Redrawn from [27] with permission from IEEE.

cost. Their findings revealed that the higher the microgas turbine waste-heat utilization efficiency, the less electricity was purchased from the grid (higher energy savings) and the less CO_2 was emitted (more environmentally friendly).

1.8 Solid-oxide FC and phosphoric-acid FC CCHP system

According to [8], there are several ongoing investigations on FC-based CCHP systems, although not much on electrolysis, i.e. hydrogen production from water using electricity, on which their paper was based. Their evaluation system included a phosphoric-acid FC (PAFC) and a solid-oxide FC (SOFC), thermal and technical economies, including environmental protection factors. Fig. 9 exemplifies their CCHP system. It consisted of four subsystems, namely (i) hydrogen production, (ii) power supply, (iii) heating and (iv) cooling. The operation of their CCHP system was such that the hydrogen produced by electrolysis by the power grid was stored in a high-pressure hydrogen-storage tank, which was used as fuel for the FC stacks to generate electricity, which fed an inverter to supply the power grid to meet the building electrical load. The heat generated by the FC stack passed through the heat exchanger and was transferred to cold water, making it hot, and the hot water was then stored in a high-temperature water tank that was used to heat the building during winter. During the summer period, heat was passed through a lithium bromide absorption chiller unit to produce cold to cool the building. In addition, there was an auxiliary electric-heating network to heat the water if necessary. In summary, the economy of the SOFC-based CCHP system is better than that of the PAFC-based CCHP system. Furthermore, reducing the cost of H_2 production, acquiring affordable H_2 and minimizing the cost of FC materials are key to the commercial development of H_2 FCs in the future.

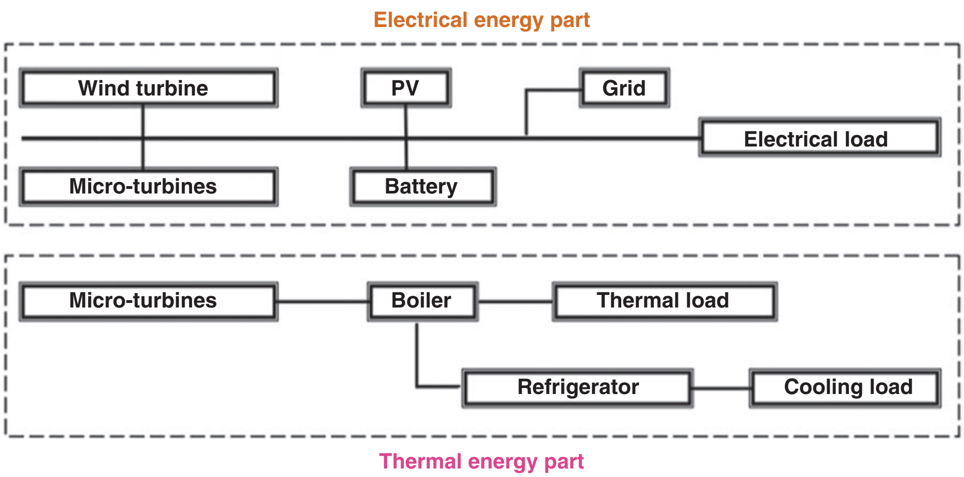

Fig. 8: Wind-turbine, PV and micro-turbine CCHP system. Redrawn from [26] with permission from IEEE.

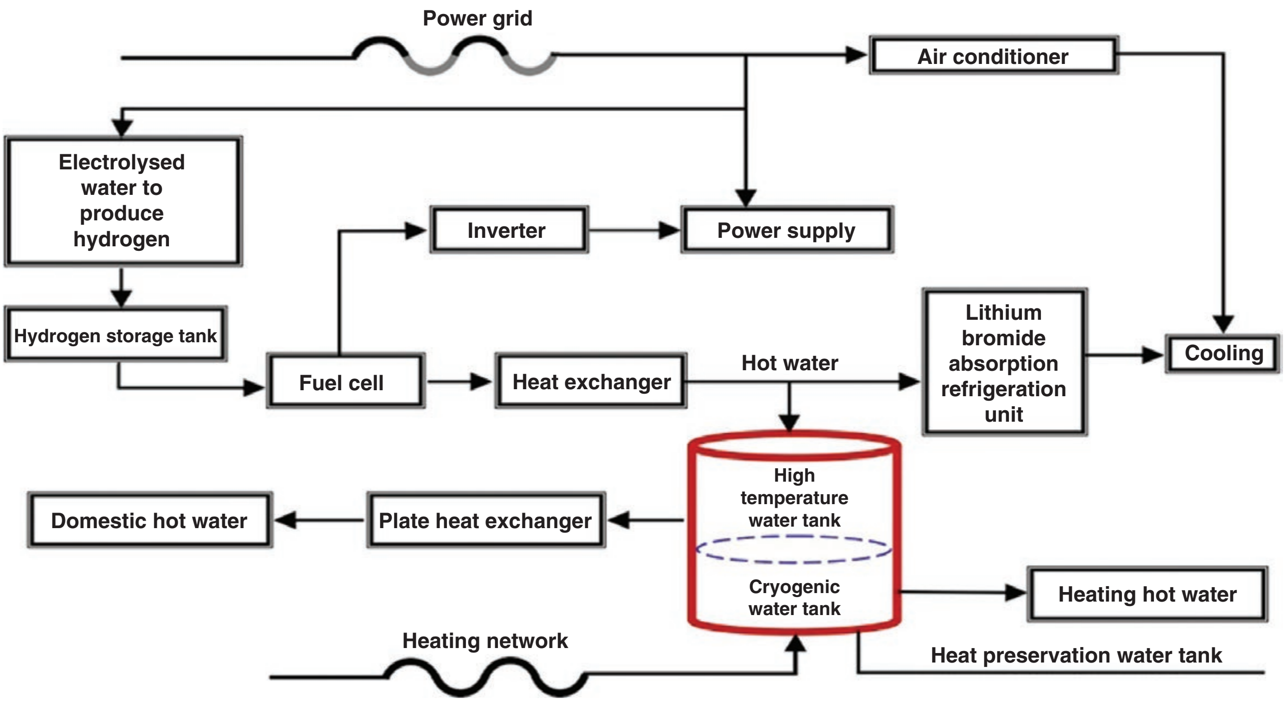

Fig. 9: Hydrogen FC CCHP system. Redrawn from [8] with permission from IEEE.

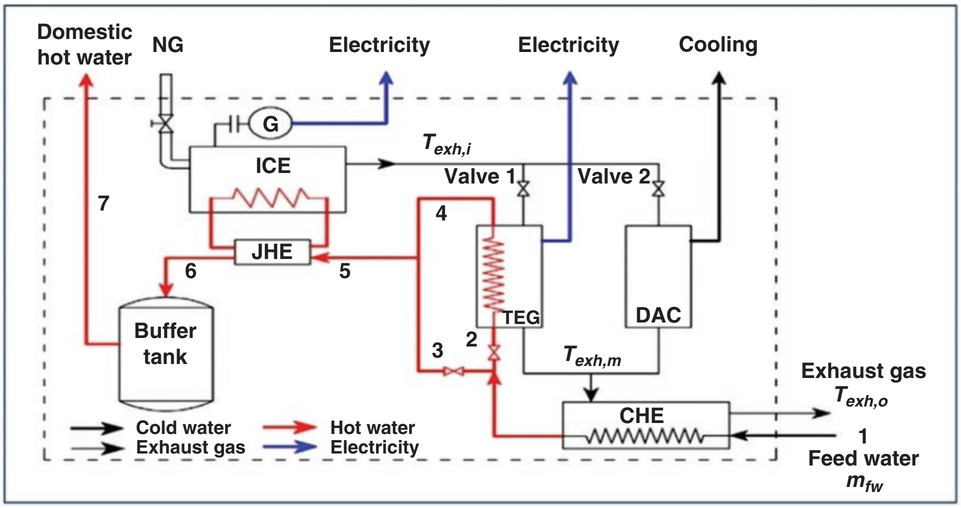

Fig. 10: ICE and TEG CCHP system. (JHE: jacketed heat exchanger; DAC: distributed absorption cooling; CHE: condensing heat exchanger.) Reprinted from [11] with permission from Elsevier.

1.9 ICE and condensing heat exchanger–thermoelectric generator CCHP system

As proposed by [11], the CCHP system was based on an ICE for electricity production, cooling and heating of household water, whereas a condensing heat exchanger and thermoelectric generator (TEG) were used to efficiently recover the waste heat of the ICE exhaust gas. Their scheme was devised using the concept of energy-cascading utilization. Fig. 10 illustrates their system. In summary, the deep recovery of exhaust gas and TEG methods were applied in the CCHP system. The electrical output of the TEG changed from 231 W to 1180 kW, and the total recoverable waste heat increased by between 13% and 16%. Their findings also revealed that the primary energy efficiency of the CCHP system could reach 94.4% and this was due to the condensing heat recovery from the exhaust gas. The PESR and the cost-saving ratio could, respectively, reach 30.4% and 41.7%, whereas the investment in the overall increase in the CCHP system was 11.1%.

1.10 Low-temperature polymer electrolyte membrane FC CCHP system

The aim of the research as per [18] was to evaluate the performance and energetic viability of a unique domestic micro CCHP system using a low-temperature polymer electrolyte membrane (LT-PEM) FC power unit and a half-effect LiBr absorption chiller. The numerical results showed a good execution in terms of exergy and energy in the full functional field of the trigeneration system. Fig. 11 represents their CCHP system. The PEM FC power unit and the absorption chiller were, respectively, modelled using 1D and thermochemical models, and validated using available experimental and literature data. The performance of their CCHP system was analysed using the energy-utilization factor (EUF), the exergy utilization factor (ExUF) and the trigeneration primary energy savings (TPES), and the numerical result showed good performance in terms of EUF and ExUF. Their CCHP system was tested under three modes, namely without producing cold, without producing heat and producing heat and cold. In the three modes, their respective EUFs and ExUFs were 75% and 40%, 56% and 45%, and 61% and 46%. It shows that the EUF performed best during heating and worst during cooling, and the best performance was achieved at lower loads.

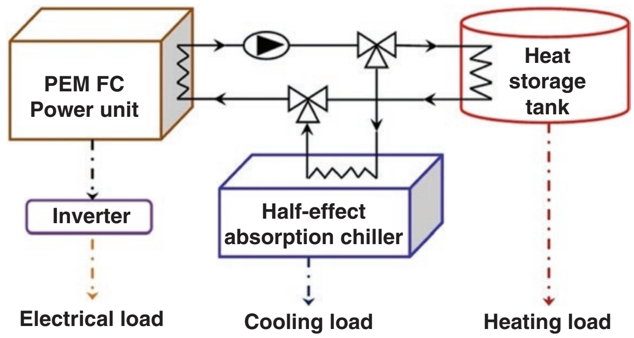

Fig. 11: LT-PEM FC CCHP system [18].

1.11 Inlet air throttling gas-turbine CCHP system

In [9], with reference to a CCHP system, inlet air throttling (IAT) schemes for gas turbines were used together with FTL and FEL and following the hybrid thermal-electric load (FHL) techniques to assess the CO_2 emission (CDE), principal energy consumption (PEC) and operation costs (COST). The operation of the CCHP system was such that the turbine inlet temperature was maintained to generate more high-temperature flue gas, which led to more cooling and heating production in the heat-recovery equipment. The similarities between the various working approaches and the energy reference requirements were analysed, and the results showed that their CCHP scheme was advanced to the individual scheme on a yearly analysis, irrespective of which working method was applied. The FEL operation method was found to have the highest reduction in total annual CDE and COST at 13.50% and 14.82%, respectively. Furthermore, the FEL strategy had the shortest payback period of 4.91 years. Fig. 12 shows their CCHP system.

1.12 GSHP micro-gas-turbine and solar CCHP system

The system proposed in [16] as shown in Fig. 13 was a local energy-supply system with the usual CCHP scheme central to it, as well as combined with the production of GSHP and PV power. Their research revealed an efficient method for optimization of a joined CCHP multi-energy system design optimization

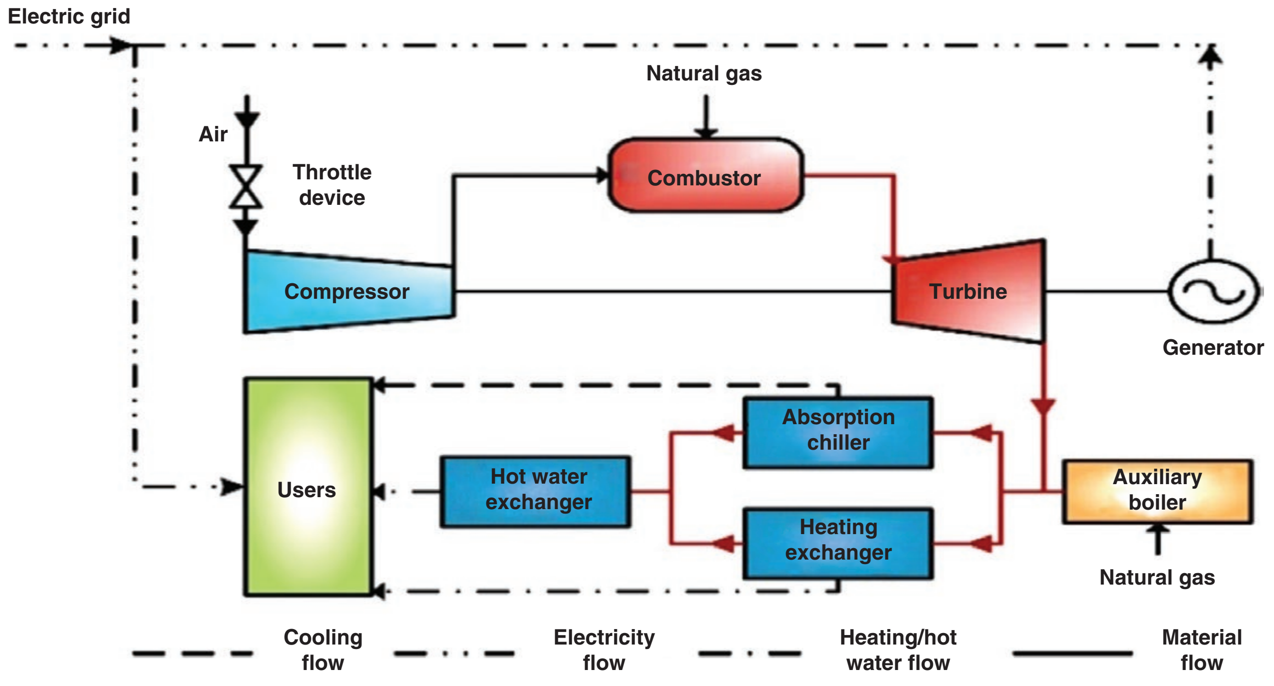

Fig. 12: IAT gas-turbine CCHP system. Reprinted from [9] with permission from Elsevier.

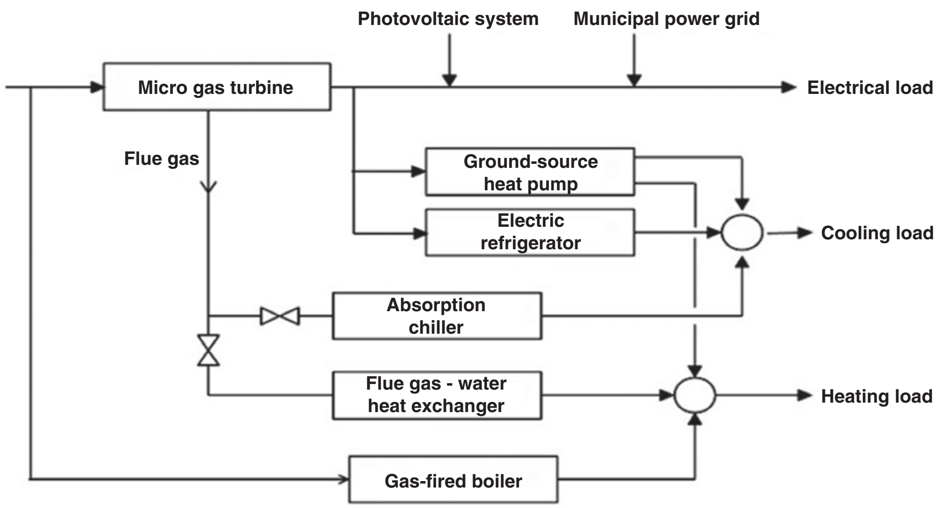

Fig. 13: GSHP micro-gas-turbine and PV CCHP system. Reprinted from [16] with permission from Elsevier.

and derived an innovative approach to addressing related optimization problems. Their optimization solution was based on sequence control configuration methods, a sequential quadratic programming algorithm and a feedback correction mechanism (FEM). The result was a CCHP coupling multi-energy system optimization tool developed using MATLAB®. Their optimized economic benefit of the CCHP system was tested in a commercial area and the total annual operating cost was significantly reduced by 36.2% relative to the traditional subsystem. The CCHP operational time during the heating and cooling seasons was 64% and 66%, respectively, and the GSHP system correspondingly ran 74% and 88% of the time to ensure that the system operated on time. Additionally, their CCHP system handled 84% of electrical, 44% of heating and 37% of cooling loads in both seasons, proving that their system works with good reliability.

1.13 ICE and GSHP CCHP system

According to [15], two GSHP coupling set-ups were investigated as shown in Fig. 14a and b, respectively, one without a heat exchanger and the other with a heat exchanger, to improve the execution of the CCHP–GSHP coupling system. The set-up with a heat exchanger outperformed the set-up without a heat exchanger by a factor of 0.34419 and 0.31118, respectively. Compared to traditional FTL, FEL and FHL strategies, the other strategies of following the maximum comprehensive performance (MCP) of the system and following the maximum electrical efficiency of the ICE unit may both be more desirable for the CCHP–GSHP coupling system with a heat exchanger having better comprehensive performance. On the other hand, the strategy of following the MCP of the system was the best technique to enhance the comprehensive performance with a maximum index value of 0.43264. Using a hotel building as a case study, a comprehensive evaluation and indicator comprising a primary energy-consumption savings ratio and a life-cycle cost-savings rate were compared with a separate generation (SG) system and by selecting a simple genetic algorithm (SGA) and quantum genetic algorithm (QGA) to solve the optimization problem. It revealed that the QGA was better than the SGA for the optimal configuration of the energy system under the FTL strategy, as well as under the other strategies.

1.14 ICE with CCHP refrigeration and dehumidification system

In [14], a hybrid CCHP cooling and dehumidification system was postulated, in which ICE was used as the PGU. A 'jacket water of ICE' was applied to allow the absorption dehumidifier to dehumidify. The hybrid cooling system consisted of an electric compression cooler and an absorption chiller. The design and functioning technique of the system was optimized using an analytic hierarchy process and a constrained non-linear programming (NLP) solution to institute a thermo-economic model of the ICE CCHP scheme. Fig. 15 illustrates the ICE CCHP system. A sensitivity analysis was performed and showed that, when the electricity price was <0.078 $/kWh and the fuel price was >0.62 $/m^3, the CCHP system was economically less advantageous relative to the SG systems. It also revealed that fuel and electricity prices had an impact on the economic performance but not on the thermal dynamic performance of the ICE CCHP system. They concluded that the absorption dehumidifier had a better improvement in the thermal dynamic performance of their ICE CCHP system but little improvement in the economy of their ICE CCHP system.

1.15 5-kW PEM FC CCHP system

According to [12], a multicriteria investigation was carried out on a residential CCHP system based on a 5-kW PEM FC as depicted in Fig. 16. Their CCHP system thermodynamic model was partly proven, whereby a parametric analysis scheme was applied to assess the system executions based on four evaluation indices, namely pollutant emission reduction, yearly cost, exergy efficiency and energy efficiency. The system was optimized with an evolution algorithm to obtain 3D Pareto solutions and an optimum functional set of parameters. Their findings indicated that higher relative humidity, lower operating temperature and increased inlet-gas pressure were vital to improving system emission and exergy efficiency. The optimized system annual cost, emission reduction and exergy efficiency at the final optimal point, respectively, were $29 337.3, 1.82 × 10^7 g and 39.9%. When this was compared with the non-optimal system, it showed better performance in both increase in emission reduction by 25.5% and exergy efficiency by 28.3%—though at the expense of the economic cost. With the increase in H_2 pressure, the system and exergy efficiency could, respectively, increase to 61.2% and 40.8% with the minimization of 1.5 × 10^7 g of emission annually.

1.16 LT-PEM FC and thermoelectric cooler CCHP system

As observed in [19], the PGU was a LT-PEM FC and the refrigerating system used was a thermoelectric cooler (TEC). The main components of the cycle, including the PEM FC and TEC, had no moving parts, were noiseless and therefore did not require maintenance. Water condensate and the low-grade heat of ~80°C were by-products. The mathematical models of FC and TEC were realized, and the simulation outcomes were consistent with existing scholarly publications, validating their micro CCHP scheme as novel. It was capable of generating 26.8 W of cold, 2.79 kW of power and 3.04 kW of heat and having an overall efficiency of 76.94%, reduction in CO_2 production reduction by ~2.58 kg/hour and 43.25% of primary fuel savings. The exergy efficiency was 53.86% and the FC caused the most exergy destruction, which increased with temperature. The compressor caused the second-most exergy destruction, followed by the pump. The pump and TEC caused the least exergy destruction. A ballpark economic calculation revealed that the primary capital cost of the micro CCHP system was <2000 USD and its weight was <100 kg. Fig. 17 shows the set-up of their trigeneration system.

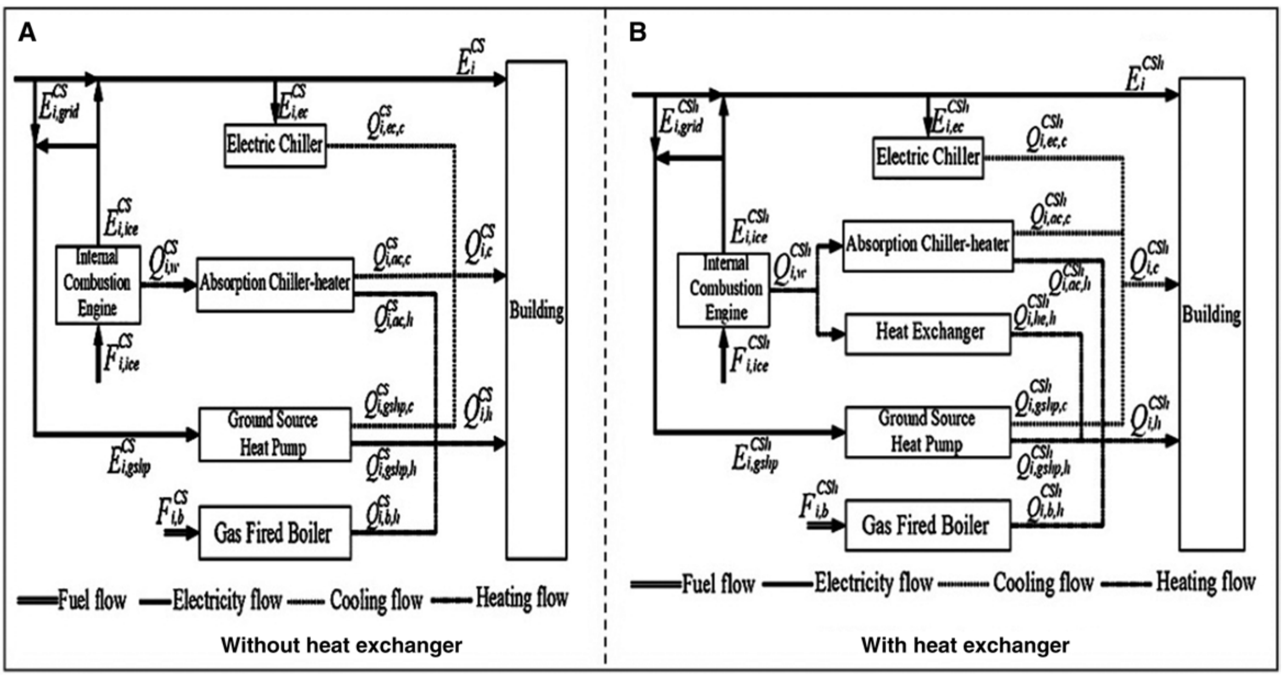

Fig. 14: ICE and GSHP CCHP system (a) without heat exchanger and (b) with heat exchanger. Adapted from [15] with permission from Elsevier.

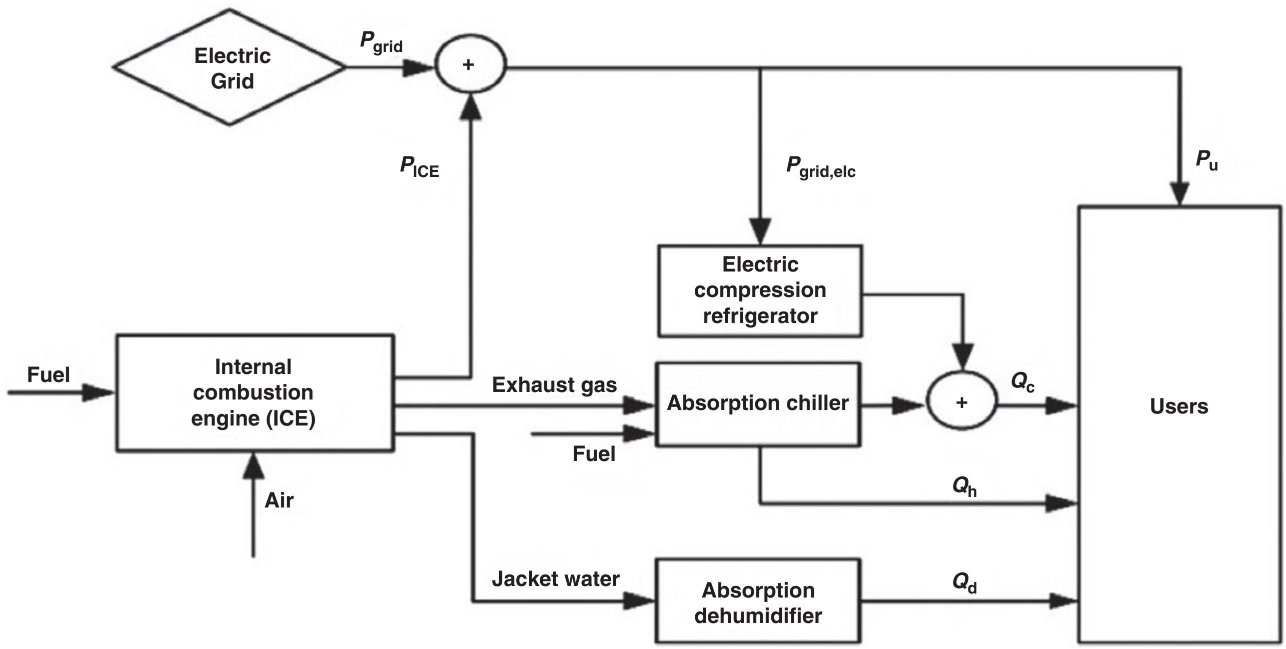

Fig. 15: ICE with CCHP dehumidification and refrigeration system. Reprinted from [14] with permission from Elsevier.

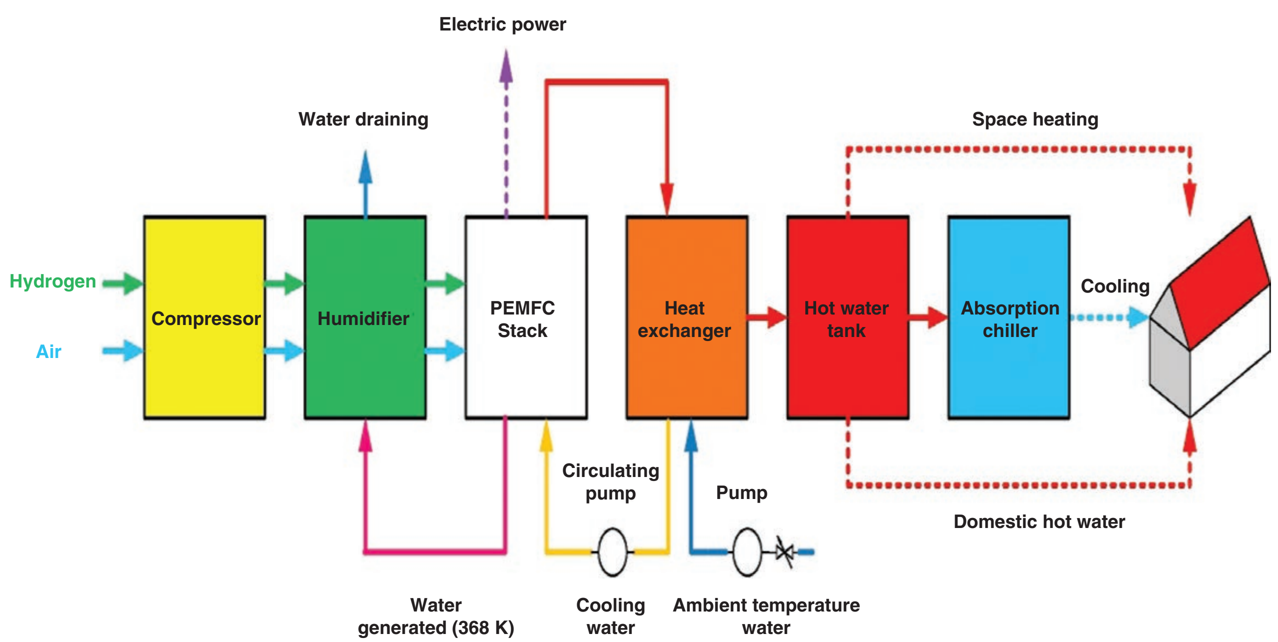

Fig. 16: 5-kW PEM FC CCHP system. Reprinted from [12] with permission from Elsevier.

1.17 Molten-carbonate FC and Stirling-engine CCHP system

Indicated in [17], the Stirling engine, molten-carbonate FC (MCFC) and a double-effect LiBr/H_2O absorption chiller hybrid CCHP system was suggested. The MCFC was the prime mover and its exhaust heat was utilized as the heat source for the Stirling engine, which subsequently supplied heat to the generator of the absorption chiller. The amounts of power, heat and cold that were produced were, respectively, 6.482, 2.137 and 1.372 MW. Fig. 18a and b, respectively, summarize their CCHP system diagram and the flow process. The results of the energy analysis showed that the total and electrical efficiencies of their proposed hybrid CCHP system were, respectively, 71.71% and 42.28%, whereas the exergy analysis disclosed that the MCFC, Stirling engine and the gas turbine had sizable efficiencies. The overall efficiency was ample, most notably due to the high degree of heat recovery from the prime mover, whereas the electrical efficiency of the cycle was relatively lower, mostly due to the power consumption by the process components, such as the compressors and pumps.

1.18 ICE with integrated organic Rankine cycle and solar-thermal utilization CCHP system

The research in [34] was a new integrated solar-thermal (ST) organic Rankine cycle (ORC) CCHP system shown in Fig. 19. ICE was the main prime mover and, together with the ORC, both could simultaneously generate power. Unlike conventional

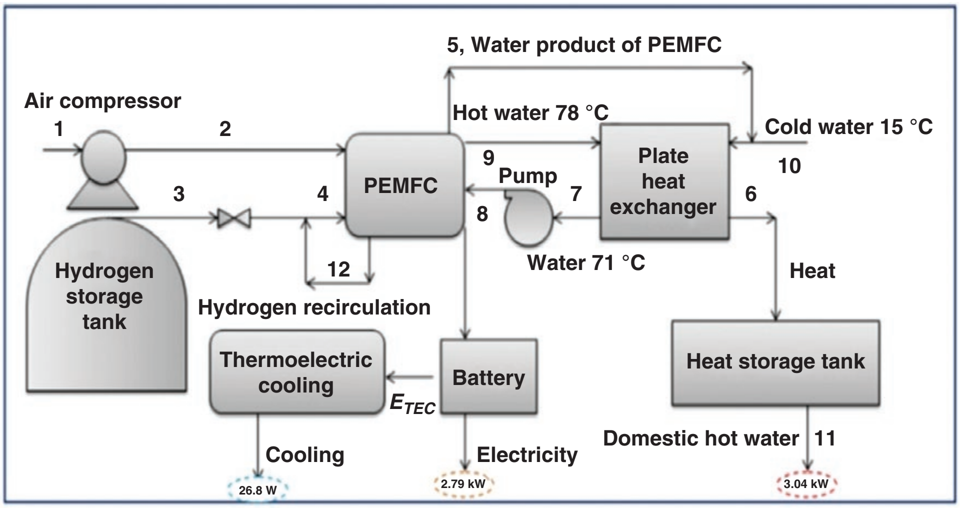

Fig. 17: PEM FC and TEC CCHP system. Adapted from [19] with permission from Elsevier.

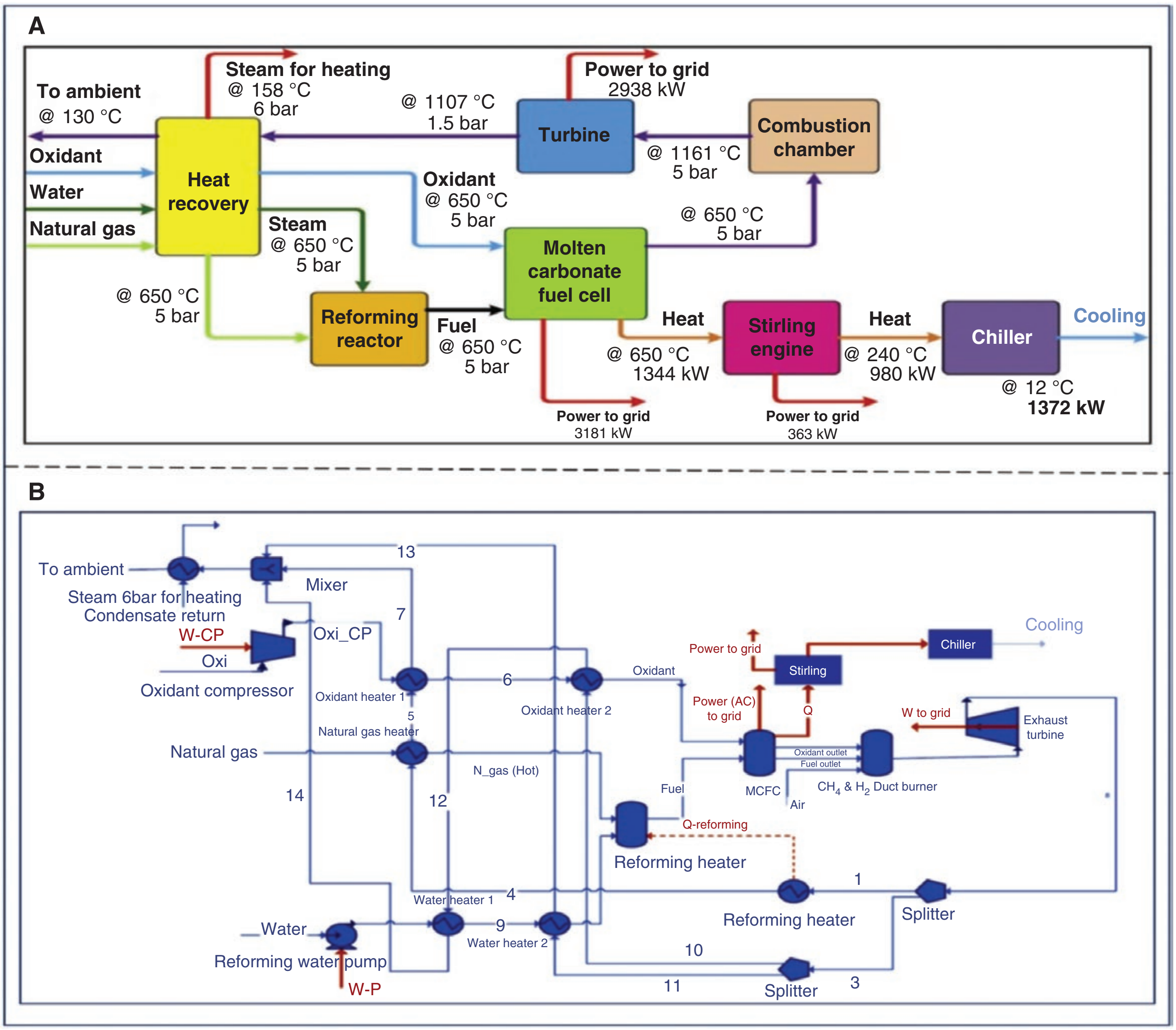

Fig. 18: Stirling-engine and MCFC CCHP system. (a) Stirling-engine and MCFC block diagram and (b) Stirling-engine MCFC flow process. Adapted from [17] with permission from Elsevier.

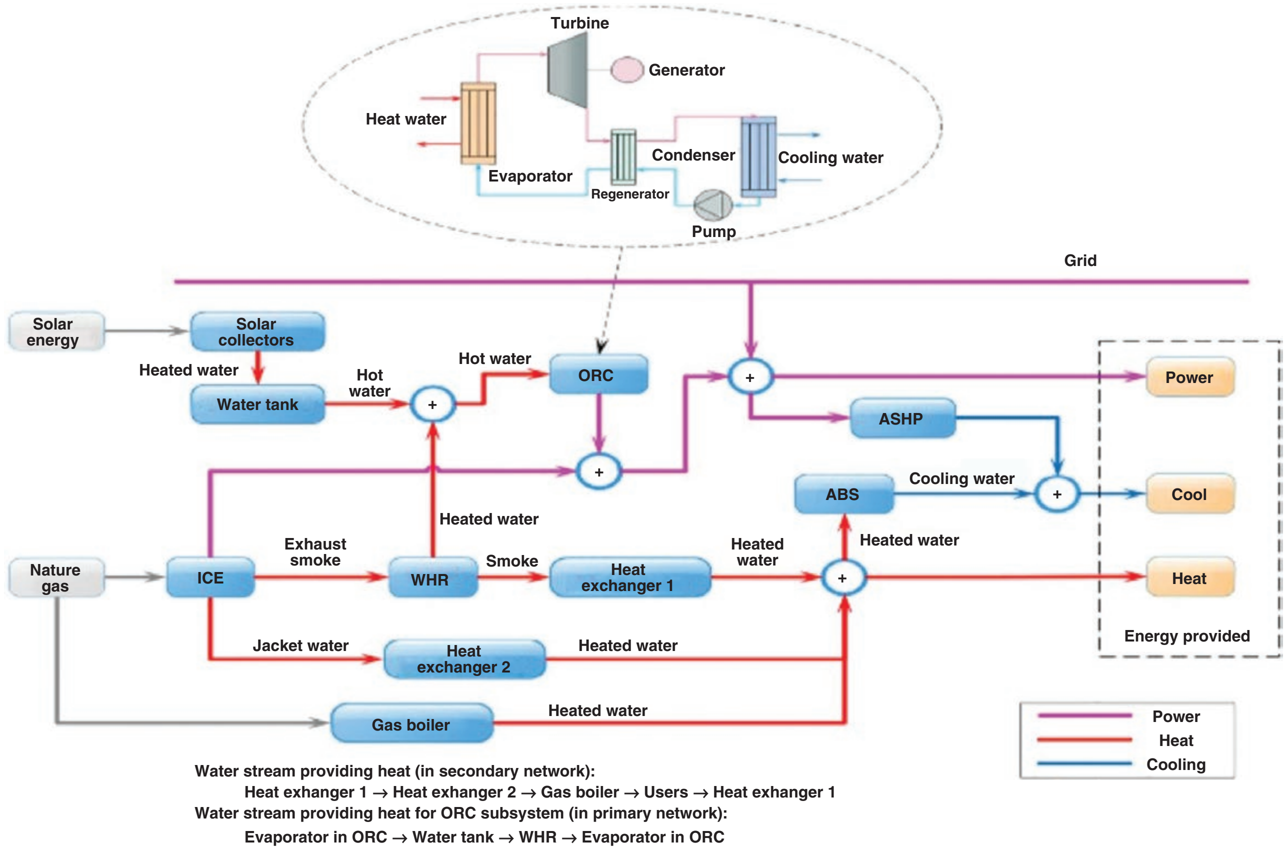

Fig. 19: Integrated ORC and ST use of the CCHP system. Reprinted from [34] with permission from Elsevier.

CCHP and CCHP–ST systems, the CCHP–ST–ORC system harmonized fossil fuel with renewable energy and its performance was evaluated based on thermodynamics. Their findings revealed that their CCHP–ST–ORC system (i) could produce an extra 5.1 kW of electricity relative to the traditional CCHP and CCHP–ST systems, (ii) had a higher energy ratio of 22.6% more than the ordinary CCHP system, (iii) consumed 12.4% less energy than the CCHP–ST system, (iv) had a partial load ratio of 100% and could generate up to 108 kW of electricity and heat, (v) could meet the heat requirements without gas boilers but by using solar collectors and an ICE and (vi) had a similar exergy efficiency of 40% compared to the traditional CCHP and CCHP–ST systems. One drawback was that the ST collector only worked when there was sunlight. Their results lent themselves to coupling CCHP system design, development, functioning and applications of the CCHP system.

1.19 CCHP system integrated with PV/thermal panels and thermal energy storage

As reported in [35], the CCHP system is becoming a popular technology to provide cascaded efficient energy and the performance of the CCHP system can be enhanced by integrating PV/thermal panels and energy storage, controlled by an effective operation strategy to manage the energy flow. They formulated a mathematical model of their postulated system and determined the optimal size of the main components using particle swarm optimization (PSO). The four scenarios tested were (i) CCHP system with PGU, heat-recovery system (HRS), PV/T, thermal energy storage (TES), heat exchanger, boiler, absorption chiller and electric chiller; (ii) same as in (i) but without TES; (iii) same as in (i) but without PV/T; and (iv) same as in (i) but now without TES and PV/T. Each of the Scenarios (i) to (iv) was then repeatedly tested based on the five operating strategies: (a) FEL with electric cooling ratio (FEL–ECR), (b) FTL, (c) FHL, d) following the maximum PGU efficiency (FME) and (e) with their proposed strategy. In Scenario (i), the original value of PESR increased by 39.6%; in Scenario (ii), the original value of PESR rose by 17.6%; and in Scenario (iii), the original value of PESR increased by 7.3%. The FTL and FME operation strategies gave the worst PESR, and FHL gave better PESR than FTL and FME, but the worst cost savings. Their proposed strategy gave the best PESR and total cost savings, followed by FEL–ECR. Fig. 20 shows their system.

1.20 Multi-energy-oriented CCHP system: energy-flow optimization method

The study in [36] and shown in Fig. 21 was a multi-energy CCHP system that incorporated gas, solar and wind energy as well as power storage controlled by the PSO method. By defining the reliability index for the supply of a particular energy form, an index for heat and power losses probability was constructed, also taking into consideration the cost of the investment, CO_2 emission and primary energy consumption. Renewable energy was prioritized for power generation under FEL, during which it could reach >50% in the peak load period or when it was windy at night and demand was low. As a result of these fluctuations, the fossil-fuel PGU was on standby to track the load power demands. Their study concluded that CCHP set-ups were better than separate energy-production set-ups, with the FEL operation strategy being superior compared with orthodox operation strategies and offering better energy efficiency, economy, environmental protection and reliability.

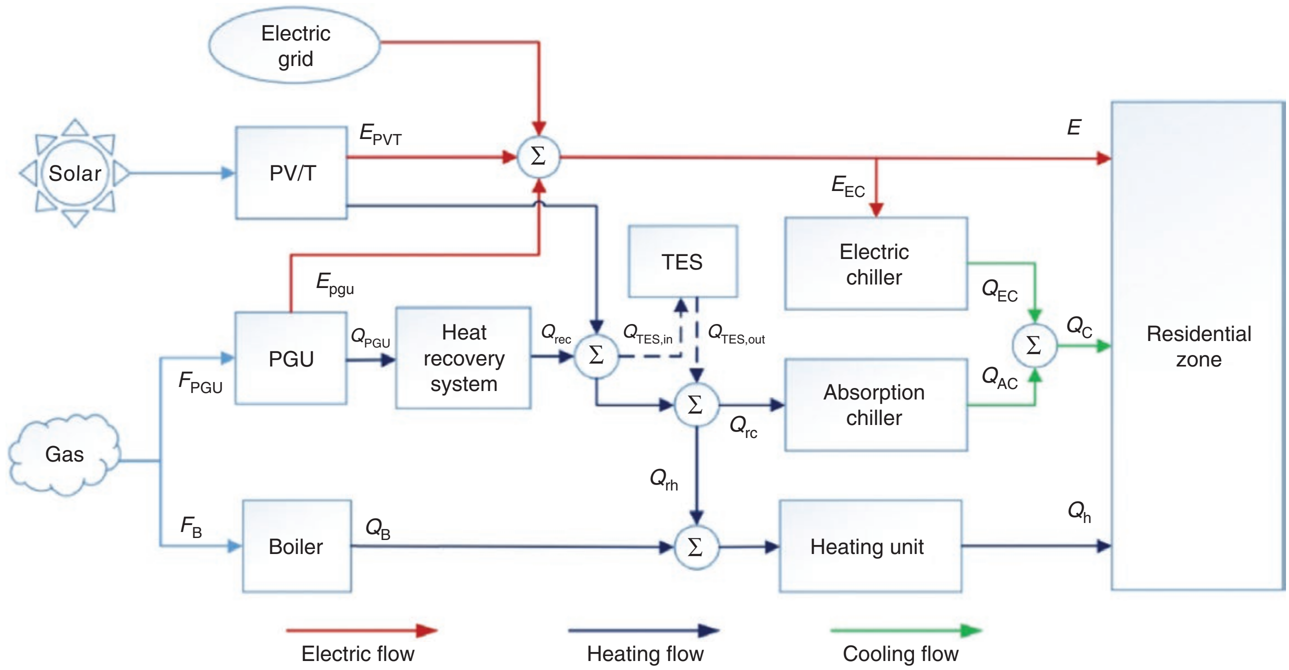

Fig. 20: CCHP system integrated with PV/thermal panels and TES [35].

1.21 Improved CCHP system based on developed owl search algorithm

Examined in [37] and depicted in Fig. 22 is an enhanced CCHP system based on a developed owl search technique based on the Levy flight mechanism and circle mapping, in which the energy flow for the capacity and operation of a CCHP system were optimized to reduce the main use of electricity in the Kerman area in Iran. In their proposed system, the waste heat of the hot gases was recycled while at the same time producing power to enable an energy efficiency of >85%. Their system was analysed and optimized with respect to the cost of operation and emission reductions, as well as energy utilization. Their simulation revealed that with the use of optimal parameters, the efficiency of the main components could be enhanced. System analysis revealed that the PESR and CO_2-emission minimization of the CCHP system was appreciable compared to an existing reference system; however, overall yearly cost savings reduced the capacity. The optimal value for the PGU capacity of the CCHP system was 500 kW.

1.22 Smart energy-management system for residential buildings equipped with the CCHP system

Postulated in [38] and exemplified in Fig. 23 is a concept of a smart energy-management system (EMS) of a CCHP–microgrid system for buildings, to control the schedules of its energy-storage and renewable systems. Their assumption was that smart meters collect measured data from different devices; nevertheless, the refinement and processing of these data seemed necessary before utilizing them in the EMS. They presented a smart EMS (SEMS) for application in a residential microgrid with high penetration of distributed energy resources. The cost of building the energy operation was minimized for stochastic and deterministic scenarios, and the effectiveness and applicability of the suggested concept were tested using the day-ahead optimum energy planning. A stochastic model based on a Monte Carlo simulation was considered to determine the effects of uncertainties on the daily energy management of the building. The conclusion drawn was that using a CCHP system fitted with a smart controller could significantly lower the energy operating costs.

1.23 Geothermal-driven CCHP systems integrating ejector transcritical CO_2 and Rankine cycles

According to [39], the benefits of CCHP systems are becoming notable due to the inclusion of efficient thermodynamics cycles and renewable energy. In their proposed model shown in Fig. 24a was a geothermal CCHP system with the ejector transcritical CO_2 (TRCC) fitted with a traditional Rankine cycle and, in Fig. 24b, the gas cooler was substituted with an internal heat exchanger (IHE) and tested for a wide range of practical operating conditions. Parametric analysis and thermodynamic modelling were performed to study the influences of design variables. Under typical operating conditions, their findings noted that the replacement of the gas cooler resulted in the Fig. 24b system having 30.9% exergy efficiency, 49.1% net power output and 75.8% cooling output increments, though at the expense of decrements in the heating output by 39.1% and thermal efficiency by 9.2% relative to the Fig. 24a system. Furthermore, the turbine inlet pressure was proportional to the net output power and exergy efficiency and inversely proportional to the heating output and thermal efficiency. In summary, their proposed systems had better output power performance when compared with similar systems.

1.24 Thermodynamic and economic analyses of different cogeneration and trigeneration systems based on CO_2 vapour compression and refrigeration systems

In [40], various new integrated cogeneration and trigeneration systems were investigated, which were suggested using a CO_2 parallel compression economization–vapour compression refrigeration cycle with a capacity of 1 MW and evaporator temperatures of between –35°C and 45°C. The main contribution

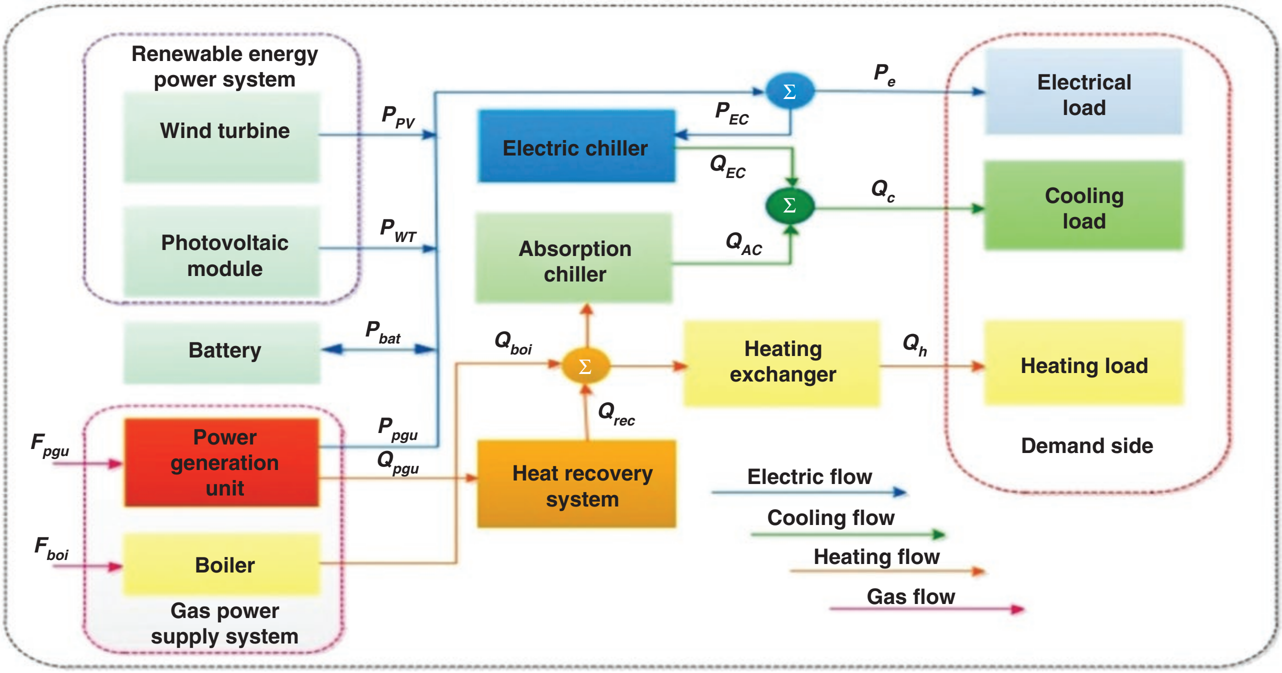

Fig. 21: Multi-energy-oriented CCHP system. Reprinted from [36] with permission from Elsevier.

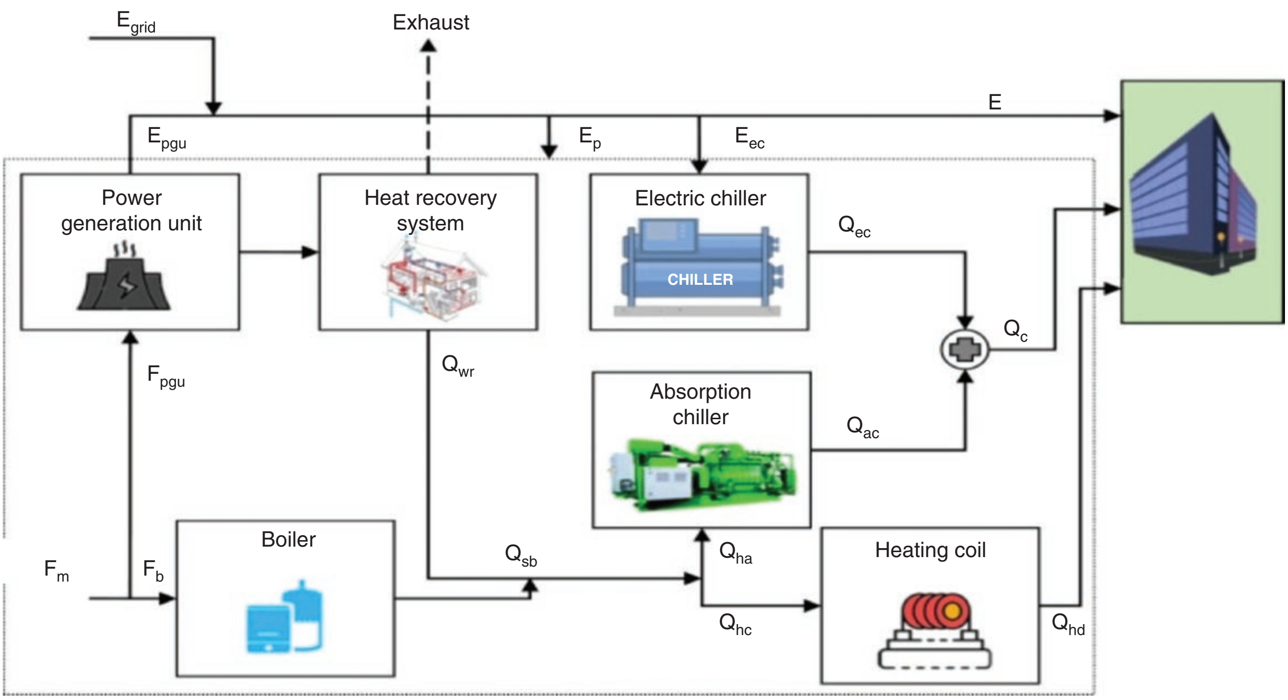

Fig. 22: Improved CCHP system based on the developed owl search algorithm [37].

of the research was an in-depth techno-economic assessment of numerous possible variations for these systems for assorted practical uses. Fig. 25a shows a trigeneration system for refrigeration, air conditioning and hot-water production. Fig. 25b shows a trigeneration system for refrigeration, air conditioning and power. A parametric study was also conducted to establish the impact of various modalities and critical design dynamics, as well as the performance of the functioning parameters on the suggested systems. Thermo-economic results showed that recovering the obtainable thermal energy of CO_2 exiting the compressor would be appealing environmentally, economically and thermodynamically to give various vital outputs. Respective refrigeration and air conditioning effects of >147 and >478 kW could be generated with cogeneration set-ups. Furthermore, power of between 59.52 and 185.8 kW could be produced depending on the organic fluid and configurations used, thus enhancing the coefficient of performance (CoP) by ≤18.0%. Furthermore, the trigeneration configuration could obtain 7763–9360 m^3 of domestic hot water annually, thus minimizing the cooling cost by ≤13%.

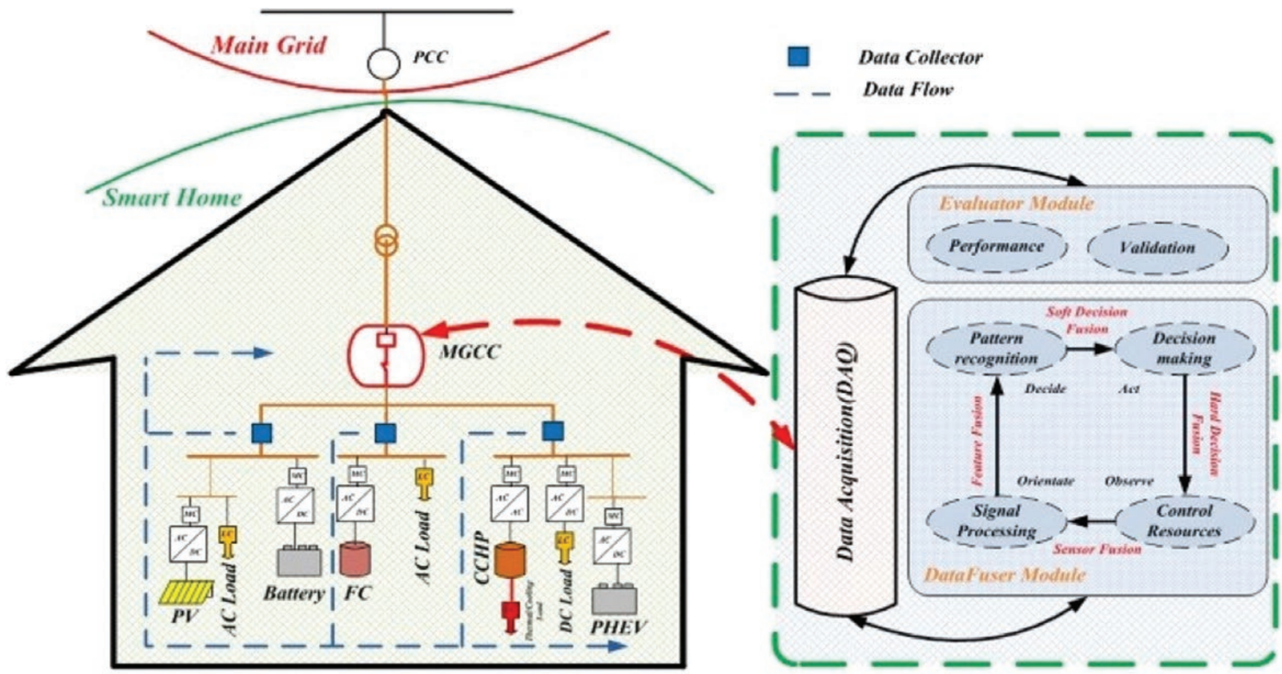

Fig. 23: Smart EMS for residential buildings fitted with the CCHP system. Reprinted from [38] with permission from Elsevier.

1.25 Energy, environmental and economic evaluations of a CCHP system driven by Stirling engine with hydrogen and helium as working gases

The research in [41], summarized in Fig. 26, was a dual Stirling-engine CCHP system with hydrogen and helium as operating gases. The engine was assessed with a non-ideal adiabatic model and the absorption chiller energy assessment was articulated using the engine waste heat. The effects of the vital specifications of the Stirling engine such as the heater temperature, regenerator length, CCHP efficiency, CoP of the absorption chiller working gases, CCHP primary energy savings, CO_2-emission reduction, operation costs reduction and engine rotational speed were investigated and compared to traditional energy systems. The power production, cold production, heat production, CCHP efficiency and CoP results using helium were, respectively, 15.24 kW, 19.65 kW, 12.65 kW, 70% and 64.4%, and the power production, cold production, heat production, CCHP efficiency and CoP results using H_2 were, respectively, 22.52 kW, 21.65 kW, 14.43 kW, 72.29% and 66.7%. In summary, hydrogen gave better results.

1.26 Thermodynamic and thermo-economic analysis of the ammonia–water mixture cycle

Proposed in [42] and illustrated in Fig. 27 was a new CCHP system based on the ammonia–water mixture driven by a low-temperature heat source (LTHS) that was a custom version of a Kalina cycle. Thermodynamics and thermo-economic balance equations for performance analysis of the thermal system were used to investigate the viability of the recommended system. The energy and exergy efficiencies were calculated to be 49.83% and 27.68%, respectively. Electrical, cooling and heating capacities were, respectively, 0.253, 1.610 and 1.972 MW. More energy efficiency could be obtained by raising the evaporation temperature and the basic ammonia concentration, or by reducing the separator pressure, heating-unit temperature and the terminal temperature difference of the vapour generator. More exergy efficiency could be attained by increasing the Separator 1 pressure or by decreasing the Separator 2 pressure, heating-unit temperature, evaporation temperature and basic ammonia concentration. The total product cost of the cycle could be minimized with evaporation temperature and maximized with ammonia concentration.

1.27 A configuration optimization framework for renewable-energy systems integrating with electric-heating energy storage in a remote tourist area

The system studied in [43], and pictured in Fig. 28, was a CCHP system of wind, solar and natural gas for a remote tourist area. Taking into account the complexity of the system, a CCHP energy hub was established to concentrate and distribute power and heat, as well as cold. An integrated optimization framework reduced yearly economic, maintenance and fuel costs by inserting the constraints on energy-supply reliability and renewable-energy penetration indices, and it could inform the reliability of power, heat and cold supplies. The PGU supplied most of the power during wind and solar outages, and heat- and power-storage devices also assisted in this regard to reduce waste and to enhance the system's performance, though at the expense of the complexity of the system. Five different CCHP configuration scenarios were tested and the scenario having PV energy, wind energy, PGUs, gas-fired boilers, electric energy-storage device, heating energy-storage (HES) device, electric chillers, absorption chillers and heat exchangers yielded the best performance having the optimum capacity configuration and operation economy, although with higher initial installation costs of the devices used.

1.28 ORC co-generator and adsorption-chiller CCHP experimental prototype

Examined in [44], and summarized in Fig. 29, was a CCHP system based on PV, a micro-ORC plant and an adsorption chiller with a built-in real bioclimatic nearly-zero-energy building (NZEB) modelled using TRNSYS® software. The analyses performed

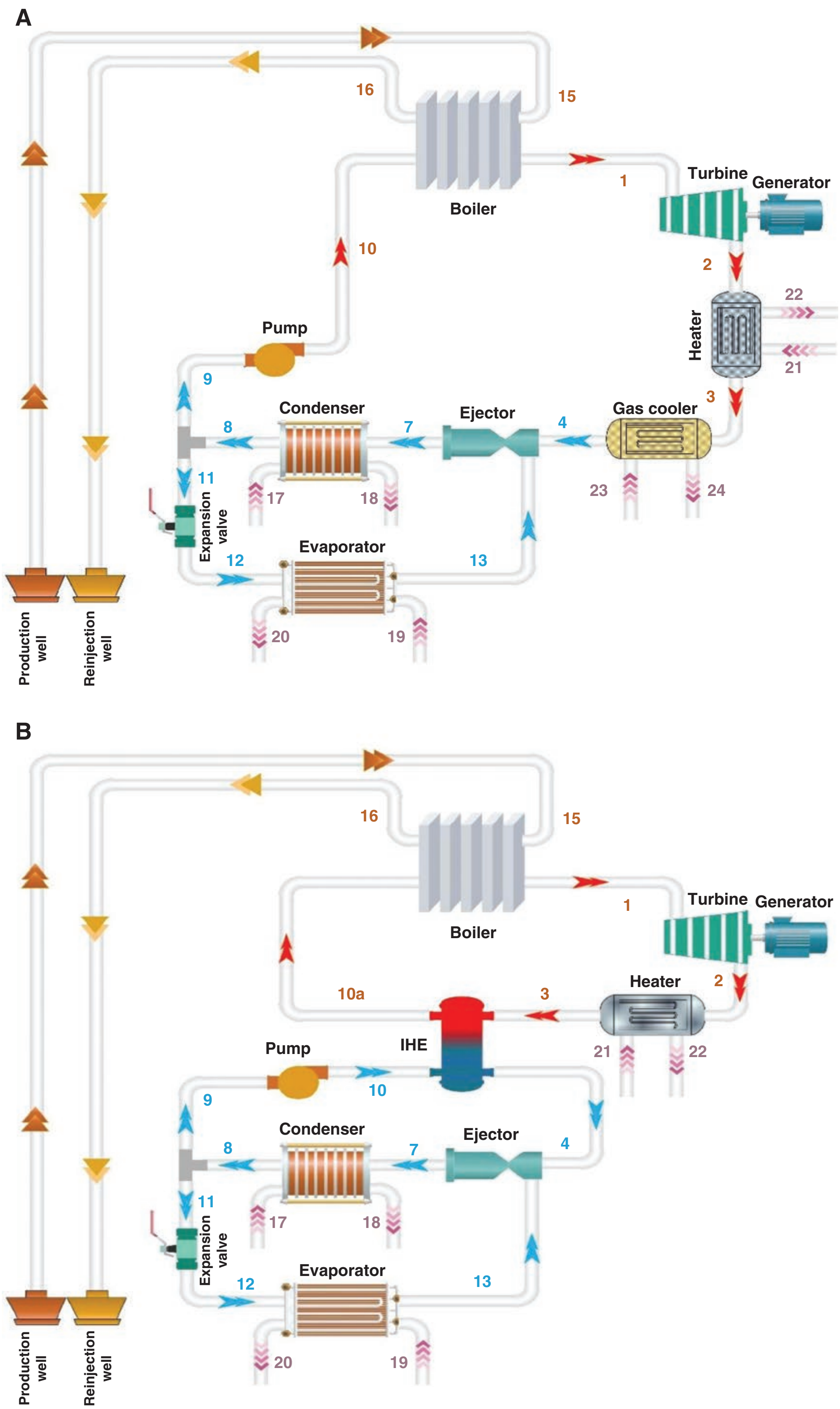

Fig. 24: Postulated CCHP systems based on (a) TRCC cycle and (b) TRCC with an IHE. Reprinted from [39] with permission from Elsevier.

included energy, economic and environmental, and it was realized that the system's effectiveness was affected by solar irradiance and weather conditions. The system was analysed hourly and the sensitivity results showed that the locations had an impact on the system. The system was operated 100 days a year and the efficiency was between 32% and 42%. The system was proven to be suitable for use in home ventilation. A techno-economic evaluation was conducted and the payback period of the evaluated solution was >25 years unless economic support possibilities were considered. If the initial cost was supported by economic

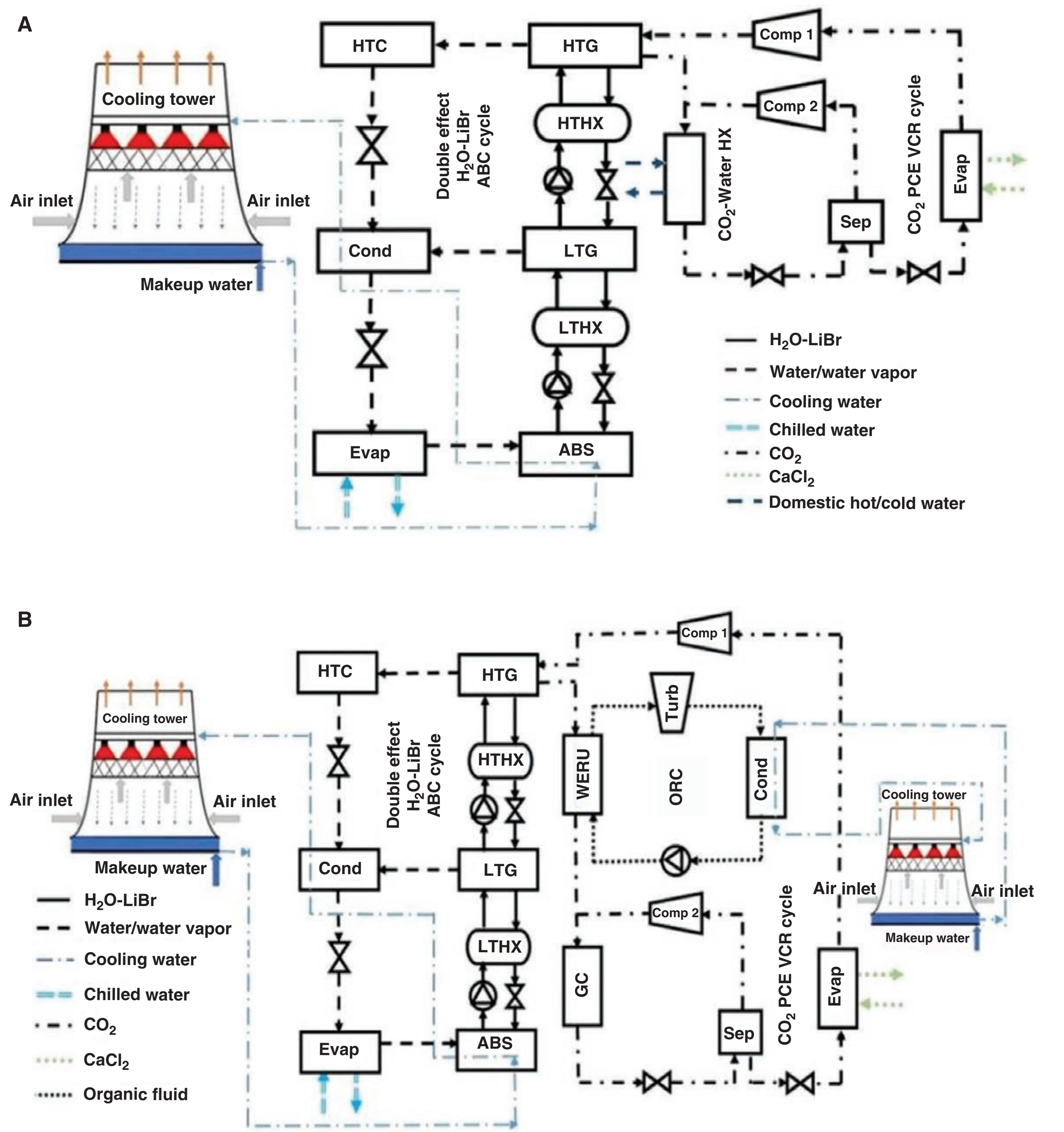

Fig. 25: Trigeneration systems for (a) refrigeration, air conditioning and hot-water production with heat exchanger and (b) refrigeration, air conditioning and power production with ORC. Reprinted from [40] with permission from Elsevier.

incentives, the assessment showed that the suggested CCHP system could attain a payback time of 6 years with a net present value of 50 000 EUR for 25 years.

1.29 Comparative study of optimization method and optimal operation strategy for multiscenario integrated energy system

Featured in [45], and captured in Fig. 30, was an integrated multiscenario CCHP system theoretical model. A novel self-adaption technique based on an exhaustive search algorithm was suggested for a minimum per-hour operation cost. Using various operation methods for remote and connected cases, the optimal capacity and operation parameters were determined. It was found that using a self-adaption technique, the remote scenario provided the minimum annual system costs of \$23.6/m² and \$19.39/m², followed by the FEL technique at \$23.68/m² and \$19.43/m², and finally the FTL strategy at \$25.17/m² and \$20.2/m², respectively, for commercial and office buildings, while in the connected scenario, the minimum annualized system cost was \$693 300 (~\$19.26/m²). A synergized optimization approach, which harmonized the

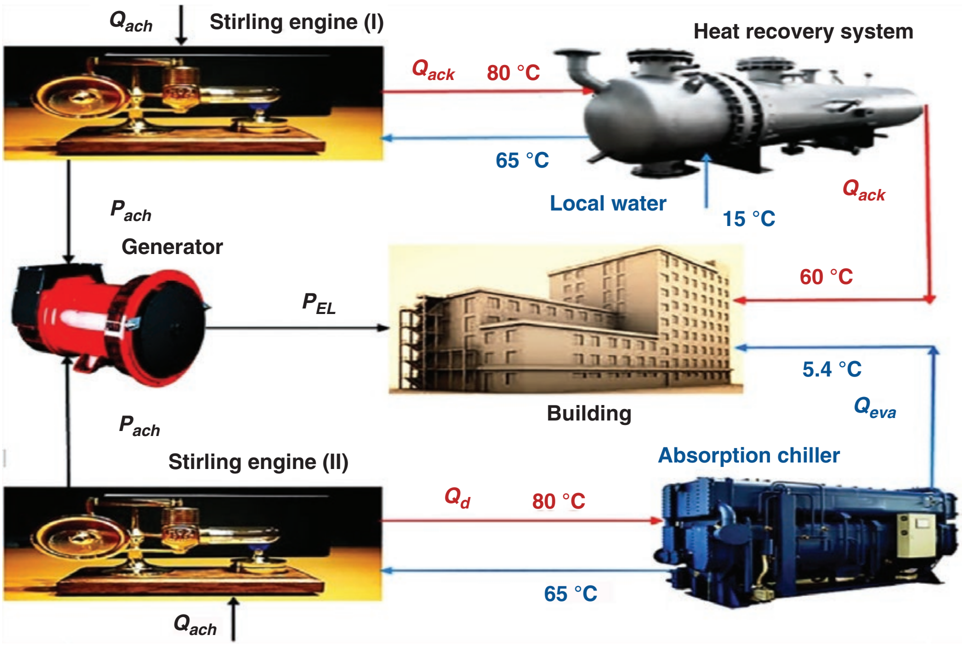

Fig. 26: CCHP system overview. Reprinted from [41] with permission from Elsevier.

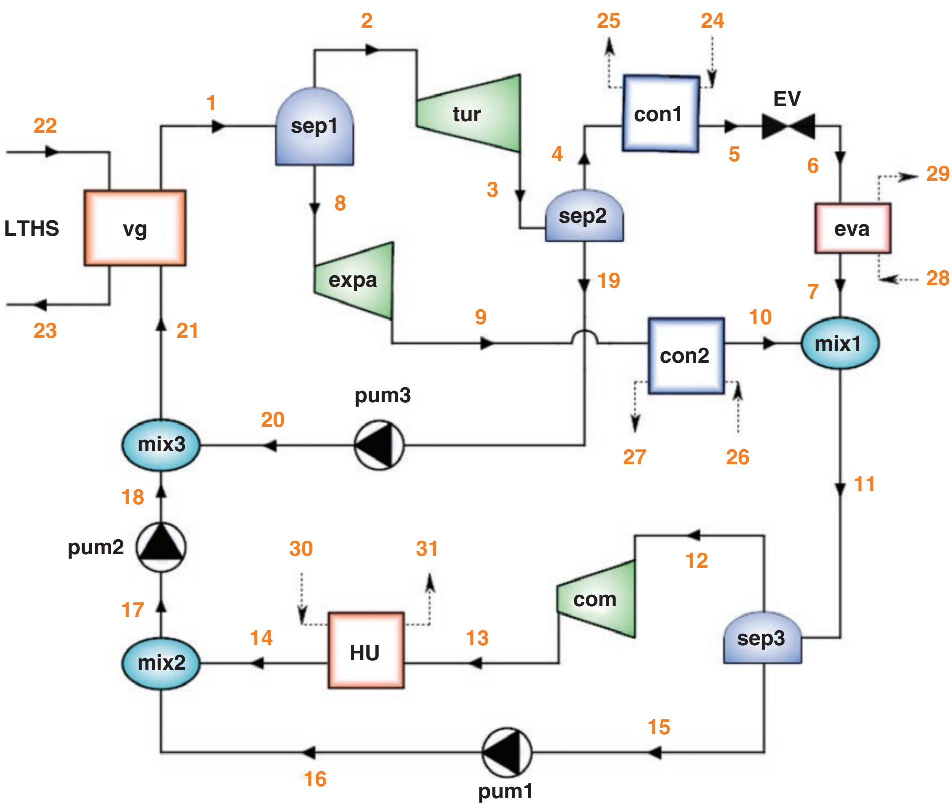

Fig. 27: LTHS CCHP system overview. Reprinted from [42] with permission from Elsevier.

genetic algorithm and the orthogonal experimental strategy, was initiated to establish multiple decision variables and the results revealed that it can reduce the yearly cost by 0.67% relative to a non-collaborative optimization. The connected CCHP system exhibited superiority in economy relative to the isolated CCHP system in the case of a large energy-supply area. In isolated scenarios, a separated energy-production system was more economical for residential buildings, irrespective of the strategies employed.

1.30 A shopping-mall CCHP–ORC distributed energy system operation simulation

Presented in [46] was a CCHP–ORC system to stabilize irregular power and heat demands, as well as to improve the versatility and changeability of the heat-to-power ratio on the source side. Using TRNSYS® software, a simulation model was developed for the functioning of the CCHP–ORC system based on the system configuration coupling analysis and the thermodynamic

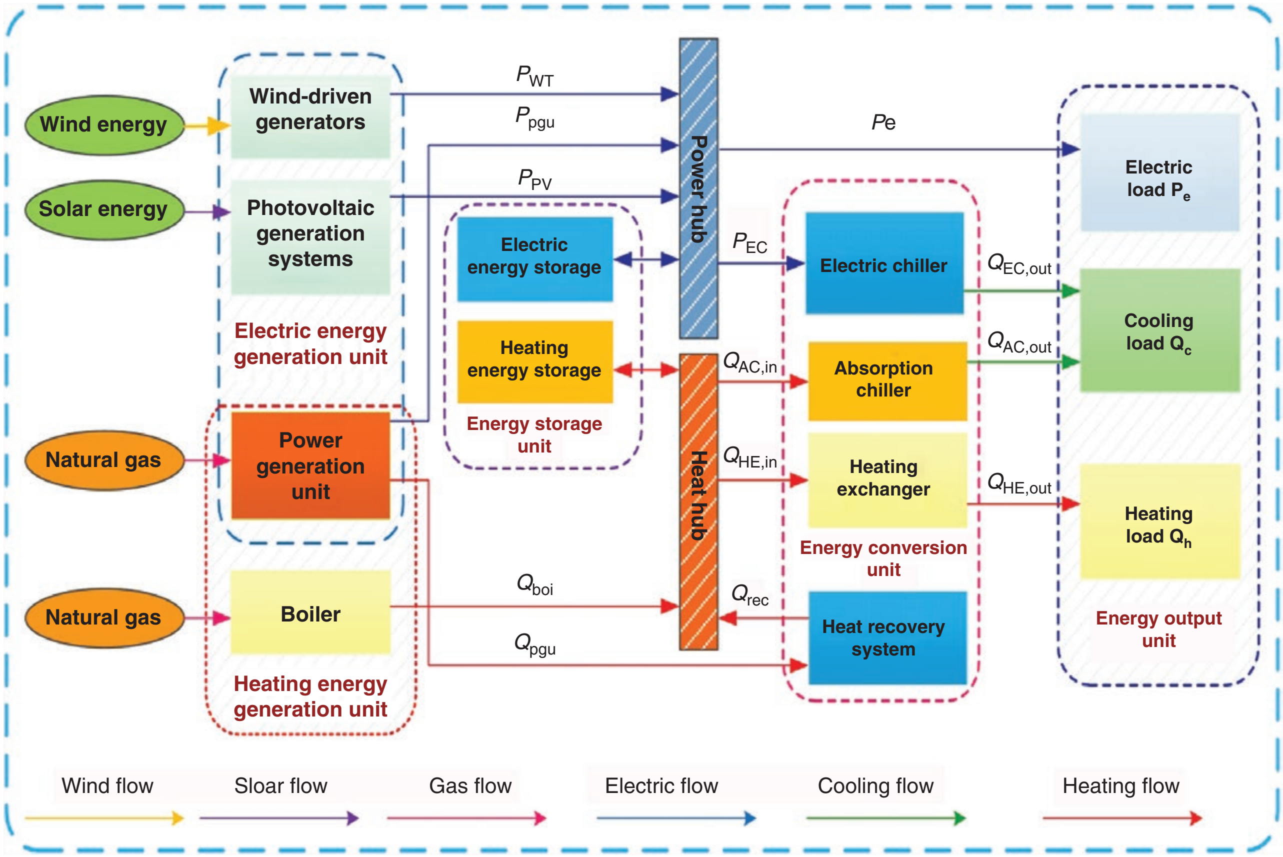

Fig. 28: Overview of the researched CCHP system (adapted from [43]).

parameters, in which the fuel mass flow of the PGU, the mass flow of supplementary fuel, the power generation of the gas engine and the power purchased by the system from the power grid were obtained. A commercial building was used as an example and Fig. 31 summarizes the study. In the heat-tracking (FTL) mode, due to the low heating and cooling loads in the transitional season, the gas consumption was minimized, so the system power generation was small and the purchased power therefore rose. Similarly, in the electricity tracking (FEL) mode, the heating and cooling loads were low in the transitional season, resulting in a lot of waste heat being generated, which could reduce the mass flow after burning, but would relatively increase the power generation.

1.31 CCHP system capacity configuration research ideas

According to [47], a cascaded CCHP system reduced emissions, although its provisions made it complex and therefore a challenge for optimal configuration and performance evaluation. This article focused on the system economy as the evaluation indicator. As a result, two operating modes, namely 'fixing power based on heat' also called 'power demand first' or FEL, and 'fixing heat based on power' also called 'heating demand first' or FTL, were evaluated, with the latter providing a better configuration economy of the CCHP system. The 'economy' of the combined supply system was tightly connected to the configuration of the system and the operational strategies. Numerical results revealed that the energy-utilization rate of the system was best when the adsorption-chiller and gas-turbine models were matched, and only then could the comprehensive energy-utilization rate of the system be optimized and the respective annual total cost of the system was minimal compared with any other instant. Fig. 32 summarizes their investigation.

1.32 CCHP system integrated with an ORC and hybrid energy-storage system design and optimization

Demonstrated in [48], and exemplified in Fig. 33, was a novel CCHP system with a built-in hybrid energy-storage system and ORC, with the objective of the research to evaluate its performance. The function of the hybrid energy-storage system was to improve the supply and operation of the CCHP system, whereas the function of the ORC was to convert the LTHS to power. Modelling/simulation and practical optimization studies were performed to assess the performance of the system. Different load profiles were used and the results, which included the load energy consumed, the power supplied and the efficiency enhancement, indicated that the performance was dependent on the load and the efficiency was attributed to the large amount of waste heat recovered. In test Case Study 1, efficiency varied between 35.70% and 42.70% with an efficiency improvement of >40% relative to traditional CCHP systems, with energy savings in summer and winter, respectively. In test Case Study 2, the overall efficiency for the six scenarios ranged from 33.49% to 56.53%.

1.33 CCHP system thermodynamic performance analyses coupled with ORC and ST utilization

Asserted in [49] and shown in Fig. 34, a CCHP system with integrated ORC and ST was studied and had better thermodynamic performance, as it was versatile with greater power-production capability and more efficient in energy and waste heat. Their

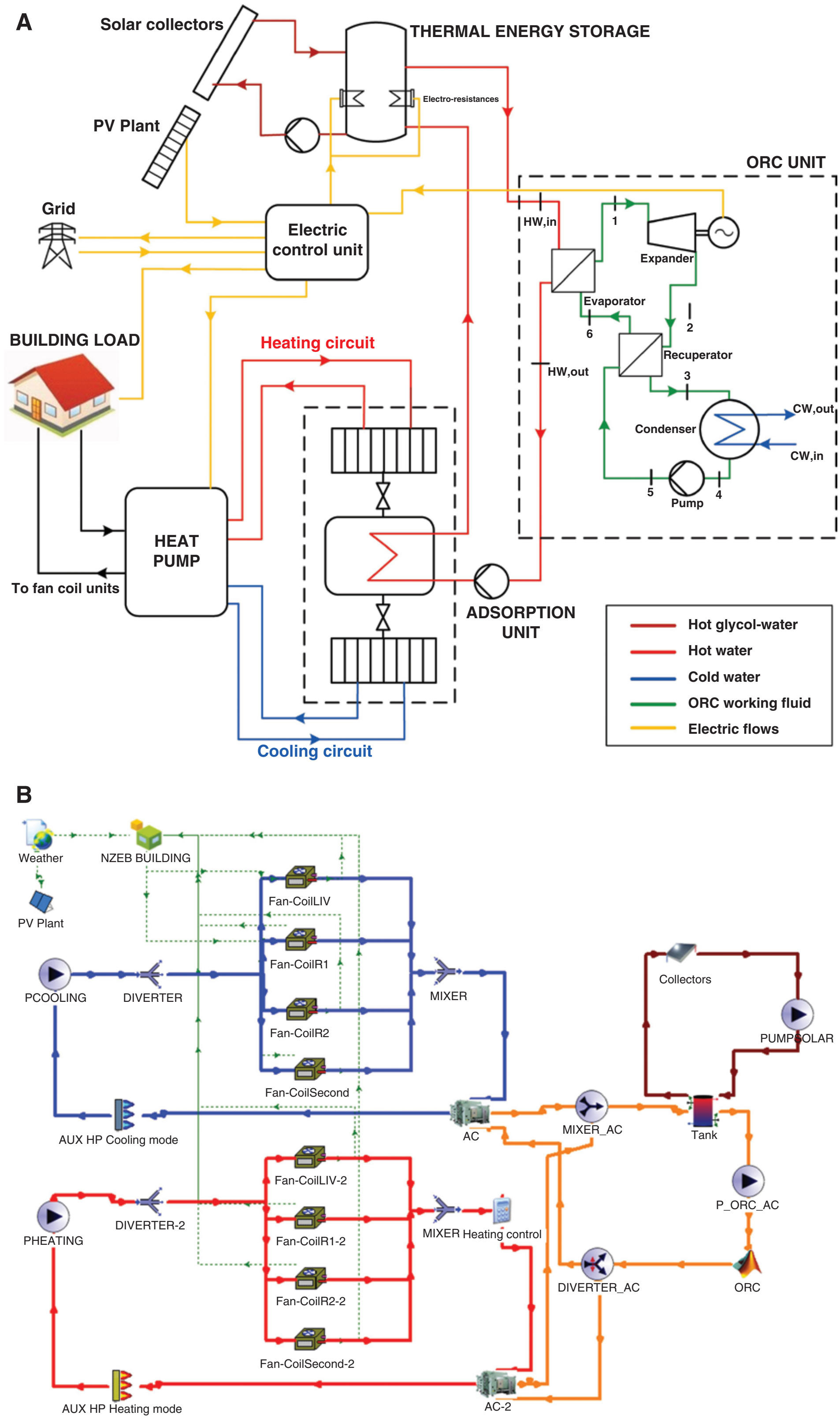

Fig. 29: The researched CCHP system. (a) Overview and (b) TRNSYS® model. Reprinted from [44] with permission from Elsevier.

proposed ORC system was driven by solar energy and exhaust heat. The energy efficiency and economy were improved by taking into account the operation technique and the optimization of the system configuration. Using the collaborative optimization approach, the researched system was applied to office and commercial buildings. With the aid of parametric analysis with a focus on the effects of the ICE-rated capacity and the ORC temperature of evaporation, the test results revealed that the typical cost per

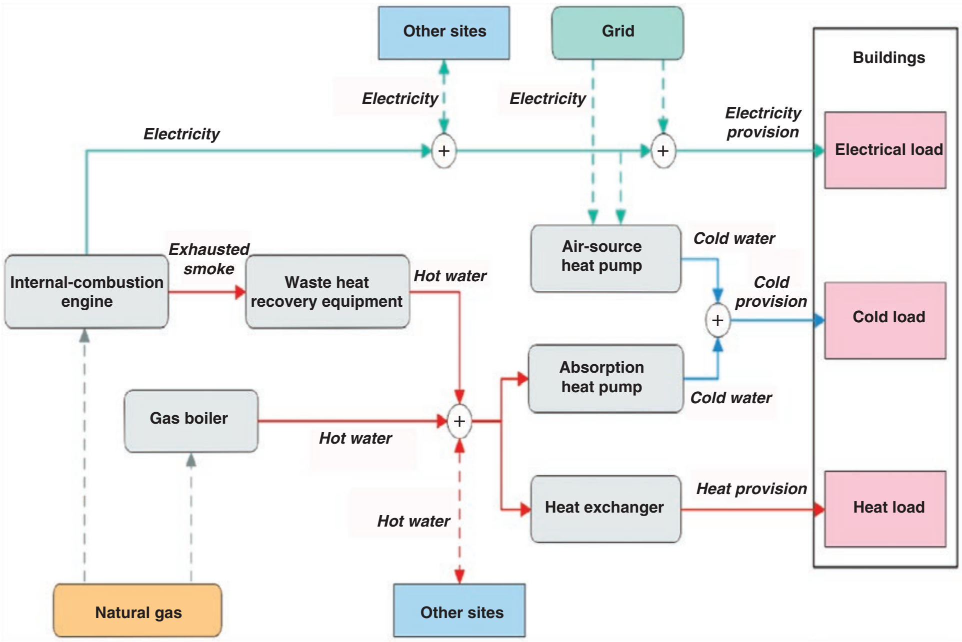

Fig. 30: Multiscenario integrated CCHP system. Reprinted from [45] with permission from Elsevier.

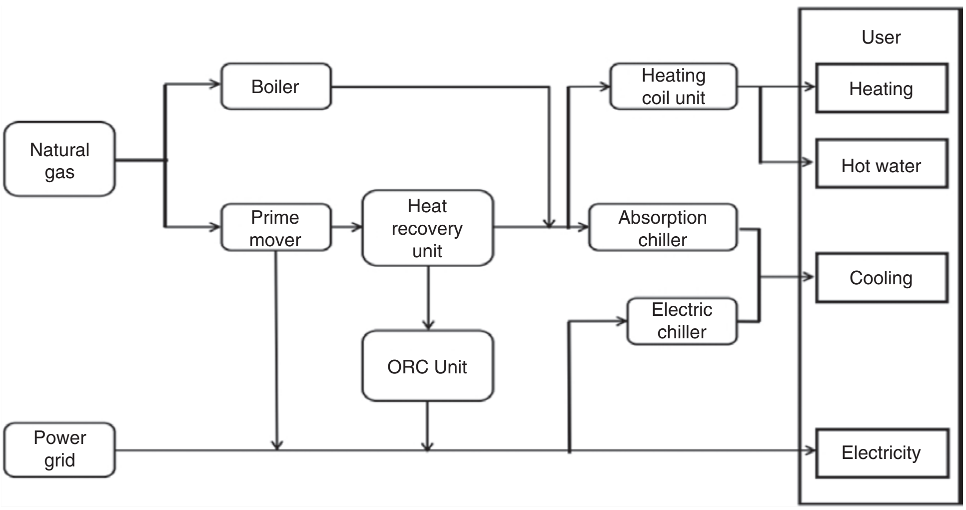

Fig. 31: A shopping-mall CCHP–ORC distributed energy system operation simulation. Reprinted from [46] with permission from IEEE.

unit of supply area of the CCHP–ORC–ST of commercial and office buildings was, respectively, \$25.9 and \$19.8 per m^2. Compared with conventional CCHP systems, this resulted in a yearly cost-savings increase of 15.0% in commercial buildings and 27.0% in office buildings.

1.34 Operation optimization of an integrated energy system in a renewable-energy-dominated future prospect considering both independence and benefit

The review in [50], summarized in Fig. 35, was an assessment of traditional CCHP systems based on fossil fuels and modern types based on integrated energy system (IESs) with renewable energy, which are less controllable and more versatile. Taking into account a stand-alone IES, optimum techniques with emphasis on independent and integrated perspectives were analysed by initially considering the holistic optimization process based on the flow of energy and optimization strategies to manage the supply and demand, and to achieve maximum benefits. Uncertainty modelling methods, such as data-driven uncertainty and multi-stage functioning methods, were evaluated to ensure the accuracy of the techniques and decrease unfavourable circumstances in the upper grid. Hybrid timescales such as a gas–electricity IES, heat–electricity IES and heat–gas–electricity IES of the various attributes of the assorted flows of energy were looked at, and game theory was considered to heighten the execution versatility of the IES. Furthermore, various energy co-ordinations were analysed to decrease all unfavourable conditions as a unit. In summary, renewable-energy CCHP systems were gradually replacing fossil-fuel CCHP systems; however, unlike fossil fuel, renewable energy was unstable due to the outages that could affect energy security; therefore, an IES approach was paramount to co-ordinate and maximize the different energy flows in both independent and dependent CCHP system set-ups.

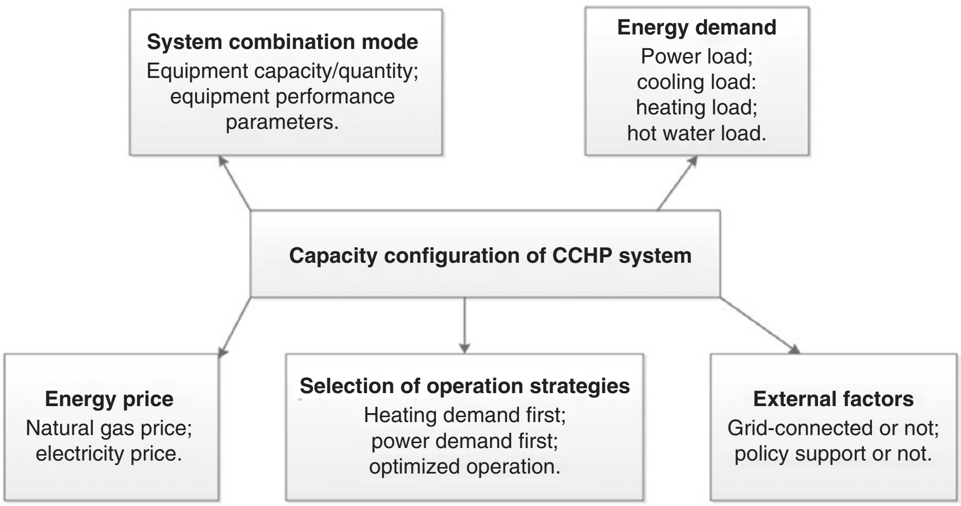

Fig. 32: CCHP system capacity configuration research ideas. Reprinted from [47] with permission from IEEE.

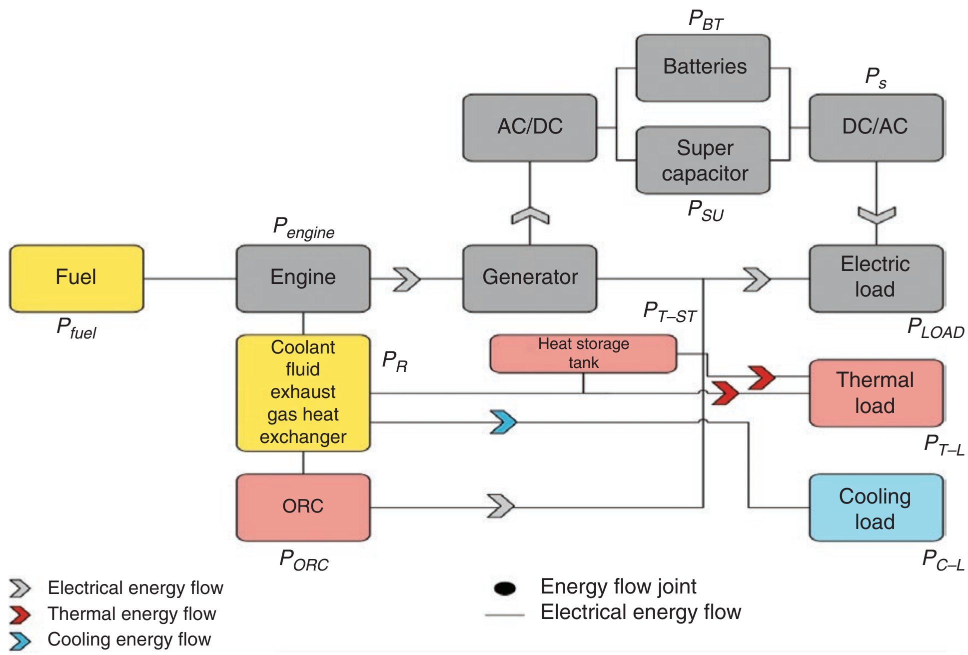

Fig. 33: The CCHP system integrated with an ORC and a hybrid energy-storage system [48].

1.35 Comprehensive performance evaluation of wind–solar CCHP system based on emergy analysis and multi-objective decision method

As researched in [51], renewable energy sources could be very promising and ease environmental pressure when used in CCHP systems. However, the use of any kind could be unreliable and costly; as a result, an evaluation method of the pros and cons of a CCHP system coupled with wind and solar (wind–solar CCHP) was required. Initially, they introduced emergy to assess the extent of sustainable development of the two systems to develop and institute a new comprehensive assessment index system by combining emergy indexes with conventional indicators. Next, a multi-objective decision-making (MODM) method rooted in fuzzy-analytic hierarchy process (Fuzzy-AHP), anti-entropy and game theory was provided to compute the weight of these indexes. Thereafter, a Kendall rank correlation coefficient was used to establish the correlation between the CCHP and the wind–solar CCHP systems. Next, considering the CCHP system as a reference, the fuzzy comprehensive evaluation (FCE) method was used to assess the integrated performance of the system. Lastly, the system was verified using a hotel in western China and sensitivity analysis was used to verify the robustness and accuracy of the suggested wind–solar CCHP system. The experimental result indicated a comprehensive performance superior to that of other CCHP systems. Their proposed method can be applied to evaluate other CCHP systems, although, when selecting, the indexes had some defects, which prevented them from finding the synthetic attributes and was rounded. Fig. 36a shows their proposed wind–solar CCHP system and Fig. 36b shows the integrated system.

1.36 Evaluation of CCHP–microgrid system: a hybrid multicriteria decision-making method

Presented in [52] was a CCHP–microgrid (MG) system that focused on the economy, environmental and energy (3E)

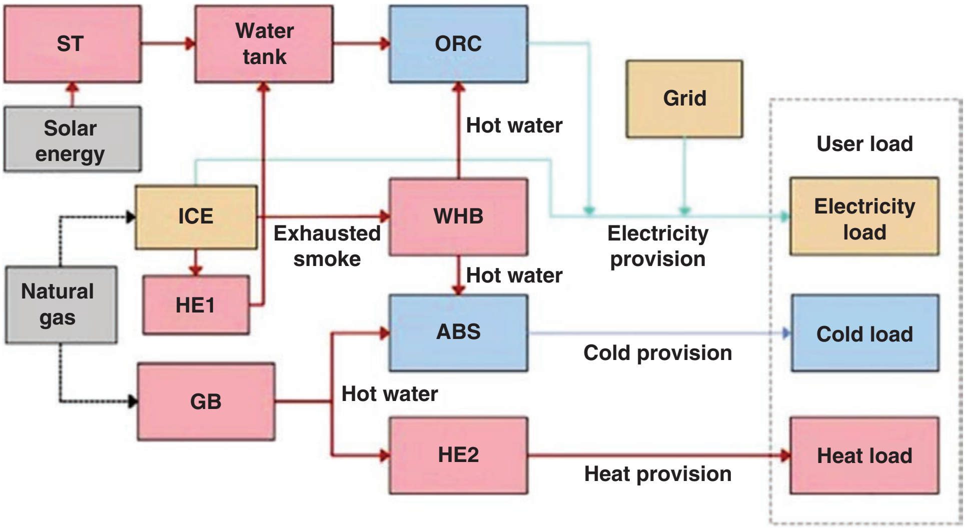

Fig. 34: CCHP–ORC–ST system under a novel operation strategy. Reprinted from [49] with permission from Elsevier.

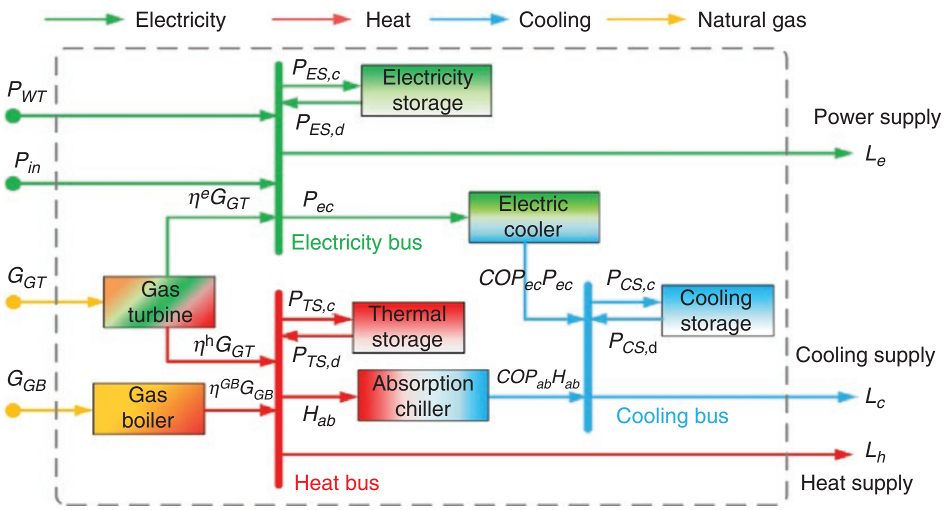

Fig. 35: The CCHP IES system in [50].

performance evaluation index construct, since CCHP–MG had these important 3E sustainable attributes. A hybrid multicriteria decision-making (MCDM) framework was then designed, which involved two modular steps as follows: (i) the integrated weighing method of indicators founded on the anti-entropy weight (AEW) method and a grey decision-making trial-and-evaluation laboratory (grey-DEMATEL) and (ii) ranking the evaluated cases by using an improved technique for order preference by similarity to an ideal solution (TOPSIS) with difference and quotient grey relation analysis (DQGRA). Their approach was tested and analysed on an eight-building-type CCHP–MG system and their findings revealed the gains of system energy supply, equivalent energy savings, energy use and equivalent emission reduction of pollutants. These are vital instruments of CCHP–MG's 3E performance and the increasing scale of the energy-supply scale, thus confirming that renewable-energy proportions were crucial to improve 3E performance. Their suggested hybrid MCDM scheme was compared with four other MCDM models and was found to have considerable potency and relevance for the 3E performance evaluation of the CCHP–MG system; however, it was essential to perform targeted modifications when applying it to other MCDM scenarios. Fig. 37a–c summarizes their research proposal.

1.37 A thermo-acoustic CCHP system for waste-heat and LNG cold-energy recovery

The study analysed in [53] was a novel theoretical study on a thermo-acoustic CCHP system for the simultaneous recovery of cold energy from liquefied natural gas (LNG) and waste heat, which are crucial to minimizing greenhouse gas emissions and removing central grids from rising power demands. Their proposed CCHP system integrated multiple energy-conversion processes into one system and enabled small-scale waste-energy utilization. Their research novelty was rooted in the acoustical matching of the impedance of the alternator and the thermo-acoustic units for total maximum exergy efficiency, in which a technique was developed to change the external electric impedance of the alternator to allow the matching of the piston displacement within the design parameters. The emission reductions, efficiency and cost savings of the optimal system were examined. Their

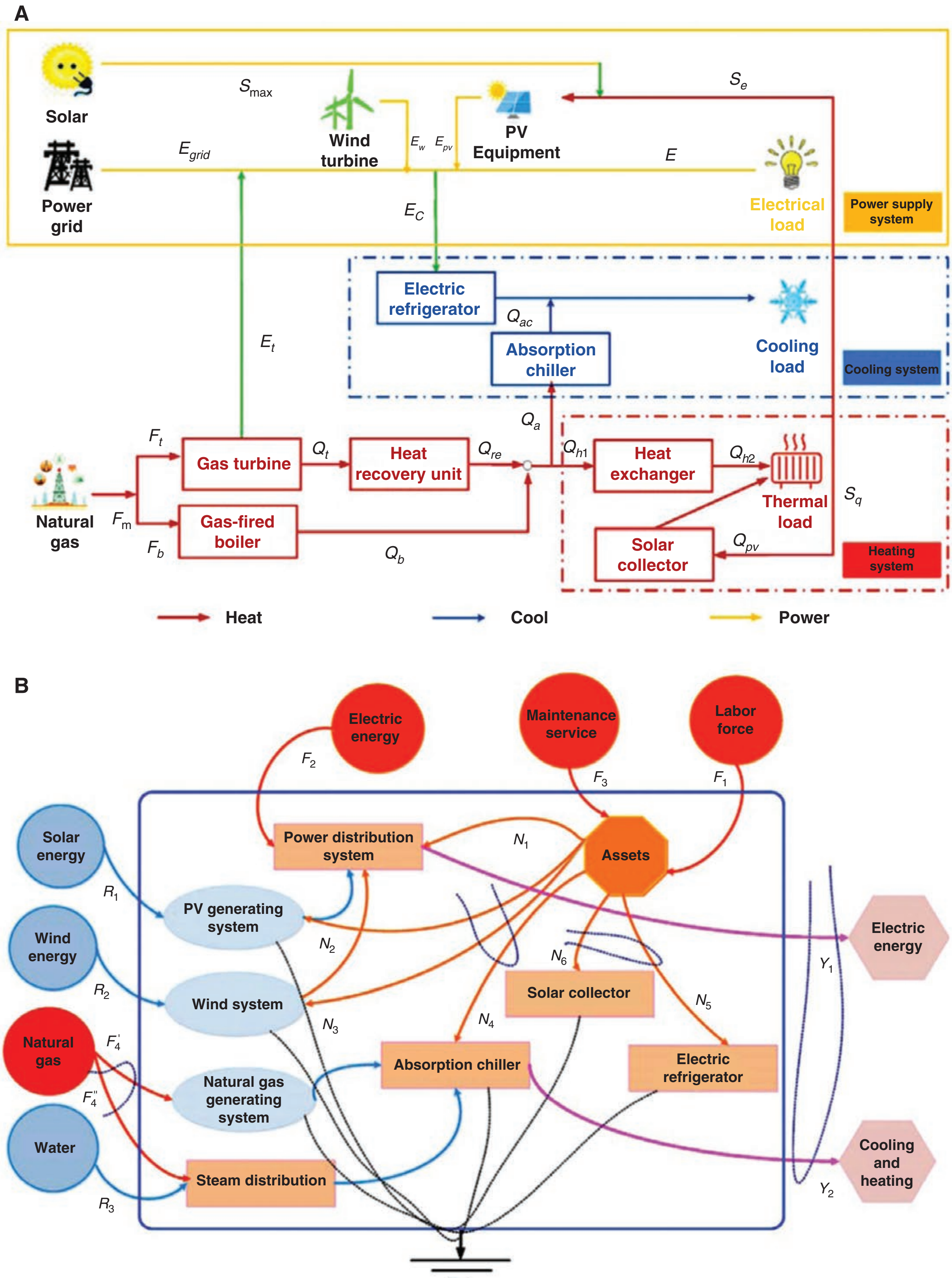

Fig. 36: (a) Wind–solar CCHP system based on emergy analysis and multi-objective decision method and (b) integrated system diagram. Reprinted from [51] with permission from Elsevier.

CCHP system, operating with a LNG cold-energy temperature of 130 K and waste-heat temperature of 500 K, attained an overall exergy efficiency of 24.1%, with a primary fuel-energy reduction of 78.4 MWh and an annual CO_2-emission minimization of 30.6 tons. Their optimized CCHP system achieved cooling of 2.19 kW at 283 K, heating of 3.55 kW at 323 K and

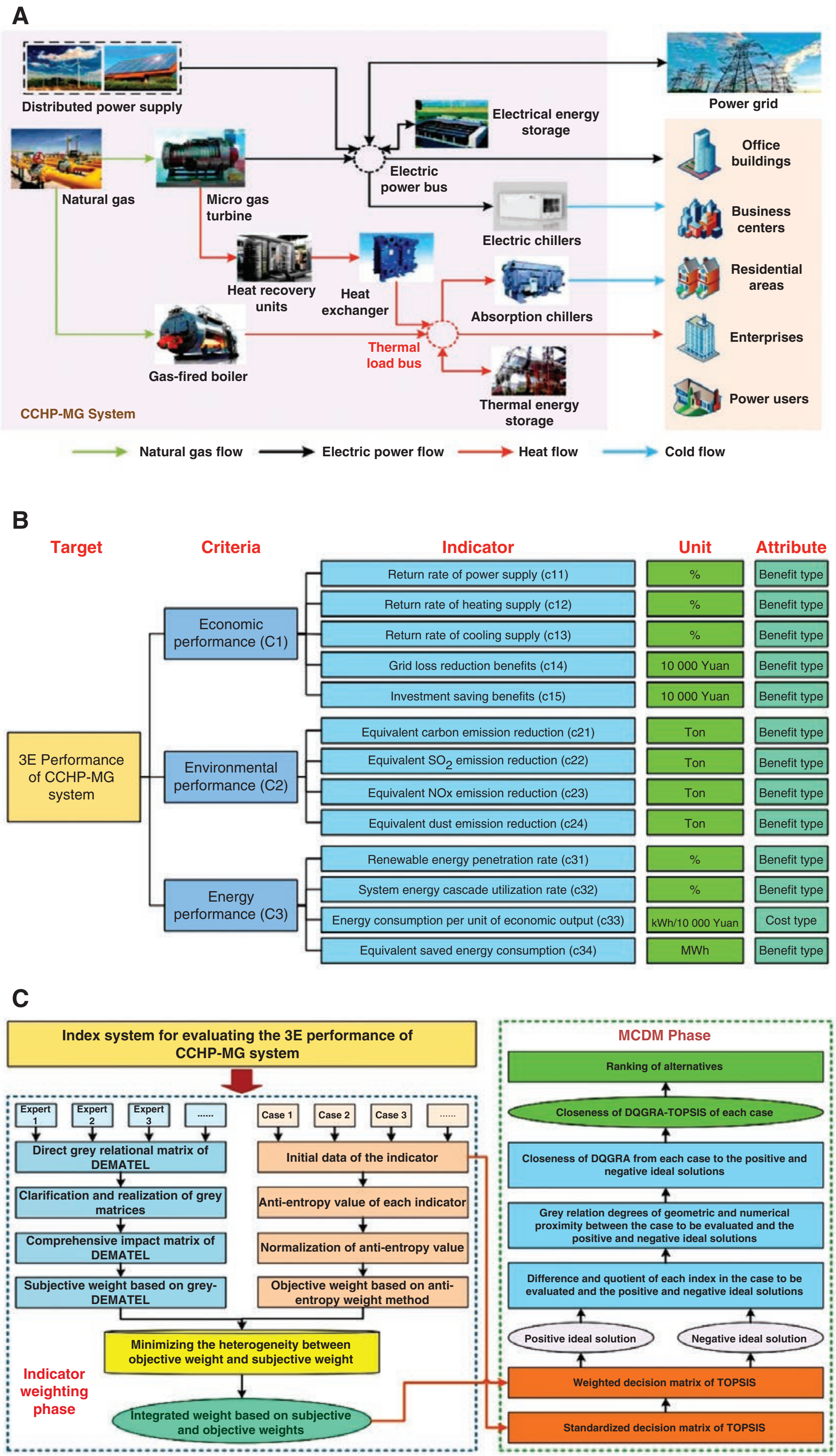

Fig. 37: (a) Energy-supply structure of the CCHP–MG system, (b) CCHP–MG system 3E performance index system evaluation and (c) hybrid MCDM model. Reprinted from [52] with permission from Elsevier.

electricity of 2.27 kW. Further correlations were done with alternative thermo-acoustic models, cogeneration systems and ORC systems, and their findings revealed that their suggested CCHP system could effectively function for assorted supply modalities, which lent itself to customization in diverse applications. Fig. 38 shows a typical example of using their thermo-acoustic trigeneration system used to recover waste energy in a LNG-fuelled vessel.

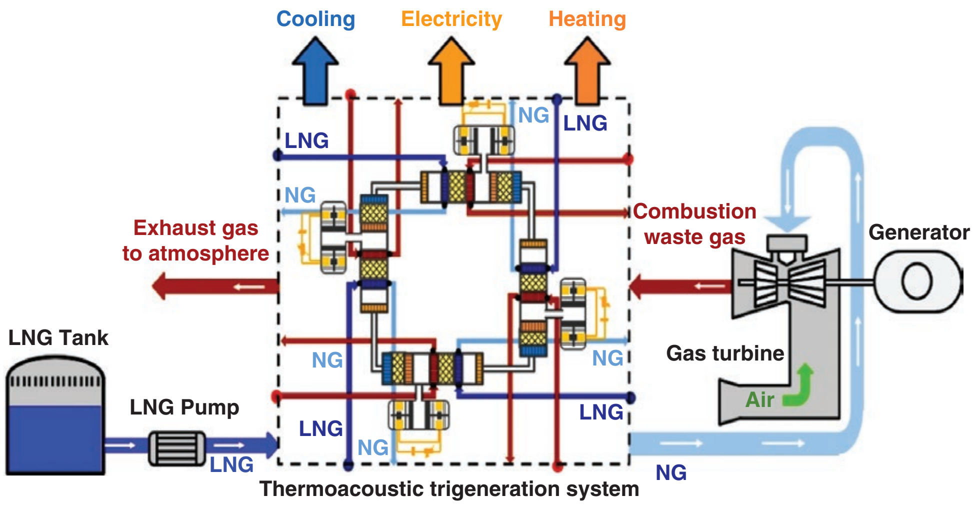

Fig. 38: Thermo-acoustic trigeneration system for waste-energy recovery in a LNG-fuelled vessel. Reprinted from [53] with permission from Elsevier.

1.38 Operation strategy for interactive CCHP system based on energy complementary characteristics of diverse operation strategies

The interactive operation of multiple CCHP systems can enhance the performance of regional IESs by exploiting the spatio-temporal augmentation of loads. However, this interaction of various energy networks in the interactive CCHP (ICCHP) system introduces new difficulties in optimization of the operation technique. As a result, [54] proposed an ICCHP system, by which an interactive operation strategy was founded on the energy-augmentation characteristics of FEL, FTL and FHL. The load heat-to-power ratio of users was initially categorized and abstracted to examine the interaction effect on the system performance and the effect mechanisms when it functions interactively between different users. In light of this, the performances of the ICCHP between two users having the same loads and between two users having different loads were investigated separately. Lastly, the effect of a third user was analysed to extend the application of the interactive operating approach to the multi-user mode. Their findings disclosed that the interaction between CCHP systems with different loads could use the complement between different loads and the energy augmentation of operation strategies to significantly enhance the performance of the ICCHP system. However, CCHP systems with identical loads could only rely on energy augmentation of the operation strategies, leading to a reduced performance improvement. Moreover, the performance of the ICCHP system would be greatly improved in the three CCHP interactive status if the third building performance was greater in autonomous operation. Fig. 39 shows their ICCHP system.

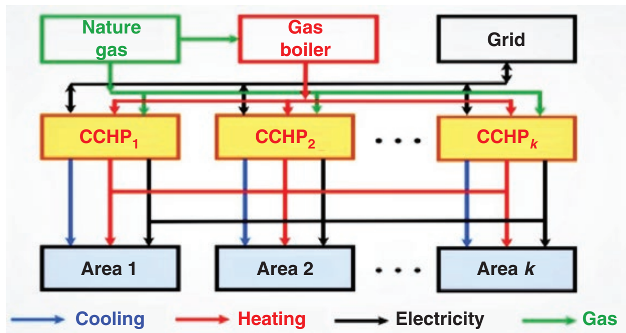

Fig. 39: The ICCHP system. Reprinted from [54] with permission from Elsevier.

1.39 Feed-forward active operation optimization for CCHP system considering thermal-load forecasting

As studied in [55], simulation software was used to obtain the energy consumption of a simulated load to optimize the functioning of a CCHP system. However, there could be a mismatch between the energy supplied and the real demand as a result of the delay and attenuation of the transmitted thermal energy. In an effort to acquire a more accurate analysis of the energy supplied, their work analysed the properties of thermal load using principal component and correlation analyses. From this model, the thermal-load forecasting model was built taking into account delay and attenuation at transmission, and a case study with real monitored data in an energy system was used, as elaborately illustrated in Fig. 40a and b. Lastly, a technique of feed-forward active operation optimization for the CCHP system was advanced, whereby dynamic correlation optimization and evaluation were performed based on the weekly forecasted thermal load in the cooling, transition and heating seasons. Their research findings showed that the linear regression correlation coefficient between the measured and forecast heating load was 90.97% and the average absolute percentage error was 6.84% for the forecasting of cooling and 5.43% for the heating loads, with a relative error distribution mainly between –10% and 10%. In summary, the performance of the CCHP system was better than those of the separate production systems based on the predicted thermal load. The maximum integrated performance index was 68.81% and was acquired during the weekend in the cooling season.

1.40 A two-stage stochastic–robust optimization for a hybrid renewable-energy CCHP system considering multiple scenario-interval uncertainties

As stated in [56], the optimal capacity of the device could force the hybrid CCHP system integrated with renewable energy to have important economic, environmental and energy benefits with low grid dependence. Nevertheless, the various uncertainties presented great difficulties in the modelling framework and the associated solution technique. In light of this, their study was undertaken and the novelty lay in the integration of stochastic and robust optimization into a two-stage stochastic–robust

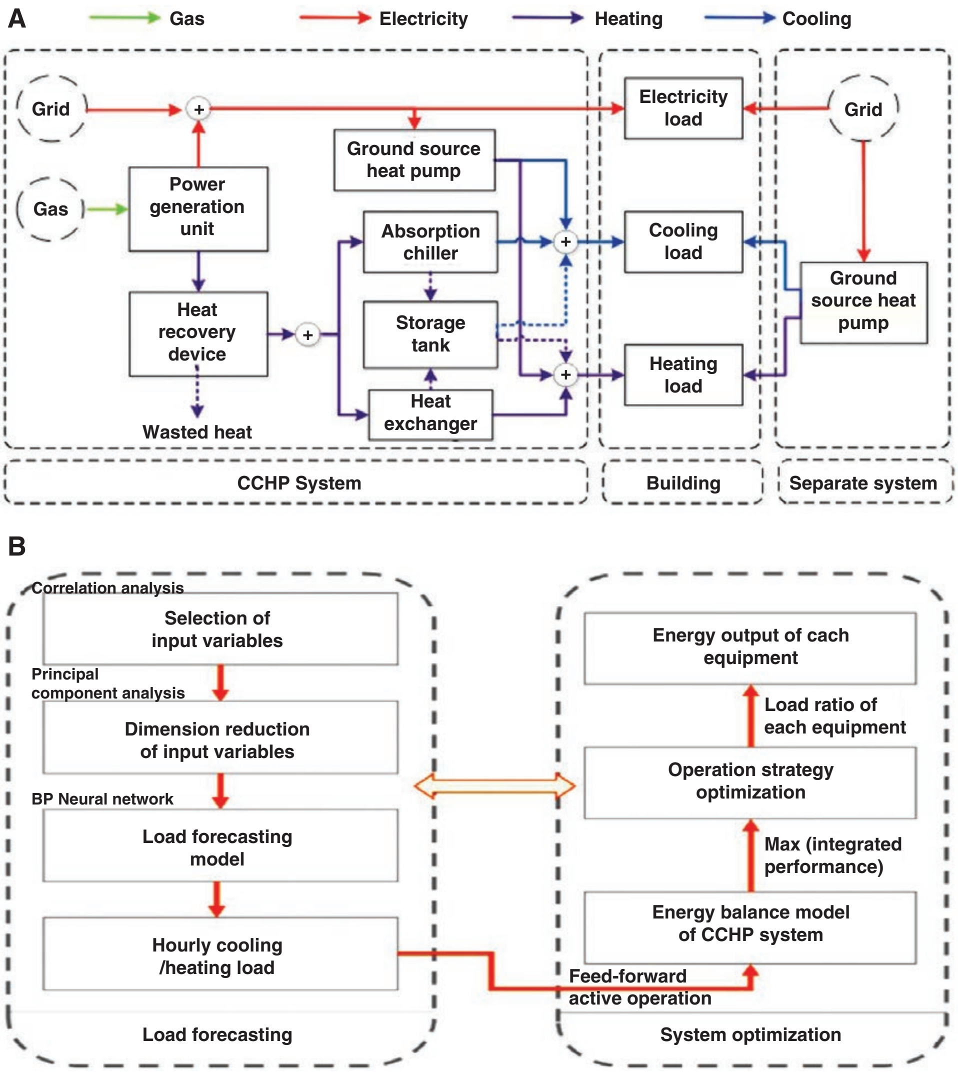

Fig. 40: (a) The CCHP and separate production systems and (b) feed-forward active operation optimization technique. Reprinted from [55] with permission from Elsevier.

capacity-optimization model to adequately address the multi-uncertainties and to robustly obtain optimal results. Fig. 41a shows the physical structure of the hybrid CCHP system and the framework of the optimization problem, while Fig. 41b illustrates the framework of the two-stage multi-objective stochastic–robust hybrid optimization, in which multiple uncertainties were integrated into their model and modelled by incorporating the stochastic hierarchy scenario-generation strategy into the robust box uncertainty set. Multistage coupling and the multi-objective optimization problems were handled, respectively, by the column-constraint generation and the ε-constraint approach. Their scheme was tested using an industrial park and their findings revealed that the appropriate scenario number could make scenario-based stochastic optimization to save 97.71% of the calculation time and safeguard the optimized results reliability. However, the uncertain budget value greatly affected the installed capacity of the successive device, while it hardly affected the discrete device numbers. The installed capacities of the renewable-energy generators (PV system and wind turbine) and the electrical energy storage (EES) tremendously determined the economic performance of the hybrid CCHP system. The rapid increase in the capacity of renewable-energy generators with a mean growth rate of 37.01% and EES with an average growth rate of 136.37% translated into a sharp growth in total cost with a higher mean growth rate of 29.07% compared to 12.09% of the total mean growth rate.

1.41 Optimal capacity configuration of CCHP system with improved operation strategies using an improved multi-objective multi-universe algorithm

Researched and established in [57] was a multi-objective capacity-optimization model to determine the optimal configuration set-up for assorted techniques. They developed improved-FEL (IFEL) and improved-FTL (IFTL) strategies to adequately control the flow of energy. The IFEL and IFTL strategies allowed full use of redundant energy produced during the operation of the CCHP system, effectively minimized fuel consumption and improved system energy efficiency of the system. In addition, they also suggested an improved multi-objective multiverse optimization (IMOMVO) algorithm that could effectively optimize the configuration of the CCHP system under different strategies. IMOMVO incorporated an opposition-based learning mechanism, population-guidance mechanism, dominance rank and seagull attacking operator

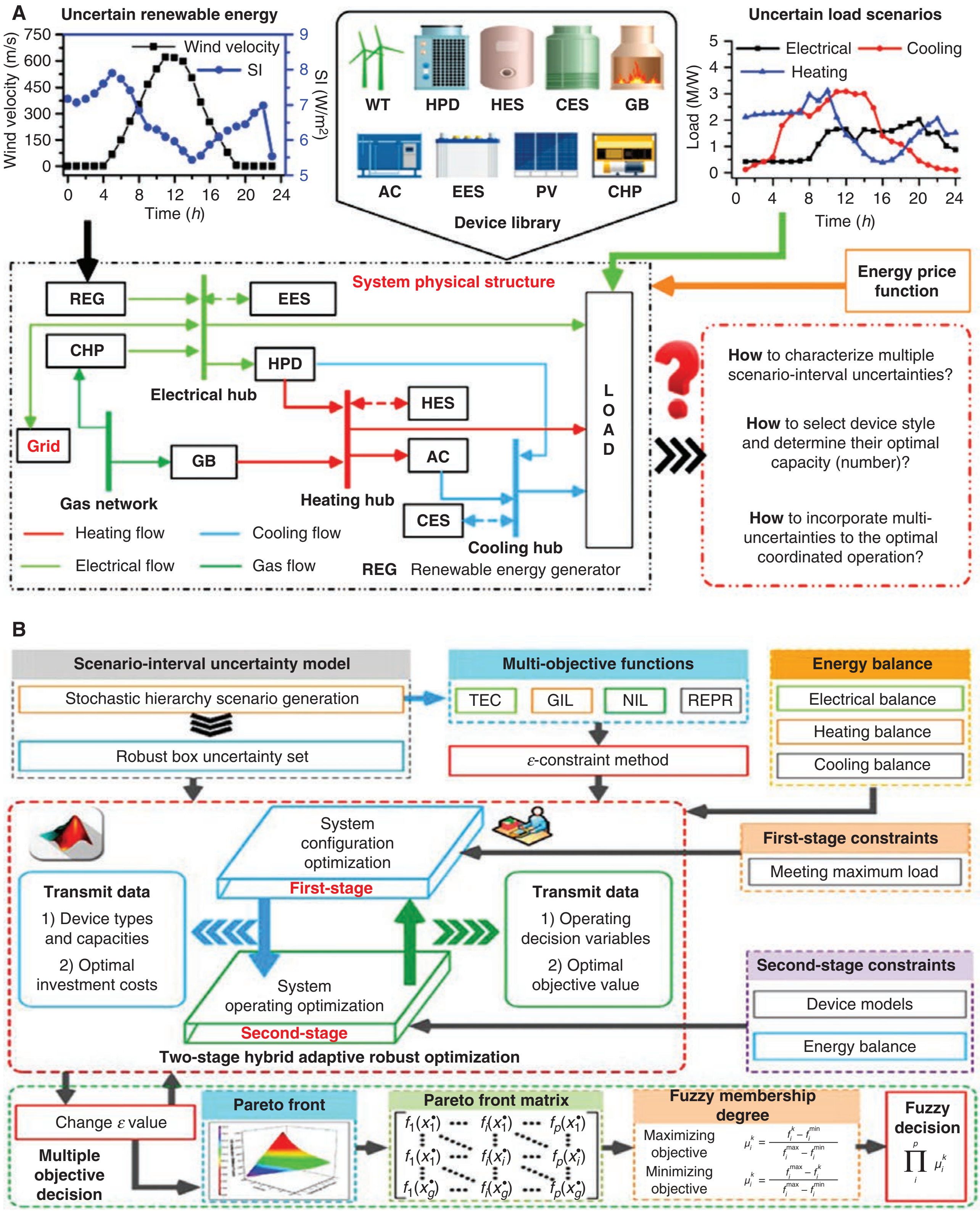

Fig. 41: (a) Physical structure and optimization problem framework of the hybrid CCHP system and (b) two-stage multi-objective stochastic–robust hybrid optimization framework. Reprinted from [56] with permission from Elsevier.

into the traditional multi-objective multiverse optimization algorithm. The TOPSIS was employed to obtain the optimal solution of each strategy under economic, energy and environment objective functions. The IFEL, IFTL, FEL, FTL and FHL operation strategies were examined in a large hotel equipped with CCHP systems. Their findings demonstrated that the Pareto solutions acquired by using the proffered IMOMVO algorithm were evenly distributed and could provide a set of representative solutions.

Furthermore, the configured system under the suggested IFEL technique could achieve energy efficiency, CO_2-emission reductions, annual cost-saving ratios and PESR of 67.09%, 47.91%, 14.94% and 31.65%, respectively; as a result, it outperformed all other strategies. Fig. 42 shows their CCHP system.

1.42 Proposal and comprehensive thermodynamic performance analysis of a new geothermal CCHP system

Proposed in [58] was a new CCHP system applied to geothermal energy. In the proposed system, a water heater was employed to use the exhaust geothermal water for heating provision, while the throttled valve of the basic flash cycle was replaced by an ejector for cooling output. Detailed mathematical models were instituted and validated to assess system performance. Based on the basic condition of geothermal water at 170°C, the suggested system exergy efficiency was 44.34% and the total power, heating and cooling output was 10.283 68 MW. Furthermore, exergy-loss analysis demonstrated that the water heater, ejector, turbine, condenser and flasher components had a sizable enhanced space to minimize the exergy destruction for the system-performance improvement. The flasher, condenser, turbine and ejector also had high exergy destruction, respectively, in order of magnitudes of 14.41%, 15.53%, 16.32% and 19.71%. Finally, the findings of the parametric analysis suggested that there was an optimal flash pressure (~140 kPa) to maximize the exergy efficiency. Within the discussed ranges, both the temperature of the increase in the water-heater outlet and the condenser temperature would damage the efficiency of the system's exergy, while a bigger evaporator temperature was advantageous for the efficiency of the system's exergy. Exergy-loss analysis showed that the greatest exergy destruction occurred in the water heater with a proportion of 24.76% of total system exergy destruction. However, the economic and environmental aspects were not covered. Fig. 43 illustrates their CCHP system.

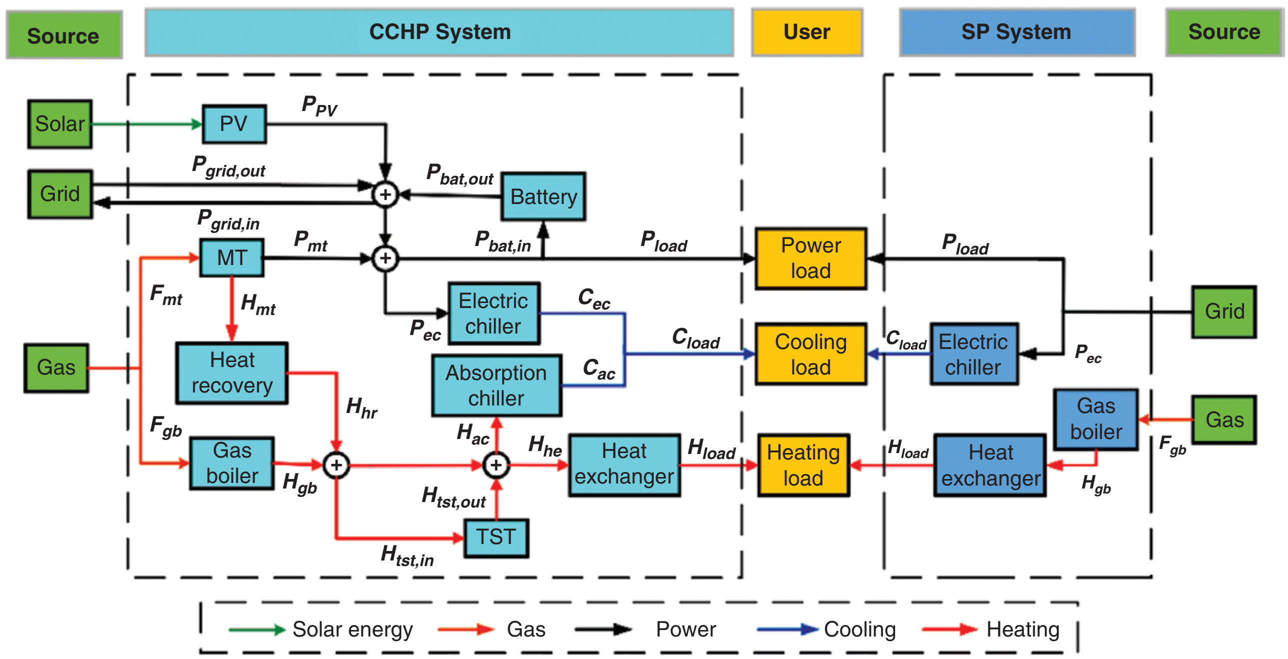

Fig. 42: Illustration of the CCHP and SP systems. Reprinted from [57] with permission from Elsevier.

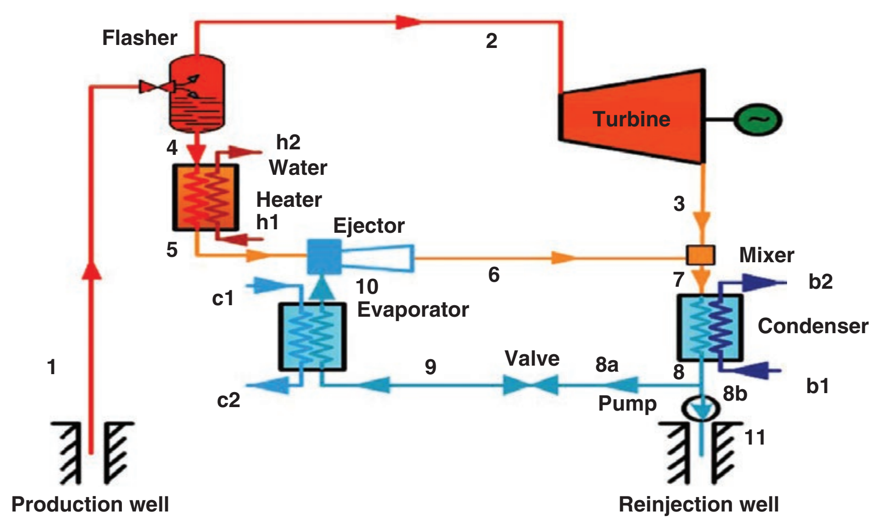

Fig. 43: Proposed CCHP system in [58].

1.43 Multidimensional analysis of solar hybrid CCHP systems with redundant design

As stated in [59], integrating PV into CCHP systems gave economic, energy-efficient and environmentally friendly benefits. However, this PV CCHP hybrid system had many components, which made it susceptible to failure at any time during operation, although at the expense of cost and bulk, redundancy could improve the availability and reliability of systems. In light of this, their work compared and analysed, with a focus on economy, environment and energy, the performance of three PV CCHP systems, namely the single-device operation PV CCHP (SPV CCHP) system, the multi-device parallel operation without redundancy design PV CCHP (MPV CCHP) system and finally the redundantly designed PV CCHP (RPV CCHP) system. A two-stage optimization technique was used and the three systems were tested in an office building in Beijing, China. Their findings disclosed that the RPV CCHP system, followed by the MPV CCHP system, was the best in terms of PESR, CO_2-emission-minimization ratio and yearly total cost-savings ratio, and, furthermore, the performance of the RPV CCHP system was 16.20% better than the MPV CCHP system and 13.99% better than the SPV CCHP system. RPV CCHP increased its subsystem's availability/reliability to >99.98% and reduced the annual failure cost by 144 654 USD. Finally, a sensitivity analysis was performed to determine how the systems would react to changes in electricity and natural-gas prices, and all three systems under-performed. Fig. 44 shows the energy flow of their redundancy-searched PV CCHP system.

1.44 Thermodynamic analysis and optimization of two low-grade energy-driven transcritical CO_2 CCHP systems

The system proposed and analysed in [60] was an efficient transcritical CO_2 CCHP system in which the ejector refrigeration (ER CCHP) cycle was incorporated into the power cycle to recover low-grade energy. Their proposed ER CCHP system was benchmarked with a throttle refrigeration cycle (TR CCHP) so that the throttle refrigeration cycle was also incorporated into the power cycle. Thermodynamic models were constructed and the effects of evaporation temperature and turbine parameters on the two systems were evaluated from energy and exergy perspectives. Their findings disclosed that due to the introduction of the ejector, the ER CCHP system could produce more net output power than the TR CCHP system. Furthermore, parametric optimizations were also conducted to attain respective maximum net output power and the optimal exergy efficiencies of both systems at different heat-source temperatures. Under design conditions and with a 230°C heat source and a turbine inlet pressure of 20 MPa, their results showed that the TR CCHP and ER CCHP systems could, respectively, produce optimal exergy efficiencies of 26.9% and 27.9% and maximum net output powers of 7.5375 and 7.9103 MW. Fig. 45a and b, respectively, illustrates the ER CCHP and TR CCHP systems.

1.45 Optimization and performance analysis of the CCHP–GSHP–SE system under different start factors

As articulated in [61], a CCHP–GSHP solar energy system (CCHP–GSHP–SE) could provide a reliable energy source; however, due to fluctuations in the building load, the energy flow of the system could not adequately meet the demand for building load, leading to a low efficiency of the equipment. Their paper proposed, taking into account the multiterminal supply of energy and the transfer properties of the loads, that the equipment performance could be improved effectively by setting a GSHP start factor (GSHP-SF). When the load level of the GSHP was set to lower than the SF, the GSHP would stop working and handed over part of the load to other equipment, which, in doing so, effectively improved the device's performance and this was tested using different values of GSHP-SF. The annual comprehensive performance (ACOP) and the annual useful ratio (AUR) were first suggested by them to characterize the devices' performance. Their findings proved that, when the SF was 0.4, the comprehensive performance

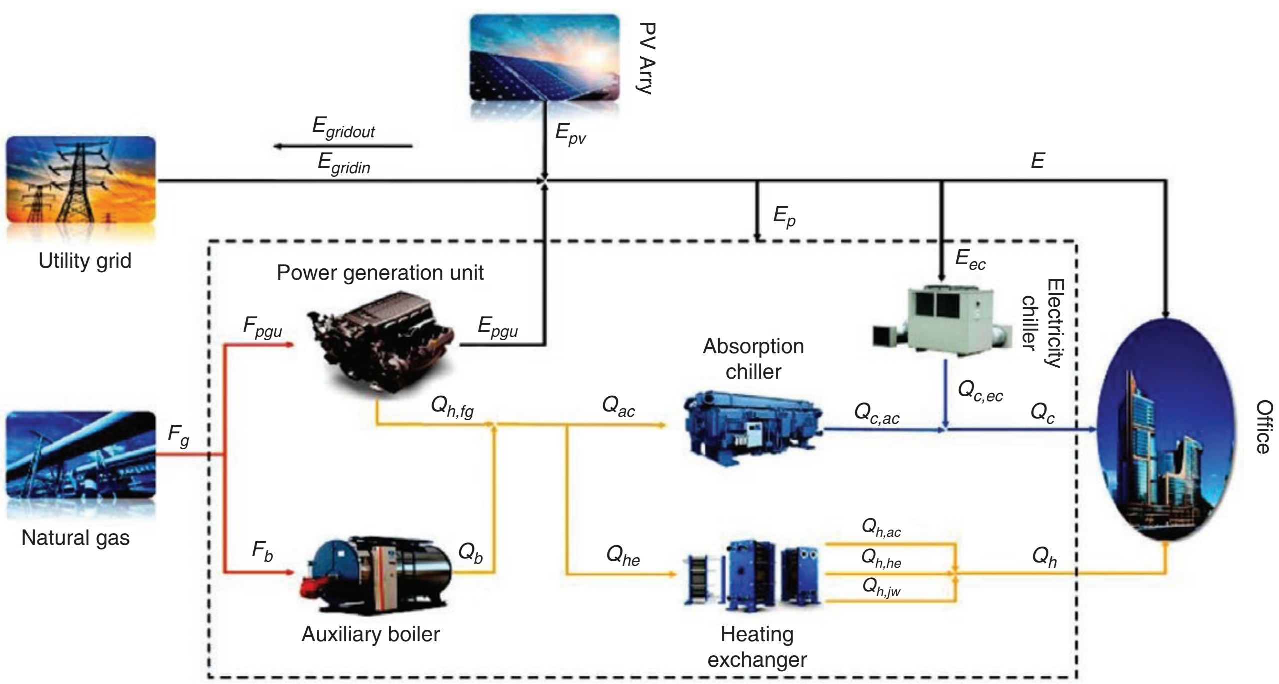

Fig. 44: The PV CCHP system energy flow. Reprinted from [59] with permission from Elsevier.

was the best. Using a traditional CCHP–SE system as a reference, two performance tests were carried out: (i) CCHP–GSHP–SE was compared to CCHP–SE and the economic-saving ratio, the energy-saving ratio and the CO_2-emission-reduction ratio were, respectively, 0.68%, 5.25% and 4.58% and (ii) CCHP–GSHP-SF–SE was also compared to CCHP–SE and the economic-saving ratio, the energy-saving ratio and the CO_2-emission-reduction ratio were, respectively, 5.35%, 14.49% and 12.93%. Finally, in terms of comprehensive performance, the CCHP–GSHP–SE and CCHP–GSHP-SF–SE systems, respectively, reached 3.05% and 10.92% relative to the CCHP–SE system. In summary, CCHP–GSHP-SF–SE gave the best performance and, with a suitable GSHP-SF setting, the double effect of GSHP for the comprehensive performance of a CCHP system could be fairly improved. Fig. 46 exemplifies their CCHP–GSHP–SE system.

1.46 4E analysis of a SOFC CCHP system with a LiBr absorption chiller

Indicated in [62], 4E is an evaluation criterion that focuses mainly on the energy, exergy, economy and environmental (4E) benefits of a CCHP system. In their work, a new CCHP system based on a solid-oxide FC (SOFC) with a LiBr absorption chiller and water tank was studied with emphasis on the influence of SOFC working conditions on its static and dynamic performances. Furthermore, the effects of the FC stack and working conditions (current density, operating temperature, inlet-gas pressure, hot-water mass flow, chilled-water mass flow and cooling-water mass flow) on the 4E multicriteria assessments (output power, system energy efficiency η_{sys}, exergy efficiency η_{exe}, annual reduction in cost C_{sys} and annual greenhouse gas emission R_{GHG}) were also examined. Their findings disclosed that operating temperature and current density could significantly affect the performance of the stack and the system, which could also be simultaneously influenced by the working conditions of the absorption chiller. Furthermore, the operating temperature proportionally increased the generated electrical power, but inversely proportionally decreased the generated thermal power. The heating power was also reduced by increasing the mass flows of the hot, cooling and chilled waters, which consequently increased the cooling power and CoP. (i) The effect of the current density: increasing the unreacted H_2 increased the waste heat and consequently increased the electrical power initially to 6.15 kW, which subsequently dropped to 5.61 kW. The thermal and cooling powers increased, respectively, by 20% and 32.03%, and the CoP decreased by 7.59%. The 4E system evaluation indices showed that the η_{sys} rose from 83.51% to 84.78%, whereas the η_{exe} fell from 29% to 16%. C_{sys} increased

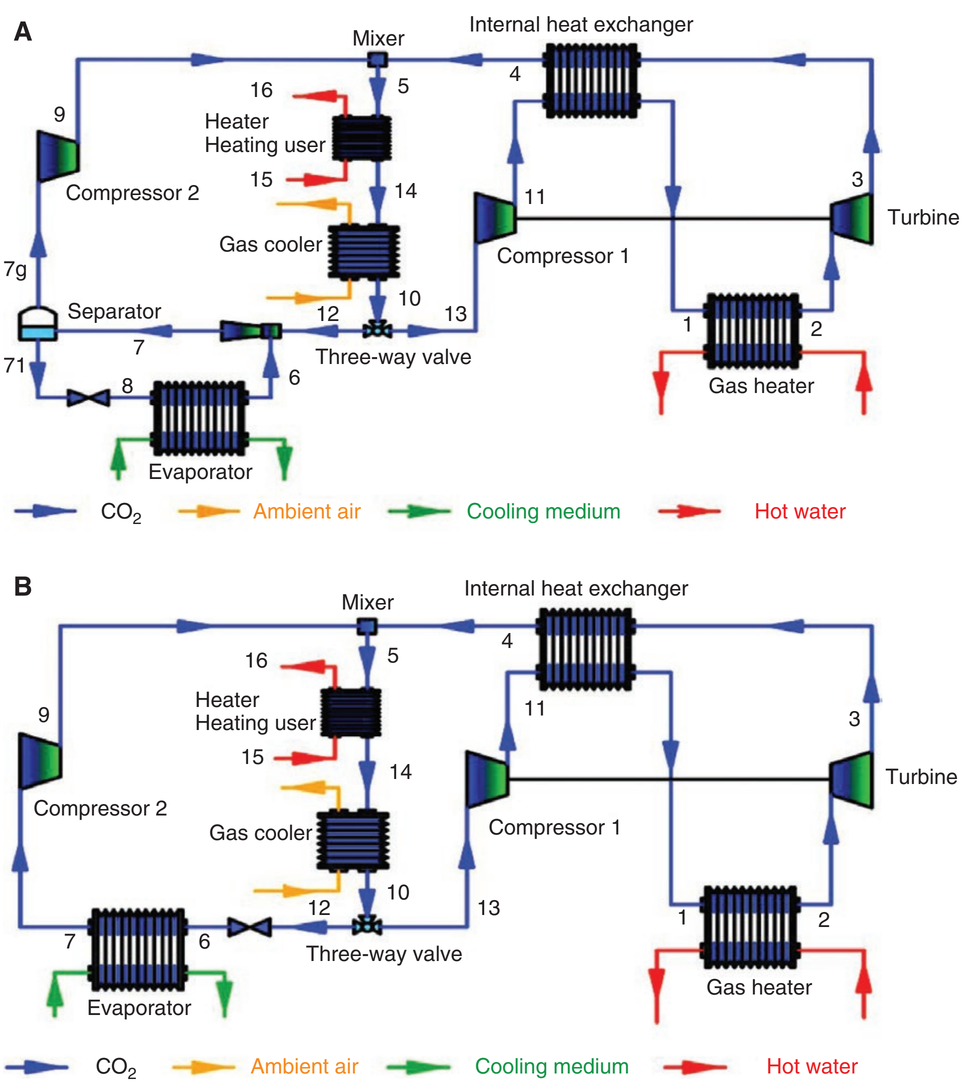

Fig. 45: (a) ER CCHP and (b) TR CCHP systems. Reprinted from [60] with permission from Elsevier.

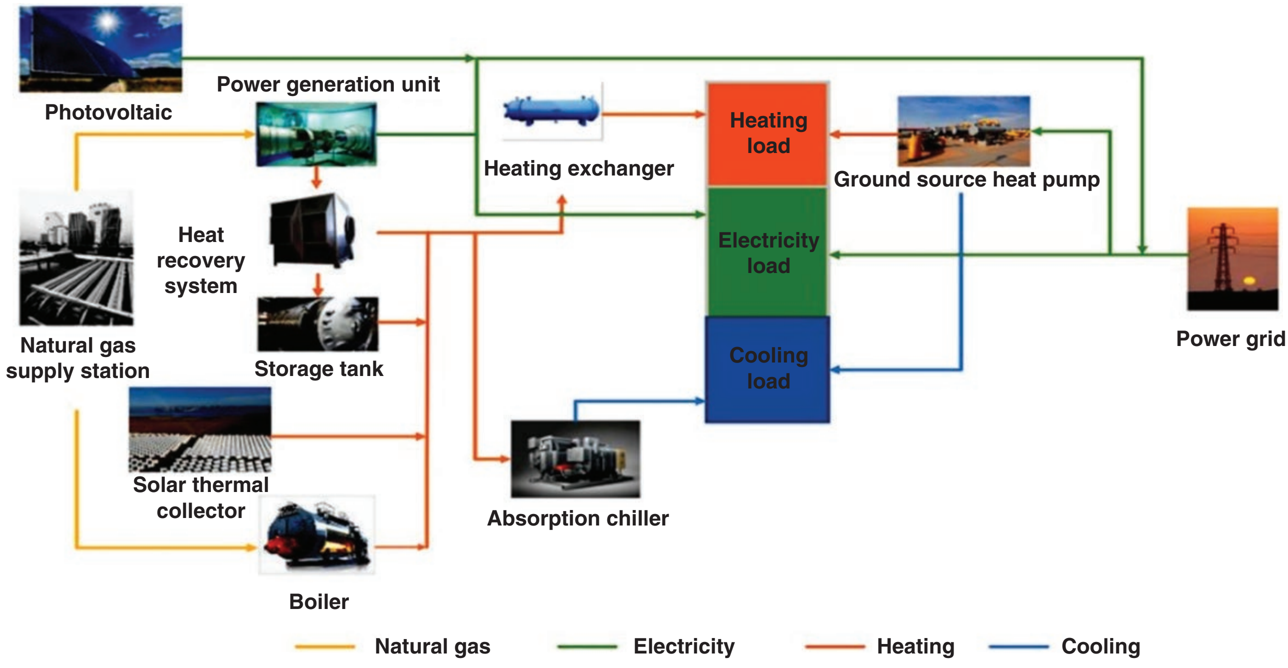

Fig. 46: The CCHP–GSHP–SE system. Reprinted from [61] with permission from Elsevier.

from 8.32 × 10^3 to 2.80 × 10^4 USD, and R_{GHG} increased from 8.16 to 30 tons. (ii) The effect of operating temperature: increasing it, respectively, increased the CoP and electrical power from 73% to 75% and from 1.98 to 6.27 kW; the cooling and thermal powers, respectively, dropped from 1.64 to 1.45 kW and from 6.12 to 3.63 kW. The 4E system evaluation indices showed η_{sys} increased from 68.85% to 77.93%, whereas η_{exe} rose from 10.56% to 22.3%. C_{sys} remained at 1.249 × 10^4 USD, while R_{GHG} increased from 17.22 to 21.07 tons. Refer to the full text on the 4E multicriteria assessments when the other four working-condition effects of (iii) inlet-gas pressure, (iv) hot-, (v) chilled- and (vi) cooling-water mass flows were varied. Fig. 47 shows the SOFC CCHP system.

1.47 Tri-objective optimization of two recuperative gas-turbine-based CCHP systems and 4E analyses under optimal conditions

Presented in [63] were two CCHP systems, with the same recuperative gas-turbine topping cycle evaluated based on exergy, energy, exergo-economic and environmentally friendly (4E) gains. The bottoming cycle of the first CCHP system (System I) consisted of a steam turbine, two absorption cooling systems, a regenerative recuperative ORC and a water heater, as shown in Fig. 48a, while in System II pictured in Fig. 48b, the recuperative–regenerative ORC was completely replaced with a condensing steam-turbine cycle. A parametric assessment was conducted to initially establish the effect of important functioning conditions of the performance of the proposed systems. These operating conditions were then used to perform a tri-objective optimization employing a Pareto envelope-based selection algorithm (PESA) II, taking into consideration the energy and exergy efficiencies, as well as the total cost rate as the objective functions. Therefore, an entropy-TOPSIS decision-maker evaluation was conducted to institute the best optimum solution from the Pareto front. Subsequently, the values of the objective functions were correlated under the optimum and base-case conditions to show the optimization benefits, which revealed that the energy and exergy efficiencies were fairly improved in both systems, with System I having energy and exergy efficiencies of 58.33% and 43.55%, respectively, compared with 58.21% and 42.93% of System II. Their overall cost rates, respectively, declined by 9% and 5.3% for Systems I and II, with corresponding cost rates of \$3727.3 and \$3930 per hour, with System I being more cost-effective. In addition, the respective payback periods for Systems I and II were 10.83 and 13.27 years. Moreover, under their optimal conditions, the total energy output and efficiencies of both systems were almost equal, although the overall cost rate of System I was considerably lower relative to System II. Furthermore, System I also had the least specific CO_2 emissions of 91.75 kg/MWh, as opposed to System II of 91.94 kg/MWh. Furthermore, the gas-turbine cycles alone of Systems I and II, respectively, accounted for 75.1% and 72.3% of the total exergy-destruction cost. Similarly, the gas-turbine cycle was also responsible for 57.1% and 63.6% of the total capital investment cost rate of Systems I and II, respectively. In conclusion, System I was a better option.

1.48 Performance evaluation of a novel CCHP system integrated with MCFC, solar gas–steam cycle and LiBr refrigeration system

In [64], a novel CCHP system was suggested, comprising a molten carbonate FC (MCFC), a combined solar gas–steam cycle (ISCC) and a double-effect absorption lithium bromide (LiBr) refrigeration system as exemplified in Fig. 49. According to the principle of energy-cascade utilization, their study began with thermal-performance analysis, whereby a portion of the high-temperature waste gas released by the MCFC was channelled to the heat-recovery steam generator (HRSG) for further waste-heat use and the remaining high-temperature waste gas was fed to the MCFC cathode to generate CO_3^{-2}. Subsequently, the influence of solar energy on the system performance was investigated, using it to substitute part of the heating load of a high-pressure economizer in the HRSG. Modelling was done using Aspen Plus® software and finally the effects on the system performance were evaluated using the exergy- and sensitivity-analysis methods; the electricity generated by the MCFC increased with temperature and rate

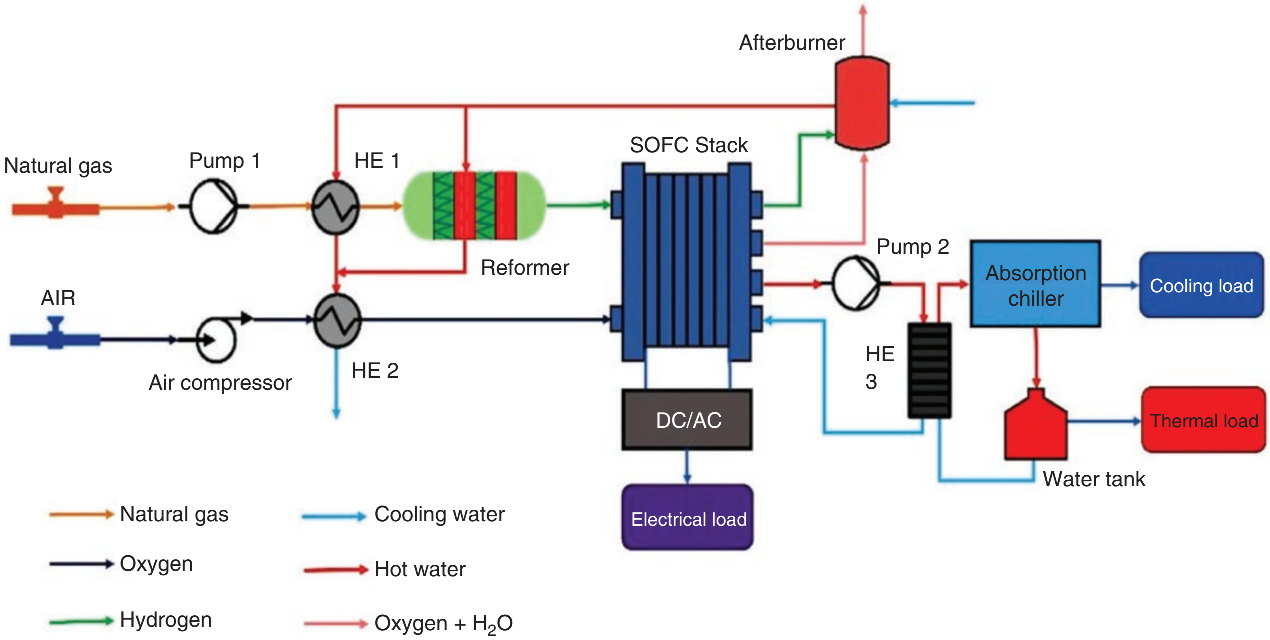

Fig. 47: SOFC CCHP system working principle. Reprinted from [62] with permission from Elsevier.

of utilisation of hydrogen. The outcome showed that the new CCHP system could generate 494.1 MW of electricity (with a total system exergy loss of 354.08 MW), 7.55709 MW of cold with 1.09 CoP and 57.95625 MW of heat. The overall thermal energy and the total system exergy efficiencies of their system, respectively, were 61.64% and 61.69%. Benchmarking the research results of their new system with a similar system that had electricity generation of 110.544 MW, exergy efficiency of 58.4% and lower specific CO_2 emission of 167.9 g/kWh, they noticed and concluded that their CCHP system had better ability to perform work and with lower CO_2 emission, as well as simultaneously meeting the demands from users for electricity, heating and cooling.

1.49 Review of environmental aspects of CCHP systems

Examined in [65] are the green features of CCHP systems when used in different sectors. They opined that urbanization and economic growth require a high energy supply to homes and that this must be done in environmentally friendly ways. One way to meet the requirement is through CCHP systems, which can also be used in different sectors including, but not limited to, health facilities, airports, wastewater-treatment plants, H_2-production plants, shopping malls, food industries, desalination systems, etc. By doing so, the benefits include mitigating high gas and electricity costs, reducing energy usage (water, heat, cold and electricity), low greenhouse gas emissions and improving productivity and performance. In addition, integrated solar energy can be used in tropical areas with high sunshine to handle the high cooling demands. They note that the key drivers to minimizing carbon and water footprints are (i) enhancing the system components such as the combustion engine and (ii) extending the system to multigeneration systems and incrementing productivity of the product with the lowest carbon footprint, which is cooling, especially where more cooling is needed. Energy-storage systems must be used and will come in handy during peak and outage periods. In general, the incorporation of absorption and electric chillers will improve the CoP of CCHP systems. Since the distance between the power plant and the cooling centres affects the performance of the system, they recommend that absorption chillers are desirable for distances of <5 km, while electric compression chillers are better for distances of >9.3 km and with the use of a water tank to improve the performance of the chillers. They claim that the use of CCHP systems can reduce coal use and can result in an 11% reduction in environmental damage, and that the carbon tax index can also help to curb carbon emissions if adequately used. CCHP systems are suitable for countries and regions with low gas prices and high electricity prices, although they can increase operating costs. Fig. 50 represents a CCHP system for home use.

1.50 Review of integration and optimization of CCHP systems

Reviewed in [66] is a comprehensive analysis of various technologies and techniques for the integration and optimization of distributed energy or CCHP systems. This is paramount, as the reduction in fossil fuels and climate change pose immense difficulties in sustainable development, and various means of addressing the growing energy demands in a cost-effective, energy-efficient and environmentally friendly way have become the focal point worldwide. In their investigations, potential forms of existing energy technologies such as cogeneration systems, fuelled systems, ST energy systems, waste-heat-recovery systems, wind energy systems, geothermal energy systems and energy-storage systems that can be integrated were foremost summed up. Next, the various application cases such as building, neighbourhood, district and city levels were summarized. Thereafter, the concerns at each level were assessed, from which whether the allocation of benefits needs to be taken into consideration was the fundamental concern at the neighbourhood level; at the district level, the main concern was how to adequately break down the district into several subdistricts; and lastly, at the city level, the key was to make provisions for worthy guidance for synergized city development. Furthermore, various optimization techniques were tailored to establish the

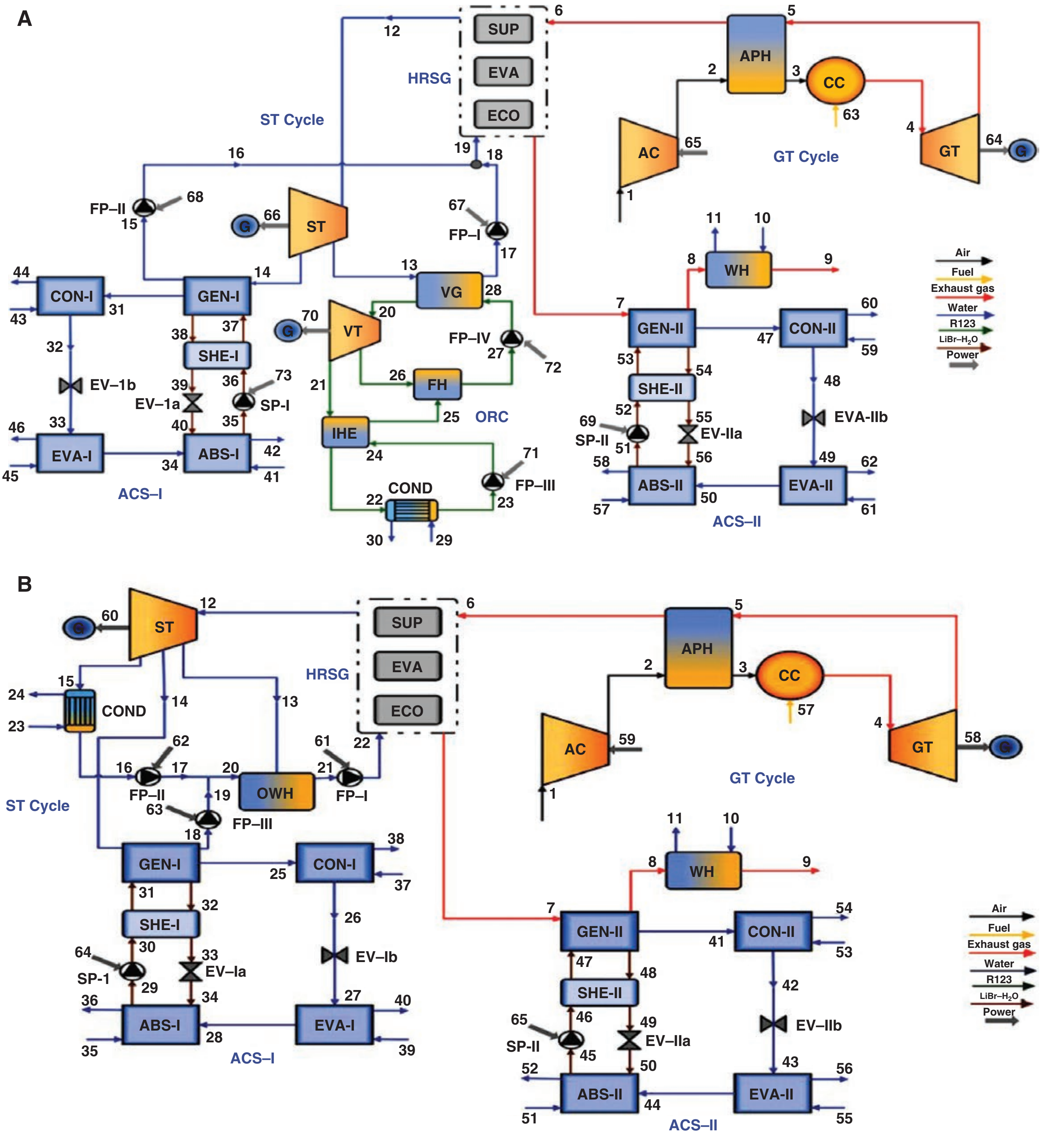

Fig. 48: (a) CCHP System I and (b) CCHP System II. Reprinted from [63] with permission from Elsevier.

optimum equipment capacity, network layout and hourly operation methods to manage and enhance the total performance of the distributed energy systems. Furthermore, dynamic trends in energy demands, technology and energy costs must also be considered. In conclusion, to advance the growth of distributed energy systems, future research difficulties can be categorized into five groups: (i) green energy sources, (ii) affordable, energy-efficient and environmentally friendly conversion technologies, (iii) accurate network framework, (iv) accurate load-prediction methods and (v) long-term planning models. Most of these aspects were discussed in detail in their full paper.

Table 1 simply summarizes the reviewed CCHP systems with highlights of the main contributions of each case study, as well as their advantages and disadvantages where applicable. Note that some highlights, advantages and disadvantages are left out not because they are not important, but because of space constraints. The goal here is to provide some insightful reference information. If necessary, the reviewed abridged case studies or the cited full papers can always be referred to.

Table 2 summarily compares the CCHP systems reviewed with emphasis on and analysis of the topological highlights of each case study under the following key aspects: (i) energy sources,

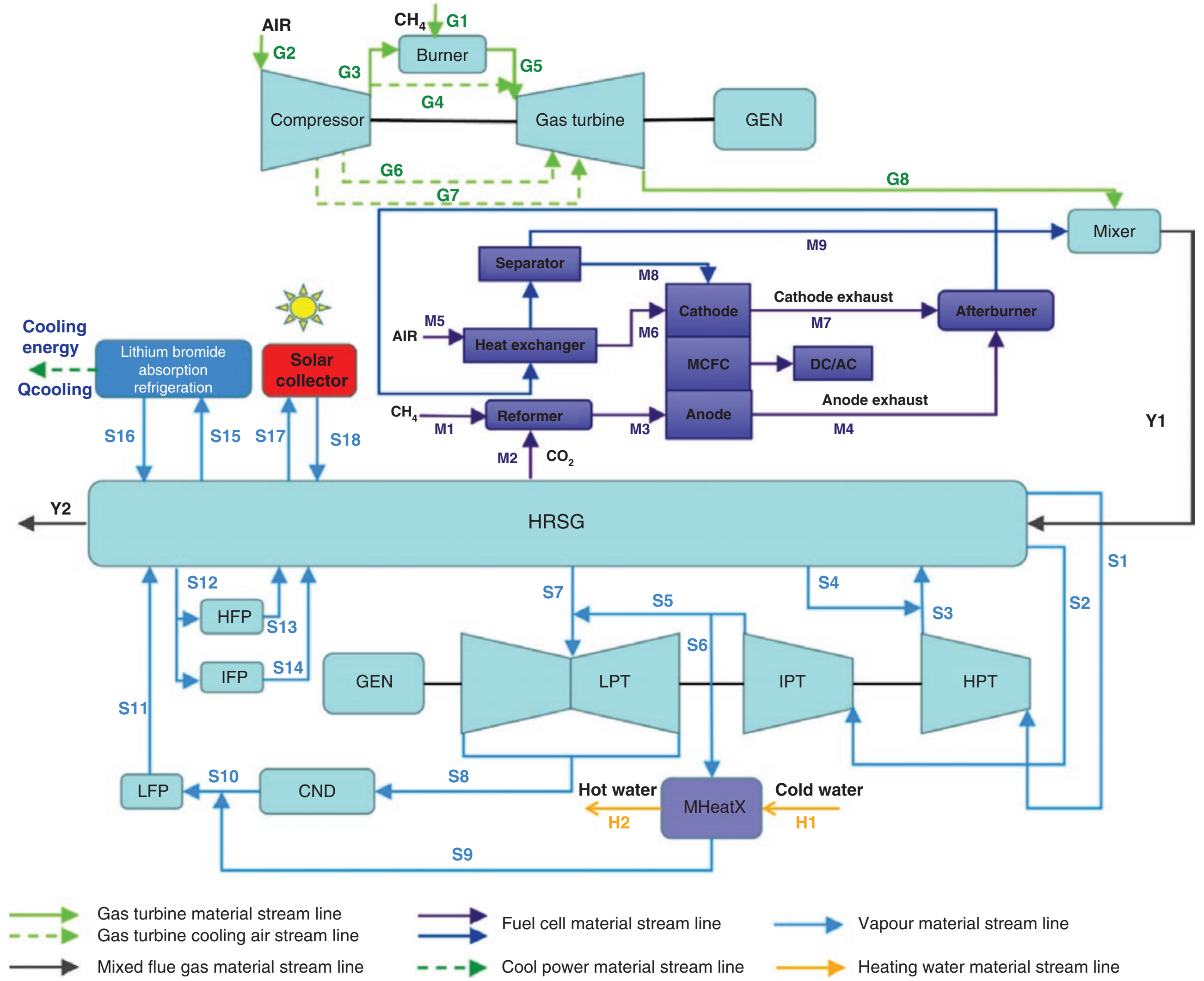

Fig. 49: The proposed CCHP system. Reprinted from [64] with permission from Elsevier.

fuels and PGU; (ii) energy-storage and energy-conversion mechanisms; and (iii) optimization and control techniques. Note that the topological analysis of Table 2 is simply obtained from the figures, textual and graphical/tabular data presented in each case study; therefore, if a particular field is left empty, it is because the original case study lacks or did not provide the information in any form that can be sensibly included in the table.

Table 3 summarily compares the reviewed CCHP systems with emphasis and analysis on the quantitative highlights of each case study mostly under the following main aspects where relevant: (i) 3E/4E—energy efficiency, exergy efficiency, economy (costs) and eco-friendliness; (ii) CCHP—cold, heat and power productions; and (iii) places where the case studies were researched. Note that the quantitative analysis summary in the Table 3 summary is simply obtained from the figures, textual, graphical and tabular data presented in each case study; therefore, if a particular field is left empty, it is because the original case study lacked or did not render the information in a way that could be reasonably summarized in the table.

2 FCs

FCs are further assessed, as CCHP systems rooted in FCs are of interest to our proposed CCHP system under research. According to [67, 68], in 1839, William Grove brought the concept of FC to light and coined it as the 'gaseous voltaic battery' and in 1842 notified Michael Faraday. As stated in [67–92], FCs are electrochemical devices that can constantly produce electricity from chemical energy and, in the process, give by-products of water and heat, provided that they are always furnished with fuel (H_2) and reactant gas (O_2) in the case of PEM FC. This process is shown in Fig. 51 and is chemically represented by the following electrochemical equation [69]:

$$4H_2 + 2O_2 \rightarrow \text{Electricity} + 4H_2O + \text{Heat} \quad (1)$$

According to [67–69, 72], hydrogen FCs (based on a PEM) are clean and renewable energy sources that are slowly becoming alternative energy sources with various uses. However, as elaborated on in [69] and depicted in Fig. 52, FCs are generally vulnerable to a phenomenon called 'fuel starvation': delay or lack of H_2 and or O_2 flow, which causes FCs to have difficulty in coping with transient current demand when loaded, thus decreasing the FC voltage. As researched in [73], fuel (H_2)/O_2 starvation must not even occur momentarily, as it will cause severe and durable destruction to the FC electrocatalyst and furthermore lower its power/energy-supply reliability, capability, durability and efficiency.

Examined in [74], a FC has low power density but high energy density; therefore, a FC cannot (i) provide the high electric power

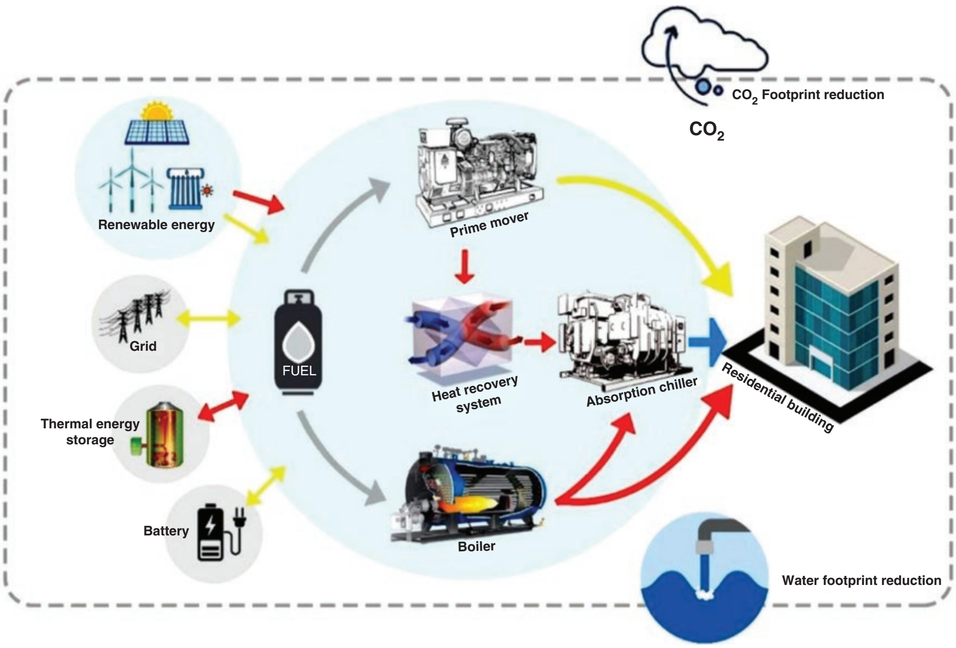

Fig. 50: Residential application of a multifunctional CCHP system in [65].

initially needed to immediately switch on a load (e.g. when a hybrid electric vehicle (HEV) starts up), (ii) rapidly react should there be an abrupt variation in the load current (e.g. when a HEV accelerates [75, 76]) and (iii) absorb the regenerative power (e.g. when a HEV decelerates or brakes). As a result, an additional device that stores energy (e.g. a rechargeable battery) and or a source of power with a faster dynamic response (e.g. an ultracapacitor bank), combined with power- and energy-conversion devices and EMS, are required to assist FCs [77–79]. Consequently, various efforts have been made to tackle this crucial issue of FC fuel starvation. In light of this, the following is a précis of some techniques that constitute but are not limited to the six noted schemes; namely (i) FC assisted with fuel-flow-rate control, (ii) FC assisted with a battery, (iii) FC assisted with an ultracapacitor/supercapacitor (UC/SC), (iv) FC assisted with a battery and SC/UC, (v) FC assisted with a CombiLit and (vi) FC assisted with PV and SC/UC.

2.1 FC assisted with fuel-flow-rate control

This approach, as presented in [69, 80], requires the flow rate of the fuel hydrogen (H_2) and the reactant gas oxygen (O_2) to be continuously controlled to follow the variations in the FC current, by controlling the current gradient of the FC, or by maintaining a regular fuel-flow rate to ensure that the FC always has adequate fuel flow. However, this approach is inefficient, as the fuel flow is habitually invariable at the highest value. Fig. 53 exemplifies this method.

2.2 FC assisted with battery

Usually, a battery (of type lithium-ion (Li-ion), nickel metal hydride, lead acid, etc.) has a higher power density [74] relative to a FC. As a result, it reacts quickly and provides peak power should there be a high transient current demand from the load, thus helping the FC to avoid sluggishness due to 'fuel starvation'. In addition, a FC can only provide electrical energy, but cannot store it. As a result, a battery also offers storage during regenerative braking [81]. However, batteries take a long time to charge and their useful life depends on their state of charge and depth of discharge [74]: the faster the rate of charge and discharge, the more likely is that the battery life will be shorter. Fig. 54 illustrates this assisting technique.

2.3 FC assisted with ultracapacitor (UC) or supercapacitor (SC)

A supercapacitor or ultracapacitor has the utmost power density and the best transient response compared with FCs and batteries. According to [82], they are therefore the preferred energy-storage devices for high-current applications, as they can be rapidly discharged or charged in a short period of time. This very fast transient response makes UC the most suitable device to help FCs to circumvent the initial phenomenon of 'fuel starvation' [74]. This method is depicted in Fig. 55.

2.4 FC assisted with battery and supercapacitor or ultracapacitor

In this approach, the battery and UC or SC are used to supply power for short intervals of peak power needs, e.g. during acceleration in the case of HEVs, in which reliable acceleration demands both high energy and high power densities [81]. As shown in Fig. 56, having both UC or SC and the battery is crucial, because relatively UC or SC has the lowest energy density but the highest power density, while the battery has moderate energy and power densities [83]; therefore, the use of both schemes helps FCs when simultaneous peak power and energy is needed. In addition, the battery provides EES.

2.5 FC assisted with CombiLit

According to [84], CombiLit is a composite device that stores energy by coalescing in a cell the electrodes of a peak-power-density supercapacitor with a high-energy-density Li-ion battery. This set-up, together with a FC, can be adapted to give changing levels of peak power discharge, increase in energy storage, lengthy cycle life and low costs. The principle is similar to that in Fig. 56.

2.6 FC assisted with solar cell and supercapacitor

In [85], a solar cell (PV array) replaces the battery energy source. Energy sources (FCs and solar cells) have high energy

Table 2: Topological analysis summary of reviewed CCHP systems

CCHP research reviewed	Energy sources/fuels/PGU Energy-storage/conversion mechanisms Optimization/control techniques	CCHP research reviewed	Fuels/PGU/energy sources Energy-storage/conversion mechanisms Optimization/control techniques
Case Study 2.1 [2] (Zhang J, *et al.*, 2018)	Natural gas (NG)/petrol/ICEs/power grid	Case Study 2.10 [18] (Cozzolino R, 2018)	LT-PEM FC with inverter
	GSHP/absorption chiller (AC)/Heat Exchangers (HE) 1 and 2		Half-effect LiBr absorption chiller/heat storage tank (HST)
	FEL/FTL/FHL		Thermochemical models/EUF/ExUF/TPES
Case Study 2.2 [4] (Badea N, *et al.*, 2010)	PV/natural gas/Stirling engine/burner	Case Study 2.11 [9] (Wang Z, *et al.*, 2018)	NG/IAT gas turbine/generator/grid
	Thermal/electrical/cold storage/chiller		AC/HE/combustor/auxiliary boiler/HST
	Summing up each part efficiency and usage		FEL/FTL/FHL
Case Study 2.3 [31] (Maraver D, *et al.*, 2013)	Biomass/biomass burner	Case Study 2.12 [16] (Lu S, *et al.*, 2018)	Grid/PV/GSHP/micro gas turbine
	Thermally activated chiller		Electric cooler/AC/flue-gas water HE/gas boiler
	Thermodynamic model/LCA		Sequence control configuration/sequential quadratic programming/feedback correction
Case Study 2.4 [7] (Xu AD, *et al.*, 2014)	Micro turbine	Case Study 2.13 [15] (Li B, *et al.*, 2019)	ICE/GSHP
	Combustor/recuperator/HE/generator		Electric chiller/AC-heater/HE/gas boiler
	Spot and peak-valley pricings		MCP/maximum electric efficiency/GA/SGA
Case Study 2.5 [25] (SU Z, *et al.*, 2016)	Biomass/biogas/PV/STC/power grid	Case Study 2.14 [14] (Jiang R, *et al.*, 2017)	ICE with cooling and dehumidification/electrical grid
	Auxiliary boiler/absorption chiller/HEs		Electric compression cooler/AC/absorption dehumidifier
	Genetic algorithm		Thermo-economic model/constrained NLP/analytic hierarchy process
Case Study 2.6 [27] (Wongvisanupong K, Hoonchareon N, 2013)	Gas turbine/PV/electrical grid	Case Study 2.15 [12] (Chen X, *et al.*, 2018)	H_2/air/5-kW PEM FC stack/power grid
	Heat-storage tank/absorption chiller/auxiliary boiler		HE/hot-water tank/AC/humidifier/compressor/pumps
	Online real-time LP using MATLAB®		Evolution algorithm/3D Pareto solutions
Case Study 2.7 [26] (Zhao H, *et al.*, 2018)	Gas micro turbine/PV/wind turbine/grid	Case Study 2.16 [19] (Ebrahimi M, Derakhshan E, 2018)	Hydrogen-storage tank/air compressor/LT-PEM FC/battery
	Battery/boiler/refrigerator		TEC/plate heat exchanger/heat ST
	HOMER optimum economic model		Simulated FC/TEC mathematical models validated using published literature data
Case Study 2.8 [8] (Wang R, *et al.*, 2018)	H_2/PAFC/SOFC/electrical grid/electrolyser/ H_2-storage tank	Case Study 2.17 [17] (Mehrpooya M, *et al.*, 2017)	NG/heat recovery/Stirling engine/turbine/MCFC
	Heat exchangers/heat-storage tank/LiBr absorption cooler unit/heater/inverter		Double-effect LiBr/H_2O absorption chiller/combustion chamber
	Use valley grid electricity period to produce H_2 and CCHP to produce power during peak/flat grid electricity periods		Energy and exergy analyses methods used to evaluate processes performance

Table 2. Continued

CCHP research reviewed	Energy sources/fuels/PGU Energy-storage/conversion mechanisms Optimization/control techniques	CCHP research reviewed	Fuels/PGU/energy sources Energy-storage/conversion mechanisms Optimization/control techniques
Case Study 2.9 [11] (Wang JL, *et al.*, 2014)	Natural gas/ICE/TEG		
	Condensing heat exchanger/hot-water-storage tank/JHE/DAC		
	Designed based on the energy-cascading utilization principle		
Case Study 2.18 [34] (Wu D, *et al.*, 2019)	Solar energy/NG/ICE/ORC/STCs	Case Study 2.27 [43] (Lingmin C, *et al.*, 2021)	Natural gas/wind/solar energy
	Heat Exchangers 1 and 2/gas boiler/WHR/absorption unit (ABS)/air-source heat pump (ASHP)		Five different configuration cases tested. Set-up having all of EES/HES/AC/EC/boiler/HE/HRS gave best results
	Traditional FEL concept by varying the electric-thermal ratio through changing various parameters to meet the user loads		Integrated optimization framework/power hub/heat hub
Case Study 2.19 [35] (Mao Y, *et al.*, 2020)	Gas/PV/thermal panels/electric grid	Case Study 2.28 [44] (Lombardo W, *et al.*, 2020)	PV/STC/micro-ORC
	TES/HRS/heating unit/boiler/AC/EC		AC/TES/heat pump/electric control unit
	PSO/FEL–ECR/FME/FTL/FHL		AC with built-in real bioclimatic NZEB, modelled using TRNSYS®
Case Study 2.20 [36] (Lingmin C, *et al.*, 2020)	Gas/PV/wind energy/power storage	Case Study 2.29 [45] (Wu D, *et al.*, 2021)	NG/ICE/electrical power grid
	AC/electric chiller (EC)/HE/HRS/boiler		Gas boiler/waste-heat recovery/air-source and absorption heat pumps/HE
	PSO/FEL/reliability indexes		Self-adaption technique/exhaustive search/genetic algorithms/orthogonal experimental algorithms
Case Study 2.21 [37] (Cao Y, *et al.*, 2020)	Power grid/NG PGU	Case Study 2.30 [46] (Ma H, *et al.*, 2020)	NG/ORC/electrical grid
	HRS/AC/EC/boiler/heating coil		Boiler/heat-recovery unit (HRU)/AC/EC/heating-coil unit
	Owl search technique based on Levy flight mechanism and circle mapping		FTL/configuration coupling analysis and thermodynamics parameters in TRNSYS®
Case Study 2.22 [38] (Farmani F, *et al.*, 2018)	PV/main grid/battery/FCs/micro turbine	Case Study 2.31 [47] (Miao N, *et al.*, 2020)	NG/gas turbine/grid-connected/policies/NG and electricity prices
	Auxiliary boiler/heat-recovery system/heat exchanger/absorption chiller		Capacity configuration: AC and gas-turbine models are the same
	Smart EMS/stochastic Monte Carlo model/data acquisition/ordered weighted average/data evaluator fuser		Fixing heat based on power (FHL)/fixing power based on heat (FEL)
Case Study 2.23 [39] (Zare V, Takleh HR, 2020)	Geothermal/TRCC/Rankine cycles	Case Study 2.32 [48] (Ji J, *et al.*, 2020)	ORC to convert LTHS to electricity/generator
	Internal heat engine/ejector/gas cooler/turbine/heater/generator/boiler, etc.		HST/AC–DC/battery/supercapacitor/DC–AC/coolant fluid exhaust gas HE
	Parametric analysis/thermodynamics modelling		Modelled/simulated practical optimization studies conducted to evaluate the system performance with different load profiles

Table 2. Continued

CCHP research reviewed	Energy sources/fuels/PGU Energy-storage/conversion mechanisms Optimization/control techniques	CCHP research reviewed	Fuels/PGU/energy sources Energy-storage/conversion mechanisms Optimization/control techniques
Case Study 2.24 [40] (Mohammadi K, Powell K, 2020)	Two trigeneration systems: one based on CO_2 exchange and the other on ORC	Case Study 2.33 [49] (Jia J, *et al.*, 2021)	Natural gas/ICE/ORC/solar energy/ST/power grid
	Refrigeration/air conditioning/hot-water production with CO_2 and power with ORC		HEs 1 and 2/gas boiler/waste heat boiler/ABS/water tank
	Techno-economic assessment/parametric analysis		Parametric analysis focused on ICE-rated capacity and ORC evaporation temperature effects
Case Study 2.25 [41] (Chahartaghi M, Sheykhi M, 2019)	H_2 and helium as the functioning gases to dual Stirling engines with generator	Case Study 2.34 [50] (Li J, *et al.*, 2021)	NG/gas turbine/power grid
	Heat-recovery system and absorption chiller		Gas boiler/thermal, electricity and cooling storage/electric cooler/AC
	Engine assessed with non-ideal adiabatic model and the AC energy assessment articulated using engine waste heat		Data-driven uncertainty and multistage functioning modelling methods to ensure accuracy of the techniques/IES
Case Study 2.26 [42] (Parikhani T, *et al.*, 2020)	NH_3–H_2O mixture driven by a LTHS – tailored version of a Kalina cycle		
	Separators 1, 2 and 3/Pumps 1, 2 and 3/Mixers 1, 2 and 3, Concentrators 1, 2 and 3/compressor/evaporator/heating unit		
	Thermodynamics and thermo-economics balance equations for performance analysis of the thermal system		
Case Study 2.35 [51] (Qian J, *et al.*, 2021)	NG/gas turbine/solar energy/PV/wind energy/wind turbine/power grid	Case Study 2.43 [59] (Yang X, *et al.*, 2022)	Utility grid/NG/gas turbine/PV array
	Gas boiler/ HRU/electric refrigerator/AC/ solar collector (SC)/heat exchanger (HE)		Auxiliary boiler/HE/AC/EC
	MODM method rooted in Fuzzy-AHP, anti-entropy and game theory/FCE/Kendall rank correlation coefficient		SPV CCHP/MPV CCHP/RPV CCHP and a two-stage optimization technique. Sensitivity analysis. Redundancy method
Case Study 2.36 [52] (Zhao H, *et al.*, 2022)	NG/micro gas turbine/distributed power supply (solar and wind energy)/electrical power grid: CCHP–microgrid	Case Study 2.44 [60] (Wang M, *et al.*, 2022)	Efficient transcritical CO_2 CCHP system/turbine
	Gas-fired boiler/HRU/HE/AC/thermal energy storage (TES)/electric chiller (EC)/ EES		Gas heater/internal heat exchanger/Compressors 1 and 2/gas cooler/valve/ heater/mixer/separator/evaporator
	MCDM framework/integrated AEW and grey-DEMATEL/ranking the assessed cases/improved TOPSIS with DQGRA		Introduced ejector refrigeration. The ER CCHP system can yield more net output power than the TR CCHP system
Case Study 2.37 [53] (Xu J, *et al.*, 2021)	LNG/NG/air/gas turbine/generator	Case Study 2.45 [61] (Deng Y, *et al.*, 2022)	PV/NG/gas turbine/power grid
	Thermo-acoustic trigeneration system		Heat-recovery system/STC/heat-storage tank/boiler/AC/HE/GSHP
	Acoustically matching the alternator and thermo-acoustic units impedance for total maximum exergy efficiency		CCHP–GSHP-SF–SE with a SF of 0.4, is better than CCHP–SE and CCHP–GSHP–SE systems. ACOP/AUR

Table 2. Continued

CCHP research reviewed	Energy sources/fuels/PGU Energy-storage/conversion mechanisms Optimization/control techniques	CCHP research reviewed	Fuels/PGU/energy sources Energy-storage/conversion mechanisms Optimization/control techniques
Case Study 2.38 [54] (Li Y, *et al.*, 2021)	Natural gas, gas turbine/power grid	Case Study 2.46 [62] (Xu Y, *et al.*, 2022)	NG/air/SOFC with DC–AC converter
	Interactive CCHP system (CCHP1, CCHP2, CCHP3 … CCHPk)/gas boiler		LiBr absorption chiller/water tank, air compressor/Pumps 1 and 2/HEs 1 and 2/reformer/afterburner
	Interactive operation strategy is based on the energy-augmentation characteristics of FEL, FTL and FHL		Operating temperature and current density as well as absorption chiller working conditions affect FCs
Case Study 2.39 [55] (Kang L, *et al.*, 2022)	Gas/gas turbine/power grid	Case Study 2.47 [63] (Nondy J, Gogoi T, 2022)	Two of the same recuperative gas-turbine topping cycle systems but different bottoming cycles to give Systems I and II
	HRU/GSHP/AC/HE/thermal storage tank		System I with a bottoming cycle with recoverative–regenerative ORC, steam turbine and two absorption cooling systems. System II with condensing steam turbine cycle in place of recuperative–regenerative ORC cycle in System I
	Principal component and correlation analyses/feed-forward active operation optimization/linear regression correlate		Tri-objective optimization/PESA-II and Entropy-TOPSIS techniques were used to get optimal results
Case Study 2.40 [56] (Yan R, *et al.*, 2022)	Uncertain renewable energy (solar and wind energy)/power grid/gas turbine	Case Study 2.48 [64] (Lu Z, *et al.*, 2022)	Gas turbine/generator/MCFC with DC–AC
	Gas boiler/CHP/EES/HES/cooling energy storage/absorption chiller/renewable energy generation/heat pump device		ISCC–DEALBR/STC/HRSG/mixer
	Stochastic and robust optimization into a two-stage stochastic–robust capacity model		Energy-cascade utilization/thermal analysis and solar influence on system
Case Study 2.41 [57] (Fu C, *et al.*, 2022)	Gas/solar/power grid	Case Study 2.49 [65] (Salimi M, *et al.*, 2022)	Renewable energy/grid/battery/ICE
	HRU/gas boiler (GB)/battery/AC/EC/HE/TST/microturbine		TES/boiler/HRS/AC
	Improved-FEL and FTL strategies/demonstrated Pareto solution with the proffered IMOMVO algorithm/TOPSIS		To minimize carbon and water footprints. (i) Enhance the system Components such as in ICE and (ii) use multigeneration
Case Study 2.42 [58] (Yang L, *et al.*, 2022)	Geothermal/flasher/turbine	Case Study 2.50 [66] (Ren F, *et al.*, 2022)	Reviewed several CCHP systems without proposing any alternative version
	Water heater/ejector/evaporator/valve/pump/mixer/condenser		Reviewed various energy-conversion and energy-storage technology systems
	Mathematical models instituted and validated to assess system performance. Parametric analysis for optimal pressure		Reviewed different control techniques with suggesting any alternative version. See indicated reference for details

Table 3: Quantitative analysis summary of reviewed CCHP systems

CCHP research reviewed	4E (energy/exergy/economy/eco-friendly)	CCHP research reviewed	4E (energy/exergy/economy/eco-friendly)
	CCHP (cold, heat and power) production		CCHP (cold, heat and power) production
	Case-study location		Case-study location
Case Study 2.1 [5] (Zhang J, *et al.*, 2018)	>35% GHG emission reduction	Case Study 2.10 [18] (Cozzolino R, 2018)	@40A; minimum (min) electrical efficiency (eff) = 35.8%; maximum (max) thermal eff = 39.4%; cooling eff = 15.2–17.1; max EUF = 75%; min ExUF = 40%
	Power = 150 + 75 + 50 kW; heat = 75 + 60 + 50 kW		@40A; the total power = 6.03 kW; total heat = 6.55 kW
	USA		Italy
Case Study 2.2 [4] (Badea N, *et al.*, 2010)	–	Case Study 2.11 [9] (Wang Z, *et al.*, 2018)	Total annual CDE = 13.50%; PEC = 3.8%; COST = 14.82%; PBP = 4.91 years
	C = 4 kWh; H = 0.14–4.68 kWh; E = 4 kWh		Various values
	Romania, South Eastern Region household		Beijing, China
Case Study 2.3 [31] (Maraver D, *et al.*, 2013)	Environmental impact Reduction of between 15% and 55%	Case Study 2.12 [16] (Lu S, *et al.*, 2018)	Total annual operating cost can be reduced by 36.2%
	–		Winter: cooling/heating = 2 501 485 kW; power = 2 550 766 kW Summer: cold/heat = 2 630 793 kW; power = 2 037 338 kW
	Spain		Tianjin, China
Case Study 2.4 [7] (Xu AD, *et al.*, 2014)	Production eff = 33%	Case Study 2.13 [15] (Li B, *et al.*, 2019)	Thermal efficiency of ICE = 50%
	Rated power = 200 kW;		Cooling = 2501 kW; heating = 1443 kW; power = 1038 kW; hot water = 370 kW
	–		Hotel in Huaian City, China
Case Study 2.5 [25] (SU Z, *et al.*, 2016)	Summer: RCSR = 0.95%; carbon dioxide emission reduction rate (CDERR) = 40.49%; primary energy savings ratio (PESR) = 20.34% Winter: RCSR = 9.20%; CDERR = 39.94%; PESR = 22.03%	Case Study 2.14 [14] (Jiang R, *et al.*, 2017)	Annual investment cost of 521 911 $/year and a payback period of 4.52 years. CEC is 0.237; annual primary energy saving ratio (APESR) = 0.263; annual total cost saving rate (ATCSR) = 0.16
	Power = 30 + 5.8 kW		Power = 1021 kW; cooling = 5843 kW
	China		Office build in Guangzhou, China
Case Study 2.6 [27] (Wongvisanupong K, Hoonchareon N, 2013)	Total eff = 70%, electrical eff = 30%, and power-to-heat ratio = 0.47–1.06; models can reduce total energy cost to ~17%	Case Study 2.15 [12] (Chen X, *et al.*, 2018)	System exergy eff = 39.9%; annual cost = 29 337.3$; annual GHG reduction = 1.82 × 107 g; maintenance cost = 5% investment
	Cooling = 41 MW; heating = 33.0935 MW; power = 23 + 7.6677 MW		Power = 5 kW
	Shopping complex, Bangkok, Thailand		China
Case Study 2.7 [26] (Zhao H, *et al.*, 2018)	Pollutants decline: CO_2 = 39.67%; SO_2 = 53.05; NO_X = 23.26%	Case Study 2.16 [19] (Ebrahimi M, Derakhshan E, 2018)	Total eff = 76.94%; Fuel Saving = 43.25%; Exergy eff = 53.86%; Cost < 2000 USD
	Cooling = 90 kW; heating = 175 kW; power = 155 kW		Cooling = 26.8 W; heat = 3.04 kW; power = 2.79 kW; CO_2 reduction rate = 2.58 kg/Hr
	Northern China		India

Table 3. Continued

CCHP research reviewed	4E (energy/exergy/economy/eco-friendly) / CCHP (cold, heat and power) production / Case-study location	CCHP research reviewed	4E (energy/exergy/economy/eco-friendly) / CCHP (cold, heat and power) production / Case-study location
Case Study 2.8 [8] (Wang R, *et al.*, 2018)	Not clearly indicated: too many various results without clarity on the 4E values	Case Study 2.17 [17] (Mehrpooya M, *et al.*, 2017)	Total eff = 71.71%; electrical eff = 42.28%
	Not clearly indicated: too many different results without clarity on the CCHP values		Cold = 1372 kW; heat = 2137 kW; power = 6482 kW
	China (Xi'an, Shaanxi) office building		–
Case Study 2.9 [11] (Wang JL, *et al.*, 2014)	System primary energy eff = 94.4%; PESR = 30.4%; cost-saving ratio = 41.7%; total investment rise = 11.1%		
	Cooling rose from 6.14 to 17.56 kW; heating rose from 12.9 to 30.31 kW; power rose from 16 to 17.18 kW		
	Hotels and residential buildings in the north of China		
Case Study 2.18 [34] (Wu D, *et al.*, 2019)	PER = 58.5–60.2 %; exergy = 39.1–40%; NG usage = 9.81 × 104 m^3 per year with 12.4% less energy consumption	Case Study 2.27 [43] (Lingmin C, *et al.*, 2021)	Various values
	Heat = 66.6 kW; electricity = 105.1 – 108 kW; no cooling value was reported		Various values
	Residential building in Weifang City, China		Isolated tourist area in Western China
Case Study 2.19 [35] (Mao Y, *et al.*, 2020)	PESR = 39.6%; ATC = 2.79 × 10^5; capital cost = 7.98 × 10^5; fuel cost = 1.86 × 10^5; electricity cost = 1.06 × 10^5; carbon tax = 2.96 × 10^4; NB: currency in Yuan	Case Study 2.28 [44] (Lombardo W, *et al.*, 2020)	Overall efficiency = 32–42%
	Power = 500 + 350 kW		Various values
	Residential zone in Beijing, China		Italy (Messina, Rome and Milan)
Case Study 2.20 [36] (Lingmin C, *et al.*, 2020)	–	Case Study 2.29 [45] (Wu D, *et al.*, 2021)	Various values
	Various values		Various values
	Guangzhou, China		Multi-function district, Beijing city, China
Case Study 2.21 [37] (Cao Y, *et al.*, 2020)	Overall system efficiency > 85%	Case Study 2.30 [46] (Ma H, *et al.*, 2020)	Various values
	00 kW PGU with 48% cooling by AC/EC		–
	Building in Kerman area in Iran		China
Case Study 2.22 [38] (Farmani F, *et al.*, 2018)	Electrical eff = 30% + 30%; thermal eff = 55% + 55%	Case Study 2.31 [47] (Miao N, *et al.*, 2020)	Various values
	Total power = 30 + 40 kW; COP_{AC} = 0.7; COP_{EC} = 3		–
	Residential building in Virginia Beach, VA, USA		China
Case Study 2.23 [39] (Zare V, Takleh HR, 2020)	Improvement in exergy efficiency = 30.9%; improvement in net power = 49.1%; improvement in cooling = 75.8%; at the expense of 39.1% heat reduction	Case Study 2.32 [48] (Ji J, *et al.*, 2020)	Total eff = 33.49–56.53%
	System A | System B Net power = 17.18 kW | 25.61 kW; heating = 69.13 kW | 42.11 kW; cooling = 12.54 kW | 22.05 kW		Had 3.61 and 1.86 kWh energy savings in summer and winter, respectively
	Urmia, Iran		China

Table 3. Continued

CCHP research reviewed	4E (energy/exergy/economy/eco-friendly) CCHP (cold, heat and power) production Case-study location	CCHP research reviewed	4E (energy/exergy/economy/eco-friendly) CCHP (cold, heat and power) production Case-study location
Case Study 2.24 [40] (Mohammadi K, Powell K, 2020)	CoP = 18%	Case Study 2.33 [49] (Jia J, *et al.*, 2021)	–
	Power = 59.52–185.8 kW; cooling = 478 kW; domestic hot water = 7763–9360 m^3/yr		Various values
	Salt Lake City, USA		–
Case Study 2.25 [41] (Chahartaghi M, Sheykhi M, 2019)	Helium | Hydrogen CoP: 64.4% | 66.7 CCHP Eff: 70% | 72.29%, TPES: 24.05% | 31.3%, TCO2ER: 31.06% | 38% CR: 75.53% | 78.8%	Case Study 2.34 [50] (Li J, *et al.*, 2021)	Energy increase from 46.6% to 58.5%; increase in exergy from 34.4% to 39.1%; cost-saving rates of the CCHP–ORC–ST system in commercial and office buildings rose by 15% and 27%
	Helium | Hydrogen Cooling = 12.65 kW | 14.43 kW; heating = 19.65 kW | 21.65 kW; power = 15.24 kW |22.52 kW		Various values
	Iran		China
Case Study 2.26 [42] (Parikhani T, *et al.*, 2020)	Energy eff = 49.83%; exergy eff = 27.68%; overall product cost = 198.3 $/GJ		
	Cooling = 1610 kW; heating = 1972 kW; power = 253 kW		
	Iran		
Case Study 2.35 [51] (Qian J, *et al.*, 2021)	–	Case Study 2.43 [59] (Yang X, *et al.*, 2022)	RPV CCHP annual total cost reduction ratio (ATCR) = 27.11%; PESR = 32.25%; carbon dioxide emissions reduction ratio (CDER) = 45.22%; increased availability of >99.98% and reduced the annual cost of failure by $144 654
	–		RPV CCHP (Npgu = 469.26 kW) > IPV CCHP (Npgu = 465.92 kW) > MPV CCHP (Npgu = 439.92 kW) > SPV CCHP systems (Npgu = 349.18 kW).
	15th-floor hotel in a city in Western China		Office building in Beijing, China
Case Study 2.36 [52] (Zhao H, *et al.*, 2022)	–	Case Study 2.44 [60] (Wang M, *et al.*, 2022)	ER CCHP Thermal Eff = 28.3%; Exergy Eff = 27.7% TR CCHP Thermal Eff = 28.4%; Exergy Eff = 26.9%
	Max cooling = 80–340 kW; max heating = 60–230 kW; max power = 150–320 kW		ER CCHP power = 7910.3 kW; heat = 35 617.6 kW TR CCHP power = 7537.5 kW; heat = 35 931.0 kW
	8 Building-type CCHP–MG systems located in an industrial park of Jiangsu Province in China		China
Case Study 2.37 [53] (Xu J, *et al.*, 2021)	Total energy efficiency of the system = 96.9%; total system energy efficiency = 24.1%; energy cost saving = 10.1 k Euro/year; CO_2-emission reduction = 30.6 tons/yr; fossil-fuel energy savings = 78.4 MWh/yr	Case Study 2.45 [61] (Deng Y, *et al.*, 2022)	CCHP–GSHP-SF–SE with SF = 0.4; economy = k$1927.212 environment = 857 385.207 kg; PESR = 14.49%; cost-saving ratio = 5.35%; CO_2-emission-reduction ratio = 12.93%
	Cooling = 2.19 kW; heating = 3.55 kW; electricity = 2.27 kW		Energy = 3 775 122 kW CCHP–GSHP-SF–SE; performance = 10.92%
	LNG-fuelled ship vessels		Hotel building in Beijing, China

Table 3. Continued

CCHP research reviewed	4E (energy/exergy/economy/eco-friendly) / CCHP (cold, heat and power) production / Case-study location	CCHP research reviewed	4E (energy/exergy/economy/eco-friendly) / CCHP (cold, heat and power) production / Case-study location
Case Study 2.38 [54] (Li Y, *et al.*, 2021)	Various values	Case Study 2.46 [62] (Xu Y, *et al.*, 2022)	When the temperature is increased: η_{sys} increased from 68.85% to 77.93%; η_{exe} rose from 10.56% to 22.3%; Csys remained at 1.249 × 104 USD; R_{GHG} increased from 17.22 to 21.07 tons
	Various values		Cooling from 1.64 to 1.45 kW; power from 1.98 to 6.27 kW; heating from 6.12 to 3.63 kW
	A railway station, an office building and a hotel building in northern China		China
Case Study 2.39 [55] (Kang L, *et al.*, 2022)	PECR = 24.65–63.41%; CDER = 35–73.79%; OCR = 29.69–67.66%	Case Study 2.47 [63] (Nondy J, Gogoi T, 2022)	System I: energy eff = 58.33%; exergy eff = 43.55%; low total cost rate = 3727.3 $/h; specific CO_2 emissions = 91.75 kg/MWh
	PGU power generation = 10 650–12 200 kW		Net cooling = 16.10 MW; process heat = 1.22 MW; net power = 56.61 MW
	Office building in Tianjin, China		India
Case Study 2.40 [56] (Yan R, *et al.*, 2022)	Various values	Case Study 2.48 [64] (Lu Z, *et al.*, 2022)	Energy eff = 61.64; exergy eff = 61.69; specific CO_2 emission = 130.92 g/kWh
	Various values		Cooling = 7557.09 kW; heating = 57 956.25 kW; electric power = 494.1 MW
	An industrial-park case located in China's Baoding City		Dunhuang, Gansu Province, China
Case Study 2.41 [57] (Fu C, *et al.*, 2022)	Energy eff = 67.09%; CO_2 emission reductions = 47.91%; PESR = 31.65%; annual cost-saving ratios = 14.94%	Case Study 2.49 [65] (Salimi M, *et al.*, 2022)	CCHP systems can reduce coal usage, which can result in a 11% reduction in environmental damage
	Power generation = 100 + 173.4 + 376.9 kW		
	Large hotel published as a reference building by the US Department of Energy		–
Case Study 2.42 [58] (Yang L, *et al.*, 2022)	Thermal Eff = 55.92%; Exergy Eff = 44.34%	Case Study 2.50 [66] (Ren F, *et al.*, 2022)	–
	Cooling = 5498.14 kW; heating = 3454.17 kW; power = 1331.37 kW; CCHP output = 10 283.68 kW		–
	China		–

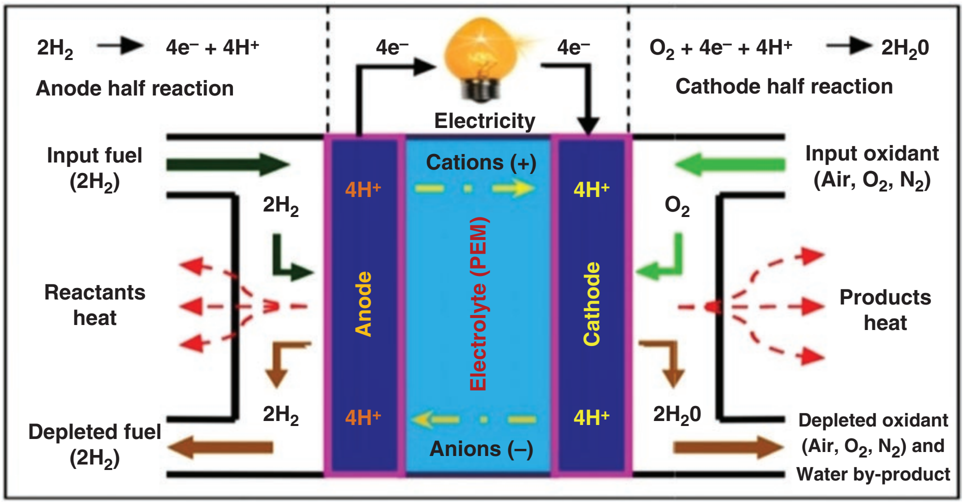

Fig. 51: PEM FC operation principle overview.

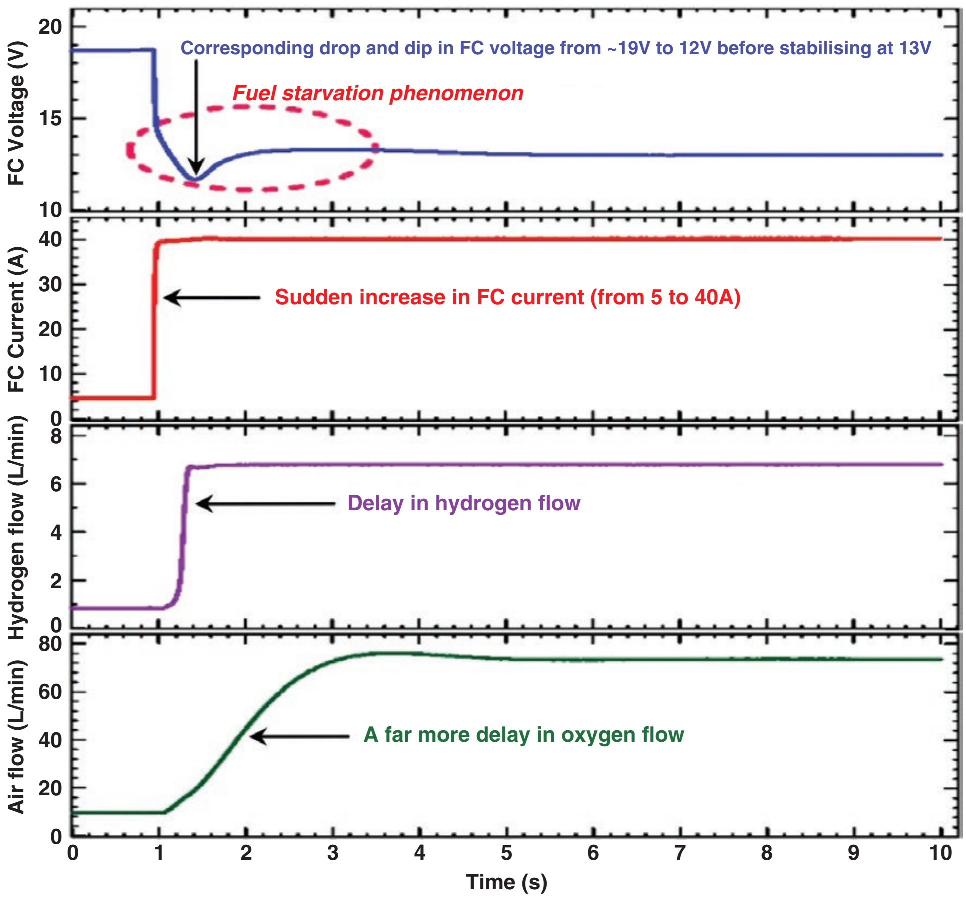

Fig. 52: FC fuel-starvation phenomenon. Adapted from [69] with permission from IEEE.

densities, whereas the power source (UC or SC) has a high power density. The power source provides the high current during transient conditions and is recharged from the core energy source(s) when the demand is lower. The drawback of this scheme is that solar cells can only provide energy when there is sunlight. Fig. 57a and b, respectively, shows the set-up and dynamic responses of the FC, solar cell and supercapacitor.

Presented in Table 4 is a summary of fuel-starvation-assisted techniques from various FCs.

3 FC types and comparisons

From [67, 68, 86–94], FCs can be grouped into seven types (apart from direct methanol (DM) FCs, since it is practically a PEM FC, since its electrolyte is still PEM, except that it uses methanol as

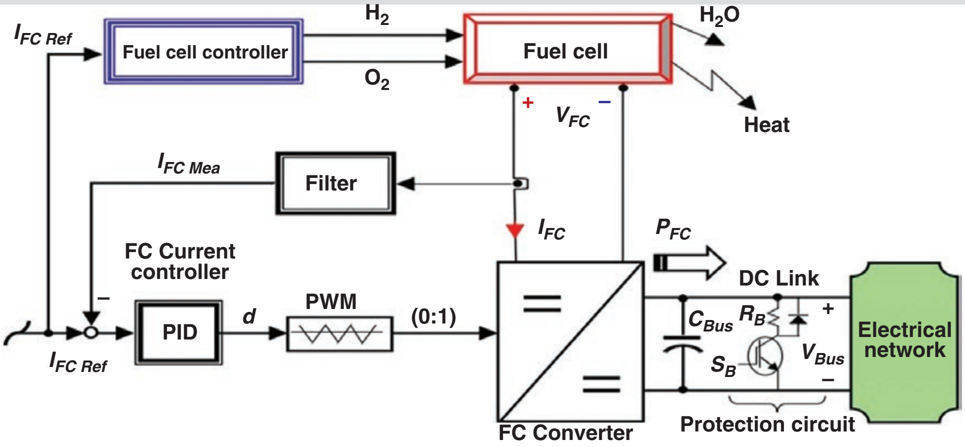

Fig. 53: FC assisted with fuel-flow-rate control. Redrawn from [69] with permission from IEEE.

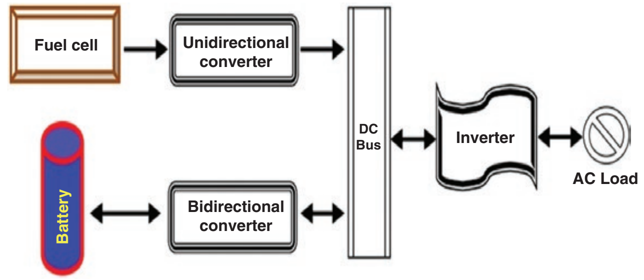

Fig. 54: FC assisted with battery.

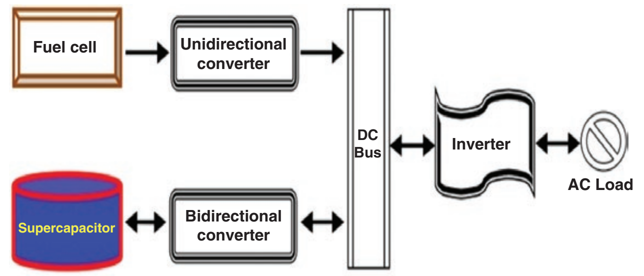

Fig. 55: FC assisted with supercapacitor or ultracapacitor.

fuel). Table 5 compares these seven most commonly used FCs and their properties.

4 Postulated green CCHP system model

Best practices and a research gap established from the reviews are applied to formulate a unique CCHP system based on PEM FC, Li-ion battery, ultracapacitor, thermoelectricity (TEG and TEC), power converters with proportional integral derivative (PID), energy management and storage. Fig. 58 exemplifies our proposed system under research using MATLAB®/Simulink®. In the CCHP system, the FC (HT-PEM) is the prime mover; the Li-ion battery and the ultracapacitor bank serve as the storage devices and also assist the FC during peak power demand. The TEG is used to convert the waste heat produced by the FC to DC power, thereby increasing the DC power output/efficiency, whereas the TEC provides cooling (which can also provide heating by reversing the current flow or voltage polarity)

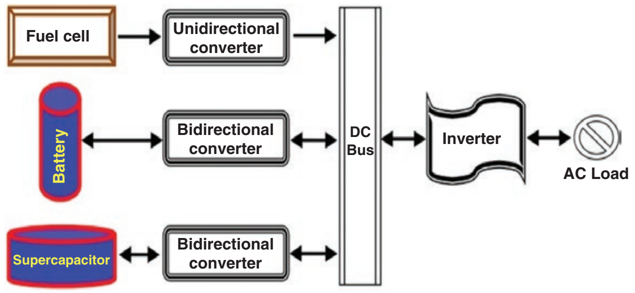

Fig. 56: FC assisted with battery and supercapacitor or ultracapacitor.

when supplied with DC power. The power converters convert and maintain the required levels of DC and/or AC voltages, and the PID EMS controls the entire trigeneration scheme accordingly. A unique option is to alternatively use a PEM regenerative FC as the PGU.

5 Conclusions

Energy insecurity is now a global problem caused by diverse factors. Various potential solutions are being sought and, in particular, clean energy is becoming the sustainable energy of choice in most countries. Therefore, as our contribution to this quest, this article concisely presented a unique topological review of 50 CCHP studies and FC research. CCHP systems simultaneously provide cold, heat and power, and these three forms of energy are fundamentally a necessity in most households and businesses. Our rationale was to holistically review miscellaneous CCHP systems in one document from a practical perspective at the system/application levels, rather than at the component or parameters level. This approach enables a better understanding of various CCHP systems and how they can be implemented or developed prudently for commercial and residential applications. To achieve this, 50 studies of CCHP systems were structurally, qualitatively and quantitatively analysed, and the fundamental findings were summarized in Tables 1–3. It was inferred that the efficiency of CCHP systems is based not solely on entirely hardware, but also on the integrated control software, predominantly based on advanced optimization algorithms and EMS techniques. The reviewed studies reported that their proposed methods performed better relative to existing methods. Therefore, it is obvious that the employment of

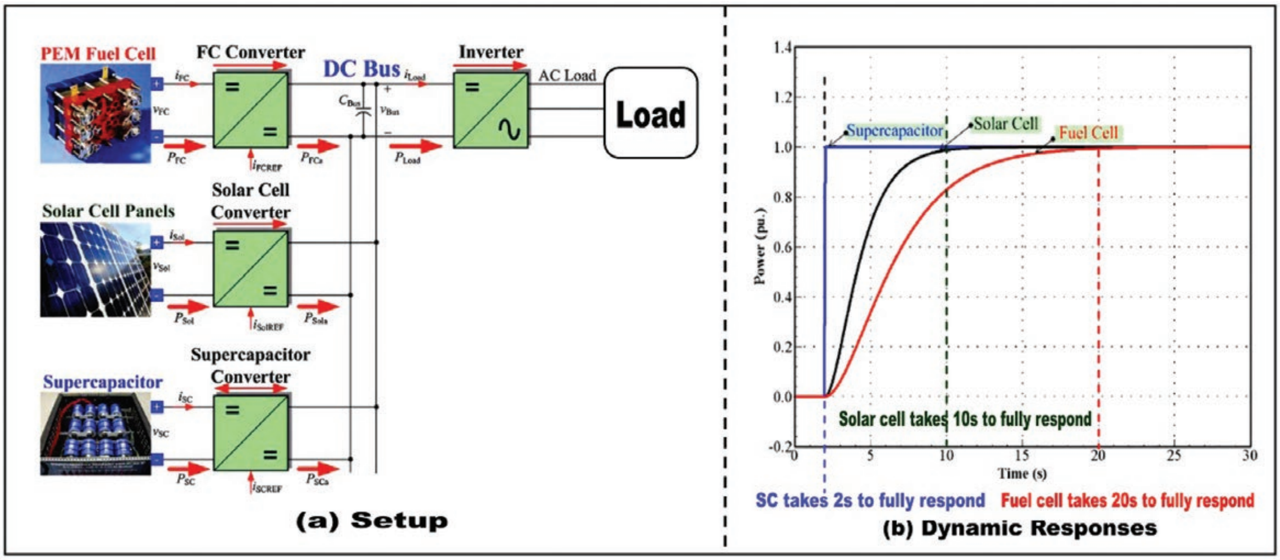

Fig. 57: FC assisted with solar cell and supercapacitor. (a) Set-up and b) dynamic responses. Adapted from [85] with permission from Elsevier.

Table 4: Comparison and summary of FC assisted techniques

FCs assisted schemes	Highlights, advantages and disadvantages
Fuel-flow-rate control [69, 80]	H_2 and O_2 are continually controlled to track the FC current variations, noticing the FC current slope and sustaining a steady flow rate of the fuel to ensure that the FC at all times has sufficient fuel flow. Although this method ensures that the fuel cell is not deprived of H_2 and O_2, it is nevertheless not efficient, because the fuel flow is generally stable, particularly at the highest value
Battery (e.g. Li-ion) [73, 81]	The battery has a higher specific power relative to FCs, and thus retorts swiftly and provides the peak power should there be a transient current. Batteries, unlike FCs, store energy. On the contrary, the battery needs time to charge and will degrade if it is discharged and charged faster and frequently in high-current uses
Ultracapacitor (UC) or supercapacitor (SC) [73, 82]	SCs/UCs have the fastest transient response and highest power density compared with batteries and FCs; therefore, they are the most ideal energy-storage devices for peak current use, as they charge rapidly and help to circumvent FC slowness, but they have the lowest energy density (discharges fastest)
Battery and SC or UC [73, 81, 83]	The most suitable FC-assisted technique is this, as using both aids the FC when peak power and utmost energy are needed at the same time. The drawback is that it is a bit costly due to more components
CombiLit [84]	CombiLit is a composite device that stores energy by merging, in the same cell, the electrodes of a high-energy Li-ion battery and a peak power density. In need of costly repairs when faulty
Solar cells and SC [85]	The solar cell has maximum energy density and the SC has peak power density that assists the FC during transients. However, constant sunlight is required and the response performance depends on the SC

a particular CCHP system and its successful implementation depend on various factors; these include, but are not limited to, location, policies, costs, load types, user activities, availability of energy sources and the efficiency of conversion, storage and control mechanisms. Additionally, the 4E evaluation index is the main performance criterion that is now used to justify a CCHP system. It was also noted that the inclusion of renewable energy greatly improved CCHP systems, while absorption chillers offered better performance compared with compression types. The FEL operation mode and its variations seem to be the most widely used method, by which power production is prioritized over heat and cold. Producing more cold is environmentally friendly. Our interest was centred on CCHP systems with a FC as the prime mover since FC-based CCHP systems from an applicability viewpoint are more diverse and meritorious, especially the PEM FCs. As a result, FCs were further investigated, with an emphasis on the FC fuel-starvation phenomenon, as well as FC types. It was realized that the FC assisted with the battery and supercapacitor technique was the most suitable. In light of all of these highlighted findings, a unique HT-PEM FC CCHP system model that constitutes a Li-ion battery bank, an ultracapacitor bank, thermoelectricity (TEG and TEC), power converters and EMS that are clean and can also address the FC fuel-starvation phenomenon assisted with a TEG was postulated as an alternative and entirely green model, which is currently undergoing research.

Table 5: Comparison and summary of FC types

FC type	Electrolyte	Reactions	Advantages	Disadvantages
Polymer electrolyte membrane FC (PEM) [67, 68, 72, 86, 90]	Solid organic polymer poly-perfluorosulfonic acid LT: 50–100°C polybenzimidazole (PBI) HT-PEM: 100–200°C	Anode: $4H_2 \rightarrow 8H^+ + 8e^-$ Cathode: $2O_2 + 8H^+ + 8e^- \rightarrow 4H_2O$ Cell: $4H_2 + 2O_2 \rightarrow 4H_2O$	• Solid electrolyte lowers decay and need servicing • low to mid temperature • rapid start-up (LT-PEM) • trivial or no effluence • power efficiency of 45%	• Low temperature needs costly catalysts (Pt) • high reaction to fuel; contaminants, such as CO • HT-PEM is not durable • LT-PEM water deluge
Alkaline FC (AFC) [67, 68, 87–90]	Aqueous solution of KOH drenched in a matrix Temperature: 60–200°C	Anode: $2H_2 + 4(OH)^- \rightarrow 4H_2O + 4e^-$ Cathode: $O_2 + 2H_2O + 4e^- \rightarrow 4(OH)^-$ Cell: $2H_2 + O_2 \rightarrow 2H_2O$	• Cathode reaction faster in an alkaline electrolyte; therefore, high execution • >55% power efficiency	• Very costly CO_2 extraction from the fuel requiring air streams, thus prone to CO_2 emission • Requires pure H_2
Phosphoric-acid FC (PAFC) [67, 68, 88–90]	Liquid phosphoric acid doused in a matrix Temperature: 175–200°C	Anode: $2H_2 \rightarrow 4H^+ + 4e^-$ Cathode: $O_2 + 4H^+ + 4e^- \rightarrow 2H_2O$ Cell: $2H_2 + O_2 \rightarrow 2H_2O$	• Approx. 85% efficiency if use CHP systems • power efficiency of ~40% • uses impure H_2 fuel	• Needs expensive Pt catalyst • low power and current • bulky size and weight • aggressive electrolyte
Molten carbonate FC (MCFC) [67, 68, 87–90]	Liquid solution of lithium or sodium or potassium carbonates drenched in a matrix Temperature: 600–1000°C	Anode: $H_2 + CO_3^{2-} \rightarrow H_2O + CO_2 + 2e^-$ Cathode: $0.5O_2 + CO_2 + 2e^- \rightarrow CO_3^{2-}$ Cell: $H_2 + 0.5O_2 + CO_2 \rightarrow H_2O + CO_2$ (CO_2 is made at the anode and used at the cathode)	• High-temperature conditions result in no need for overpriced catalysts • Flexibility to use other fuels • The power efficiency of >50%	• High temperature speeds rust and degradation of FC components • Long start-up time • Expensive thermal management
Solid-oxide FC (SOFC) [67, 68, 86, 88, 90]	Solid zirconium oxide with small amount of added Ytrria (Y_2O_3) Temperature: 600–1000°C	Anode: $H_2 + O^{2-} \rightarrow H_2O + 2e^-$ Cathode: $1/2O_2 + 2e^- \rightarrow O^{2-}$ Cell: $H_2 + 1/2O_2 \rightarrow H_2O$	• Can use contaminated fuels • akin to PEM, has solid electrolyte merits • power efficiency of >50%	• High temperature enhances decay and destruction of FC parts • Sluggish starting up • Poor capability at ~600°C
Plant microbial FC (PMFC) [91, 92]	Different soil types, wetland sediments, rhizo-deposits, microbes, compost Ambient temperature: ±20°C	Anode: $(CH_2O)_6 + 6H_2O \rightarrow 6CO_2 + 24H^+ + 24e^-$ Cathode: $6O_2 + 24e^- + 24H^+ \rightarrow 12H_2O$ Cell: $6H_2O + 6CO_2 \rightarrow 6O_2 + (CH_2O)_6$	• Eco-friendly, organic (B N_2, NH_4 etc.) removal in wastewater treatments, plant bio-sensing, used in wetlands/agricultural lands to generate power	• Bioelectricity generation is relatively low • periodic maintenance to replace plants • natural operational conditions require observation • photosynthesis-dependent
Regenerative or reversible FC [93, 94]	It can be O^{2-}-conducting and/ or proton (H^+)-conducting (the different types just depend on the FC electrolyte used)	*FC mode: could be any of the above fuel cells* *Electrolyser mode:* Anode: $O^{2-} \rightarrow 0.5O_2 + 2e^-$ Cathode: $H_2O + 2e^- \rightarrow H_2 + O^{2-}$ Cell: $H_2O \rightarrow 0.5O_2 + H_2$	• Can be efficiently used in dual operating modes depending on the needs of the target application • More sustainable and can be renewably used in space applications	• A bit more complex and has more components and could be more bulky • Expensive due to the additional components and processes involved

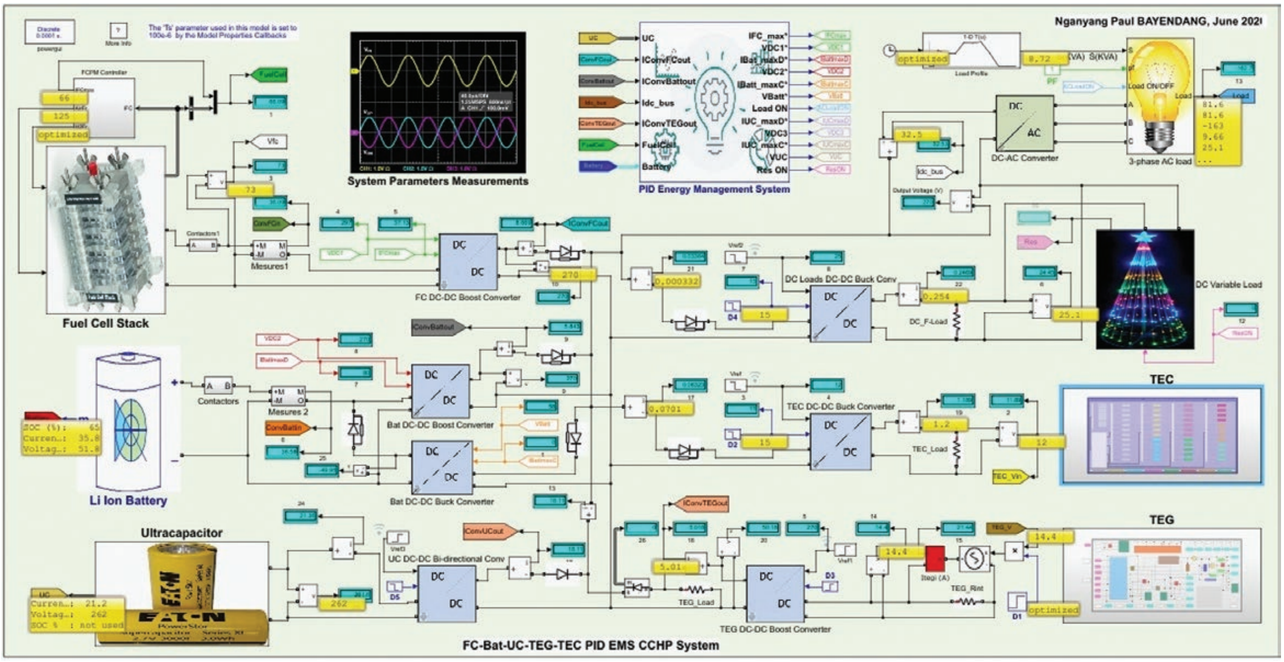

Fig. 58: PEM FC, battery, UC, TEG, TEC and PID EMS CCHP system research model.

Acknowledgements

Conceptualization: N.P.B.; methodology: N.P.B.; software: N.P.B.; validation: N.P.B. and M.T.K.; formal analysis: N.P.B. and M.T.K.; investigation: N.P.B., M.T.K. and V.B.; resources: N.P.B., M.T.K. and V.B.; data curation: N.P.B.; writing—original draft: N.P.B.; Writing—review and editing: N.P.B., M.T.K. and V.B.; visualization: N.P.B.; supervision: M.T.K. and V.B.; project administration: N.P.B., M.T.K. and V.B.; funding acquisition: V.B.

Funding

This research work has been supported by CPUT CPGS and UWC HySA Systems.

Conflict of interest statement

None declared.

Data availability

Research data are available at this stage only to the researchers involved.

References

[1] Eberhard A, Gratwick K, Morella E, *et al.* Independent power projects in sub-Saharan Africa: investment trends and policy lessons. *Energy Policy*, 2017, 108:390–424.

[2] Zhang J, Cao S, Yu L, *et al.* Comparison of combined cooling, heating and power (CCHP) systems with different cooling modes based on energetic, environmental and economic criteria. *Energy Conversion and Management*, 2018, 160:60–73.

[3] Ming Z, Qiqi Q, Haojing W, *et al.* Economy benefit comparison of CCHP system and conventional separate supply system. In: *2015 8th International Conference on Intelligent Computation Technology and Automation (ICICTA)*, Nanchang, China, 14–15 June 2015, 402–406; doi: 10.1109/ICICTA.2015.107.

[4] Badea N, Vlad C, Stolan A. Comparative study of energy performance for two mCCHP systems used in domestic residence. In: *2010 3rd International Symposium on Electrical and Electronics Engineering (ISEEE)*, Galati, Romania, 16–18 September 2010, 321–326; doi:10.1109/ISEEE.2010.5628489.

[5] Bozchalui MC, Sharma R. Optimal operation of commercial building micro-grids using multi-objective optimization to achieve emissions and efficiency targets. In: *2012 IEEE Power and Energy Society General Meeting*, San Diego, California, USA, 22–26 July 2012, 1–8; doi:10.1109/PESGM.2012.6345600.

[6] Wu DW, Wang RZ. Combined cooling, heating and power: a review. *Progress in Energy and Combustion Science*, 2006, 32:459–495.

[7] Xu AD, Lin S, Lei JY, *et al.* Operation optimization model for micro-turbine based CCHP systems. In: *2014 IEEE PES General Meeting | Conference & Exposition*, National Harbor, Maryland, USA, 27–31 July 2014, 1–5; doi:10.1109/PESGM.2014.6939384.

[8] Wang R, Guo Y, Liu K, *et al.* Performance analysis of building hydrogen comprehensive utilization system based on CCHP system of hydrogen fuel cell. In: *2018 2nd IEEE Conference on Energy Internet and Energy System Integration (EI2)*, Beijing, China, 20–22 October, 2018, 1–6; doi:10.1109/EI2.2018.8582349.

[9] Wang Z, Han W, Zhang N, *et al.* Analysis of inlet air throttling operation method for gas turbine in performance of CCHP system under different operation strategies. *Energy Conversion and Management*, 2018, 171:298–306.

[10] Zhang K, Li XR, Liu JM. Research on minimum schedulable power optimization of CCHP system. In: *2019 IEEE Innovative Smart Grid Technologies—Asia (ISGT Asia)*, Chengdu, China, 21–24 May 2019, 4210–4214; doi: 10.1109/ISGT-Asia.2019.8881422.

[11] Wang JL, Wu JY, Zheng CY. Simulation and evaluation of a CCHP system with exhaust gas deep-recovery and thermoelectric generator. *Energy Conversion and Management*, 2014, 86:992–1000.

[12] Chen X, Zhou H, Li W, *et al.* Multi-criteria assessment and optimization study on 5 kW PEMFC based residential CCHP system. *Energy Conversion and Management*, 2018, 160:384–395.

[13] Zhang X, Li H, Liu L, *et al.* Optimization analysis of a novel combined heating and power system based on biomass partial

gasification and ground source heat pump. *Energy Conversion and Management*, 2018, 163:355–370.

[14] Jiang R, Qin FGF, Yin H, *et al*. Thermo-economic assessment and application of CCHP system with de-humidification and hybrid refrigeration. *Applied Thermal Engineering*, 2017, 125:28–936.

[15] Li B, Hu P, Zhu N, *et al*. Performance analysis and optimization of a CCHP-GSHP coupling system based on quantum genetic algorithm. *Sustainable Cities and Society*, 2019, 46:101408.

[16] Lu S, Li Y, Xia H. Study on the configuration and operation optimization of CCHP coupling multiple energy system. *Energy Conversion and Management*, 2018, 177:773–791.

[17] Mehrpooya M, Sayyad S, Zonouz MJ. Energy, exergy and sensitivity analyses of a hybrid combined cooling, heating and power (CCHP) plant with molten carbonate fuel cell (MCFC) and Stirling engine. *Journal of Cleaner Production*, 2017, 148:283–294.

[18] Cozzolino R. Thermodynamic performance assessment of a novel Micro-CCHP system based on a low temperature PEMFC power unit and a half-effect Li/Br absorption chiller. *Energies*, 2018, 11:3151–3121.

[19] Ebrahimi M, Derakhshan E. Design and evaluation of a micro combined cooling, heating, and power system based on polymer exchange membrane fuel cell and thermoelectric cooler. *Energy Conversion and Management*, 2018, 171:507–517.

[20] Qu Z, Ma T, Yu X, *et al*. Parametric study on thermoelectric power generator and micro-turbine combined power generation system. *Chemical Engineering Transactions*, 2018, 70:61–66.

[21] Li Z, Xu Y. Dynamic dispatch of grid-connected multi-energy micro-grids considering opportunity profit. In: *2017 IEEE Power & Energy Society General Meeting*, Chicago, IL, USA, 16–20 July 2017, 1–5; doi:10.1109/PESGM.2017.8274205.

[22] Zhang Q, Cui G, Zhang L, *et al*. Energy integration and economical optimization of small scale CCHP system. In: *2006 International Technology and Innovation Conference (ITIC 2006)*, Hangzhou, China, 6–7 November 2006, 2198–2203; doi:10.1049/cp:20061136.

[23] Ming G, Onifri M, Lin Z, *et al*. Experimental studies on a CCHP system based on a micro-turbine. In: *2011 2nd International Conference on Mechanic Automation and Control Engineering*, Hohhot, China, 15–17 July 2011, 2159–2162; doi: 10.1109/MACE.2011.5987405.

[24] Garcia-Saez I, Mendez J, Ortiz C, *et al*. Energy and economic assessment of solar organic Rankine cycle for combined heat and power generation in residential applications. *Renewable Energy*, 2019, 140:461–476.

[25] Su Z, Sun B, Zhang C, *et al*. Optimal operation strategy of biomass and solar CCHP system. In: *2016 35th Chinese Control Conference (CCC)*, Chengdu, China, 27–29 July 2016, 8612–8616; doi:10.1109/ChiCC.2016.7554731.

[26] Zhao H, Hu E, Wang Z, *et al*. Optimal configuration of grid connected micro-grid considering CCHP and analysis of energy saving and emission reduction. In: *2018 2nd IEEE Conference on Energy Internet and Energy System Integration (EI2)*, Beijing, China; 20–22 October 2018, 1–9; doi:10.1109/EI2.2018.8581657.

[27] Wongvisanupong K, Hoonchareon N. Optimal scheduling of hybrid CCHP and PV operation for shopping complex load. In: *2013 10th International Conference on Electrical Engineering/Electronics, Computer, Telecommunications and Information Technology*, Krabi, Thailand, 15–17 May 2013, 1–6; doi:10.1109/ECTICon.2013.6559594.

[28] Chen P, Jiang Z, Tang Z, *et al*. Effect of electricity feed-in tariff on the planning of CCHP Micro-systems. In: *2016 IEEE PES Asia-Pacific Power and Energy Engineering Conference (APPEEC)*, Xi'an, China, 25–28 October 2016, 875–879; doi:10.1109/APPEEC.2016.7779620.

[29] Ye L, Yi L. Optimal design of distributed CCHP system. In: *Proceedings 2011 International Conference on Transportation, Mechanical, and Electrical Engineering (TMEE)*, Changchun, China, 16–18 December 2011, 1961–1965; doi:10.1109/TMEE.2011.6199599.

[30] Wang X, Zhao XL, Fu L, *et al*. Research on configuration and operation of the CCHP system applicable to active distribution network. In: *IEEE International Conference on Power System Technology (POWERCON)*, Wollongong, NSW, Australia, 28 September–1 October 2016, 1–6; doi:10.1109/POWERCON.2016.7753991.

[31] Maraver D, Sin A, Sebastián F, *et al*. Environmental assessment of CCHP (combined cooling heating and power) systems based on biomass combustion in comparison to conventional generation. *Energy*, 2013, 57:17–23.

[32] Cheng L, Liu C, Huang R, *et al*. An optimal operating strategy for CCHP in multi-energy carrier system. In: *IEEE Power and Energy Society General Meeting (PESGM)*, Boston, Massachusetts, USA, 17–21 July 2016, 1–5; doi:10.1109/PESGM.2016.7741902.

[33] Li X, Dong Y, Zou Y. Energy management of CCHP micro-grid considering demand-side management. In: *32nd Youth Academic Annual Conference of Chinese Association of Automation (YAC)*, Hefei, China, 19–21 May 2017, 240–245; doi:10.1109/YAC.2017.7967412.

[34] Wu D, Zuo J, Liu Z, *et al*. Thermodynamic analyses and optimization of a novel CCHP system integrated organic Rankine cycle and solar thermal utilization. *Energy Conversion and Management*, 2019, 196:453–466.

[35] Mao Y, Wu J, Zhang W. An effective operation strategy for CCHP system integrated with photovoltaic/thermal panels and thermal energy storage. *Energies*, 2020, 13:64186418.

[36] Lingmin C, Jiekang W, Fan W, *et al*. Energy flow optimization method for multi-energy system oriented to combined cooling, heating and power. *Energy*, 2020, 211:118536.

[37] Cao Y, Wang Q, Wang Z, *et al*. A new optimized configuration for capacity and operation improvement of CCHP system based on developed owl search algorithm. *Energy Reports*, 2020, 6:315–324.

[38] Farmani F, Parvizimosaed M, Monsef H, *et al*. A conceptual model of a smart energy management system for a residential building equipped with CCHP system. *International Journal of Electrical Power & Energy Systems*, 2018, 95:523–536.

[39] Zare V, Takleh HR. Novel geothermal driven CCHP systems integrating ejector transcritical CO_2 and Rankine cycles: thermodynamic modeling and parametric study. *Energy Conversion and Management*, 2020, 205:112396.

[40] Mohammadi K, Powell K. Thermodynamic and economic analysis of different cogeneration and trigeneration systems based on carbon dioxide vapor compression refrigeration systems. *Applied Thermal Engineering*, 2020, 164:114503.

[41] Chahartaghi M, Sheykhi M. Energy, environmental and economic evaluations of a CCHP system driven by Stirling engine with helium and hydrogen as working gases. *Energy*, 2019, 174:1251–1266.

[42] Parikhani T, Azariyan H, Behrad R, *et al*. Thermodynamic and thermoeconomic analysis of a novel ammonia-water mixture combined cooling, heating, and power (CCHP) cycle. *Renewable Energy*, 2020, 145:1158–1175.

[43] Lingmin C, Jiekang W, Changjie L, *et al*. A configuration optimization framework for renewable energy systems integrating with electric-heating energy storage in an isolated tourist area. *Energy Science & Engineering*, 2021, 9:865–883.

[44] Lombardo W, Sapienza A, Ottaviano S, *et al*. A CCHP system based on ORC cogenerator and adsorption chiller experimental prototypes: energy and economic analysis for NZEB applications. *Applied Thermal Engineering*, 2021, 183:116119.

[45] Wu D, Han Z, Liu Z, *et al*. Comparative study of optimization method and optimal operation strategy for multi-scenario integrated energy system. *Energy*, 2021, 217:119311.

[46] Ma H, Zhang P, Chen Z, *et al*. Operation simulation of the CCHP-ORC based distributed energy system in a shopping mall. In: *2020 5th International Conference on Power and Renewable Energy (ICPRE)*, Shanghai, China, 12–14 September 2020, 179–183; doi:10.1109/ICPRE51194.2020.9233299.

[47] Miao N, An P, Yue C, *et al*. Research ideas for the capacity configuration of CCHP system. In: *2020 IEEE/IAS Industrial and Commercial Power System Asia (I&CPS Asia)*, Weihai, China, 13–15 July 2020, 8–14; doi:10.1109/ICPSAsia48933.2020.9208366.

[48] Ji J, Ding Z, Xia X, *et al*. System design and optimisation study on a novel CCHP system integrated with a hybrid energy storage system and an ORC. *Complexity*, 2020, 1278751:1–14.

[49] Jia J, Chen H, Liu H, *et al*. Thermodynamic performance analyses for CCHP system coupled with organic Rankine cycle and solar thermal utilization under a novel operation strategy. *Energy Conversion and Management*, 2021, 239:114212.

[50] Li J, Liu J, Yan P, *et al*. Operation optimization of integrated energy system under a renewable energy dominated future scene considering both independence and benefit: a review. *Energies*, 2021, 14:1103.

[51] Qian J, Wu J, Yao L, *et al*. Comprehensive performance evaluation of Wind-Solar-CCHP system based on emergy analysis and multi-objective decision method. *Energy*, 2021, 230:120779.

[52] Zhao H, Li B, Lu H, *et al*. Economy-environment-energy performance evaluation of CCHP microgrid system: a hybrid multi-criteria decision-making method. *Energy*, 2021, 240:122830.

[53] Xu J, Luo E, Hochgreb S. A thermoacoustic combined cooling, heating, and power (CCHP) system for waste heat and LNG cold energy recovery. *Energy*, 2021, 227:120341.

[54] Li Y, Tian R, Wei M. Operation strategy for interactive CCHP system based on energy complementary characteristics of diverse operation strategies. *Applied Energy*, 2021, 310:118415.

[55] Kang L, Yuan X, Sun K, *et al*. Feed-forward active operation optimization for CCHP system considering thermal load forecasting. *Energy*, 2022, 254:124234.

[56] Yan R, Wang J, Wang J, *et al*. A two-stage stochastic-robust optimization for a hybrid renewable energy CCHP system considering multiple scenario-interval uncertainties. *Energy*, 2022, 247:123498.

[57] Fu C, Lin K, Zhou Y. Optimal capacity configuration of CCHP system with improved operation strategies using improved multi-objective multi-universe algorithm. *Expert Systems with Applications*, 2022, 199:117183.

[58] Yang L, Wang Y, Ma T, *et al*. Proposal and comprehensive thermodynamic performance analysis of a new geothermal combined cooling, heating and power system. *Cogent Engineering*, 2022, 9:2075131.

[59] Yang X, Liu K, Leng Z, *et al*. Multi-dimensions analysis of solar hybrid CCHP systems with redundant design. *Energy*, 2022, 253:124003.

[60] Wang M, Zhang J, Liu H. Thermodynamic analysis and optimization of two low-grade energy driven transcritical CO_2 combined cooling, heating and power systems. *Energy*, 2022, 249:123765.

[61] Deng Y, Liu Y, Zhang Y, *et al*. Optimization and performance analysis of CCHP-GSHP-SE system under different start factors. *Energy Conversion And Management*, 2022, 266:115827.

[62] Xu Y, Luo X, Tu Z. 4E analysis of a SOFC-CCHP system with a LiBr absorption chiller. *Energy Reports*, 2022, 8:5284–5295.

[63] Nondy J, Gogoi TK. Tri-objective optimization of two recuperative gas turbine-based CCHP systems and 4E analyses at optimal conditions. *Applied Energy*, 2022, 323:119582.

[64] Lu Z, Duan L, Wang Z. Performance evaluation of a novel CCHP system integrated with MCFC, ISCC and LiBr refrigeration system. *International Journal of Hydrogen Energy*, 2022, 47:20957–20972.

[65] Salimi M, Hosseinpour M, Mansouri S, *et al*. Environmental aspects of the combined cooling, heating, and power (CCHP) systems: a review. *Processes*, 2022, 10:711.

[66] Ren F, Wei Z, Zhai X. A review on the integration and optimization of distributed energy systems. *Renewable and Sustainable Energy Reviews*, 2022, 162:112440.

[67] Thomas S, Zalbowitz M, Cruz J. *Fuel Cells—Green Power*. Los Alamos, NM: Los Alamos National Laboratory, 1999. https://paginas.fe.up.pt/~mcnunes/QAE1sem/documentos/fuelcells.pdf (20 August 2021, date last accessed).

[68] Hoogers G. *Fuel Cell Technology Handbook*. 1st edn. Boca Raton, FL: CRC Press LLC, 2002.

[69] Thounthong P, Sethakul P. Analysis of a fuel starvation phenomenon of a PEM fuel cell. In: *2007 Power Conversion Conference—Nagoya*, Nagoya, Japan, 2–5 April 2007, 731–738; doi:10.1109/PCCON.2007.373048.

[70] Lemes Z, Vath A, Hartkopf T, *et al*. Dynamic fuel cell models and their application in hardware in the loop simulation. *Journal of Power Sources*, 2006, 154:386–393.

[71] Nehrir MH, Wang C, Shaw SR. Fuel cells: promising devices for distributed generation. *IEEE Power and Energy Magazine*, 2006, 4:47–53.

[72] Chandan A, Hattenberger M, El-kharouf A, *et al*. High temperature (HT) polymer electrolyte membrane fuel cells (PEMFC): a review. *Journal of Power Sources*, 2013, 231:264–278.

[73] Taniguchi A, Akita T, Yasuda K, *et al*. Analysis of electro-catalyst degradation in PEMFC caused by cell reversal during fuel starvation. *Journal of Power Sources*, 2004, 130:42–49.

[74] Sulaiman N, Hannan MA, Mohamed A, *et al*. Review on energy management system for fuel cell hybrid electric vehicle: issues and challenges. *Renewable and Sustainable Energy Reviews*, 2015, 52:802–814.

[75] Boettner DD, Paganelli G, Guezennec YG, *et al*. Proton exchange membrane fuel cell system model for automotive vehicle simulation and control. *Journal of Energy Resource Technology*, 2002, 124:20–27.

[76] Khaligh A, Li Z. Battery, ultra-capacitor, fuel cell and hybrid energy storage systems for electric, hybrid electric, fuel cell, and plug-in hybrid electric vehicles: state of the art. *IEEE Transactions on Vehicle Technology*, 2010, 59:2806–2814.

[77] Powers WF, Nicastri PR. Automotive vehicle control challenges in the 21st century. *Control Engineering Practice*, 2000, 8:605–618.

[78] Emadi A, Ehsani M, Miller JM. *Vehicular Electric Power Systems: Land, Sea, Air and Space Vehicles*. 1st edn. Roca Raton, FL: CRC Press, 2003.

[79] Nozu R, Lizuka M, Nakanishi M, *et al*. Investigation of the life process of the electric double layer capacitor during float charging. *Journal of Power Sources*, 2009, 186:570–579.

[80] Thounthong P, Rael S, Davat B. Control strategy of fuel cell and super-capacitors association for a distributed generation system. *IEEE Transactions on Industrial Electronics*, 2007, 54:3225–3233.

[81] Livint G, Horga V, Ratoi M, *et al*. *Control of Hybrid Electrical Vehicles, Electric Vehicles: Modelling and Simulation*. London: InTechOpen, 2011.

[82] Yu A, Chabot V, Zhang J. *Electrochemical Super-capacitors for Energy Storage and Delivery: Fundamentals and Applications*. 1st edn. Boca Raton, FL: CRC Press, 2013.

[83] Hannan MA, Azidin FA, Mohamed A. Hybrid electric vehicles and their challenges: a review. *Renewable and Sustainable Energy Reviews*, 2014, 29:135–150.

[84] Pollet BG, Pasupathi S, Swart G, *et al*. Hydrogen South Africa (HySA) systems competence centre: mission, objectives, technological achievements and breakthroughs. *International Journal of Hydrogen Energy*, 2014, 39:3577–3596.

[85] Thounthong P, Chunkag V, Sethakul P, *et al*. Energy management of fuel cell/solar cell/super-capacitor hybrid power source. *Journal of Power Sources*, 2011, 196:313–324.

[86] Nomnqa MV. Design of a domestic high temperature proton exchange membrane fuel cell cogeneration system: modelling and optimisation. *Doctor of Engineering thesis*. Cape Peninsula University of Technology, Cape Town, South Africa, 2017. https://core.ac.uk/download/pdf/151666722.pdf (15 March 2020, date last accessed).

[87] Tichagwa A. Micro combined heat and power management for a residential system. *Master's thesis*, University of Cape Town, South Africa, 2013. https://open.uct.ac.za/handle/11427/16914 (30 October 2020, date last accessed).

[88] EG&G Technical Services, Inc. Science Applications International Corporation. *Fuel Cell Handbook*. 6th edn. Morgantown, WV: US Department of Energy Office of Fossil Energy, National Energy Technology Laboratory, 2002. http://courses.washington.edu/mengr430/au07/handouts/f_c_6.pdf (7 June 2021, date last accessed).

[89] Huston J, Wyatt C, Nichols C, *et al*. *Application of Thermoelectric Devices to Fuel Cell Power Generation: Demonstration and Evaluation*. Washington, DC: US Army Corps of Engineers, Engineer Research and Development Centre, 2004. https://www.academia.edu/es/30461092/Application_of_Thermoelectric_Devices_to_Fuel_Cell_Power_Generation_Demonstration_and_Evaluation (9 December 2021, date last accessed).

[90] Gao X. HT-PEM fuel cell system with integrated thermoelectric exhaust heat recovery. *Ph.D. dissertation*. Department of Energy Technology, Aalborg University, Denmark, 2014. https://vbn.aau.dk/en/publications/ht-pem-fuel-cell-system-with-integrated-thermoelectric-exhaust-he (14 January 2020, date last accessed).

[91] Kabutey FT, Zhao Q, Wei L, *et al*. An overview of plant microbial fuel cells (PMFCs): configurations and applications. *Renewable and Sustainable Energy Reviews*, 2019, 110:402–414.

[92] Moqsud MA, Yoshitake J, Bushra QS, *et al*. Compost in plant microbial fuel cell for bioelectricity generation. *Waste Management*, 2015, 36:63–69.

[93] Bents DJ, Scullin VJ. *Hydrogen-Oxygen PEM Regenerative Fuel Cell Energy Storage System*. NASA/TM—2005-213381. Cleveland, OH: NASA, 2005. https://ntrs.nasa.gov/api/citations/20050080718/downloads/20050080718.pdf (10 January 2022, date last accessed).

[94] Pu Z, Zhang G, Hassanpour A, *et al*. Regenerative fuel cells: recent progress, challenges, perspectives and their applications for space energy system. *Applied Energy*, 2021, 283:116376.